Measuring the Ratio of Storm-Deposited Gutter Casts, Upper Cretaceous Gallup Sandstone, New Mexico, USA

By: Logan Jung-Ritchie, Hons. B.Sc.

A thesis submitted to the School of Geography and Earth Sciences, and the School of Graduate Studies in partial fulfilment of the requirements for the degree Master of Science

McMaster University MASTER OF SCIENCE (2017) Hamilton, Ontario (Science)

TITLE: Measuring the Ratio of Storm-Deposited Gutter Cast, Upper Cretaceous Gallup Sandstone, New Mexico, USA AUTHOR: Logan Jung-Ritchie, B.Sc. (McMaster University) SUPERVISOR: Professor Janok Bhattacharya NUMBER OF PAGES: 98

Abstract

Understanding unconventional petroleum reservoirs and HALO plays, areas outside existing production zones which are made up of thin-bedded or heterolithic intervals, has gained in importance in recent years with the continual demand for energy and the increased development of such prospects. Heterolithic units within deltaic successions host vast quantities of oil and gas that often go unexploited due to a lack of understanding of the sandstone shape, morphology and continuity within such reservoirs. The purpose of this work is to examine the thin-bedded units within the Late Cretaceous prodelta successions of the Gallup Sandstone in the Shiprock area of New Mexico in order to quantify the fundamental processes responsible for the deposition of these sands and to perform a correlation for such heterolithic deposits. Rock Ridge and Sanostee show heterolithic deposits, within parasequences 5a and 7a of the Gallup sandstone, and were analyzed, using measured sections and photomosaics, near the Shiprock area in order to compare the heterolithics in different stratigraphic settings. Five measured sections were collected at the centimeter scale in order to observe every facies change at a high resolution. Facies associations, such as tempestites, turbidites, and hyperpycnites, were used to identify dominant processes of deposition. Corresponding net-to-gross calculations yielded the sandstone percentage of each section with the result that storm-dominated beds present at Sanostee yielded the highest percentage of sand content. Two high resolution gigapan photomosaics of each heterolithic exposure were collected in order to perform a correlation of all the sandstones observed within the measured sections, across the entire exposure. Results show that dominant process of deposition varies along strike. Towards Sanostee, in the south, storm-waves are dominant while farther north rivers exert greater influence. However, the presence of large scale storm-deposited gutter casts at Sanostee has significant implications for lateral and vertical continuity of

sandstones in comparison to the more tabular sandstone facies found at Rock Ridge. These guttered facies have a major impact on net-to-gross and vertical conductivity due to their high degree of amalgamation and therefore may signify important areas for prospecting in such heterolithic reservoirs. Furthermore, the presence of large scale gutters beneath a sharp-based shoreface is indicative of a Falling Stage Systems Tract, leading to the conclusion that Parasequence 7a-6d were affected by forced regression.

Acknowledgements

Firstly, this work would not have been possible without the guidance, funding, patience, and unending support of my supervisor Dr. Janok Bhattacharya. He has taught me the importance of holding high standards, always striving to learn as a professional and grow as a person. I am grateful for his willingness to teach and be supportive in any way he can. The last two years have provided a wonderful example of an engaged, contributing, and passionate member of the geoscience community.

Without the unending support of my family I would never have made it into graduate school, never mind completing my Master's thesis. My dad's continual encouragement and the immense support my mom provides are the backbone that every success I have ever had is built upon.

I would be remiss not to extend my sincerest thanks to all my lab mates and colleagues who have helped me in the field, through graduate courses and the writing process. Stephanie Kimmerle, Sandeep Sharma, David Kynaston, Christina Genovese, Matt Leung, Curtis Ferron, and Kristin Dosen for their help in the lab and during the field season. A special thank you is warranted for Wen Lin, Sean Karner, Monica Wiercigroch, and Madison McAndrew for all their help as field assistants, advisors, housemates, and wonderful travelling companions during the 2016 field season. And a special thanks to Wen Lin for the endless discussions on the stratigraphy of the Gallup and helping me understand various papers and concepts that have aided in the development of this thesis and my overall growth as a scientist.

Lastly, I would like to thank NSERC and our consortium members BP and Inpex without whose generous financial support this work would never have been completed.

Table of Contents

List of Figures

Chapter 1 – Introduction

With the continued expansion of global population the demand for energy continues to increase to unprecedented levels. This puts increased demand on global petroleum reserves and necessitates the importance of understanding, exploration, and exploitation of new potential reservoirs. Many intervals in known petroleum reservoirs contain hydrocarbons but are made up of sandstone beds below the resolution of conventional logging tools or are found in mud dominated environments (Schieber et al., 2007; Wilson & Schieber, 2014) and have therefore been bypassed. Examples are found in the mud dominated prodeltas of the Gallup Sandstone within the San Juan Basin located in northwestern New Mexico, USA.

The purpose of this study is to examine the heterolithics of the Gallup prodeltas in order to: 1) determine the dominant process that controls deposition of these units within the Cretaceous Interior Seaway; 2) analyze the lateral extent of sandstones within heterolithic deposits of two different parasequences; and 3) provide a correlation of both sets of heterolithic sandstones using high resolution Gigapan photomosaics to document these types of unconventional reservoirs in outcrop. The following is a detailed study of the processes of formation and stratigraphic significance of the heterolithics below the Gallup shoreface.

1.1 Deltas

Deltas were originally defined by Barrell (1912) as, “A deposit sub-aerially built by a river into or against a body of permanent water. The outer and lower parts are necessarily constructed below water level, but its upper and inner surface must be land maintained or reclaimed by river building from the sea” indicate that in order to be properly characterized both the marine and subaerial components must be preserved. However, issue with the lack of preservation of

subaerial components, resulting in top-truncated units, has led to the repeated succession of thick sandstones and heterolithics (Bhattacharya, 2006; Bhattacharya & Willis, 2001) to be classified as 'offshore bars' (Bhattacharya & Giosan, 2003; Bhattacharya & Willis, 2001). For example, Tillman and Mereweather (1994) interpreted the Harlan Sandstone as an offshore bar package based on the lack of subaerial deposits, however Bhattacharya and Willis (2001) re-interpret this unit as deltaic due to lobate sandstone geometry, oblique offshore paleocurrents, brackish influence exhibited within the ichnofauna suites, and vertical stacking patterns of upward coarsening units. Deltaic sandstones tend to be top-truncated by erosional ravinement surfaces, sometimes recognizable with a thin, coarse transgressive lag (Bhattacharya & Willis, 2001). The tripartite model (Figure 1) has traditionally been used to classify the processes that form deltas; as river, tide, and storm dominated (Galloway, 1975) based on the morphology and structure of the sand bodies. One of the issues with this model is that waves do not always strike the shoreline at a perpendicular angle (Bhattacharya & Giosan, 2003). The asymmetric delta model (Figure 2) depicts how waves can strike at an oblique angle to the shoreline causing differences in the deposits updrift and downdrift (Bhattacharya & Giosan, 2003; Krueger et al., 2010). The updrift side is dominated by sands transported alongshore (Figure 2) and are typically texturally more mature compared to the downdrift deposits. Downdrift deposits are characterized by alternating units of river borne sand and mud (Bhattacharya & Giosan, 2003). The Gallup sandstone is hypothesized to be an asymmetric delta and therefore follows this depositional model (Krueger et al., 2010).

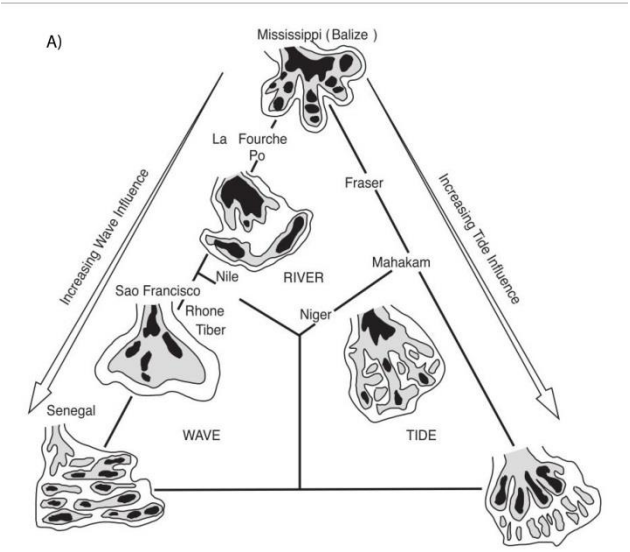

Figure 1. Processes that influence delta deposition and morphology, tripartite model of delta classification from Galloway (1975).

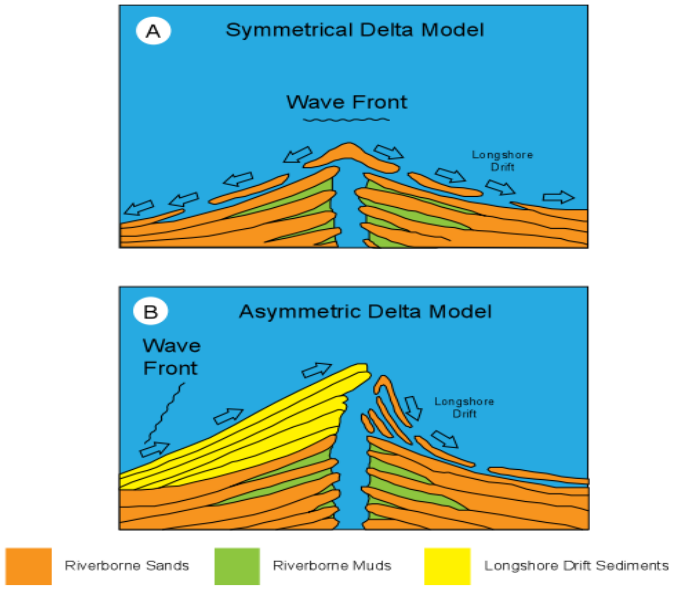

Figure 2. Wave approach of asymmetric delta model taken from LoParco (2011) and modified after Dominguez (1996). Note the dispersal of river borne sands versus marine sands down drift of the river mouth. Differences in

grain size and sorting between marine to fluvial sands cause physical differences in reservoirs within these environments.

Contrary to the original definition and models of classification (Barrell, 1912; Galloway, 1975) recent work has shown that preservation of the primary mechanism of sediment delivery to the marine basin is preserved and better observed by examining the prodelta heterolithics (Li et al., 2015) deposited below fair-weather wave base, as opposed to relying on the overlying sandstones, which many have undergone wave reworking. By looking for indicators such as repressed bioturbation, brackish fossils, evidence of fluvial influence such as hyperpycnites (Bhattacharya & Willis, 2001; Bhattacharya & MacEachern, 2009; Lamb et al., 2008; Li et al., 2015; Mulder et al., 2003) it is possible to identify deltaic deposits and the mechanism for sediment delivery by examining the prodelta heterolithics. In this study, several of the Gallup sandstone prodeltas are evaluated both for process of deposition and changes in along strike facies variability. Once the percentages of all the processes of deposition have been obtained an evaluation can be made based on the updated deltaic classification scheme of Ainsworth et al. (2011; Figure 3) where the Gallup prodeltas can be placed within the diagram. The purpose of this study is to, firstly, obtain a clear idea of the primary methods of sediment deposition into the marine realm of the delta to quantify the dominant processes. Secondly, to evaluate along-strike variability of facies due to longshore drift and asymmetry of the delta and how changes in lithology might have an effect on reservoir potential.

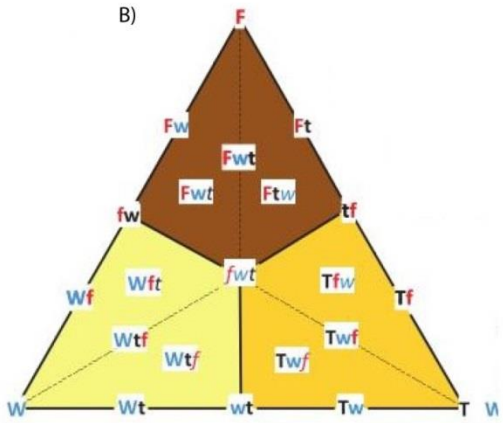

Figure 3. Updated Model from Ainsworth et al. (2011). Bold Upper Case letter signifies primary process, bold lower case is a secondary process, and italic lower case is a tertiary process. F, f, *f* = fluvial, W, w, *w* = wave. And T, t, *t* = Tidal.

1.2 Gutter Casts

The term 'gutter casts' was first described by Whitaker (1973) who defined them as erosional features caused by 'offshore directed unidirectional flow' (Myrow, 1992; Whitaker, 1973) or alternatively helical flow vortices (Noad, 2015) during storm events. Gutter casts are found to be oriented perpendicular or oblique to the paleoshoreline (Myrow, 1992) supporting the model of offshore directed storm flow being the cause of these features. Gutter scours are U or V shaped with high sloping walls (Myrow, 1992; Plint, 2010). Dimensions of recorded gutter casts vary from 2-50cm wide and 2-30cm deep, however much larger scale gutter casts have also been reported, for example, the Cretaceous Sandakan Formation in Borneo, where they reach sizes of 20m wide and 2m deep (Noad, 2015) and the Miocene Baram Delta Province, where gutters reach sizes of 10.8m wide and 2m deep (Collins et al., 2016). Due to their origin during high energy storm flows, gutters are typically filled with sands (Myrow, 1992; Noad, 2015; Plint, 2010), even when found in more distal environments, and can be

either massive or stratified, commonly characterized by hummocky cross-stratification (HCS) fill deposited during waning storm flows (Collins et al., 2016; Myrow, 1992; Noad, 2015).

In this study, large scale gutter casts are found in one of the locations documented. The size and scale of these structures aid in determining the strength and prevalence of storm deposits within the Gallup prodeltas and the prevalence of this facies along strike and the lateral transition to thinner sandstones has implications for the delivery mechanism of sediment into the delta.

Chapter 2 – Geologic Setting

The Gallup Sandstone Formation is a fluvio-deltaic clastic wedge, within the Mancos Shale, that outcrops in the San Juan Basin in New Mexico, USA (Figure 4). The Gallup Sandstone was deposited during the Late Turonian regression of the Western Interior Seaway (Campbell, 1979) and progrades northeast into the middle of the basin. The regional paleoshoreline strikes northwest- southeast and the outcrop belt extends from the Shiprock area in the north of the state to south of the town of Gallup (Figure 5).

Figure 4. The Western Cretaceous Interior Seaway, during the Late Turonian (90 Mya), extended from the Arctic Ocean to the Gulf of Mexico, and divided present-day North America in two. The Late Turonian regression led to deltaic progradation and the deposition of the Gallup sandstone and the heterolithics examined in this study (Blakey, 2014).

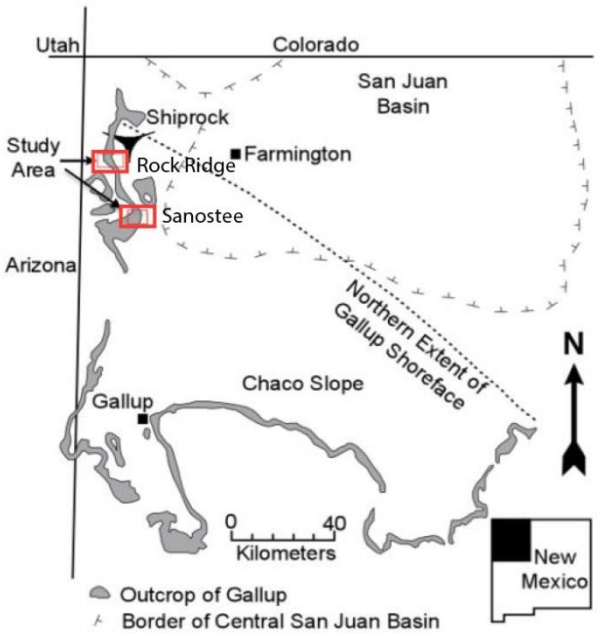

Figure 5. Map of Gallup sandstone outcrop belt in northwestern New Mexico, USA (Campbell, 1979). Red boxes indicate study area, Rock Ridge to the north and Sanostee to the south.

2.1 Stratigraphy of the Gallup Sandstone

The Gallup Sandstone has been studied for years (Dane et al., 1957; Campbell, 1973, 1971, 1979; McCubbin, 1982; Molenaar, 1973, 1974, 1983; Nummedal & Molenaar, 1995) due to its proclivity as a petroleum reservoir, however new interpretations provide an updated model of the regional stratigraphy. Regionally, the Gallup was deposited as a clastic wedge that downlaps onto the offshore Juana Lopez Member of the Mancos shale (Figure 6). The Gallup Sandstone Formation is unconformably overlain by the Tocito Sandstone Member of fluvial-estuarine origin and the Dilco Coal Member of the Crevasse Canyon Formation (Campbell, 1979; Valasek, 1995; Jennette & Jones, 1995; Molenaar & Nummedal, 1995). Traditionally the Gallup is interpreted to be composed of the deposits oftwo major environments: coastal marine and deltaic (Molenaar, 1973). The coastal strand plain

environments transition into deltaic distributary plain sands (Molenaar, 1973, 1974). The Gallup has traditionally been interpreted as having six sandstone tongues (Figure 6) that progressively prograde further into the basin due to repeated episodes of local regression (Nummedal & Molenaar, 1995).

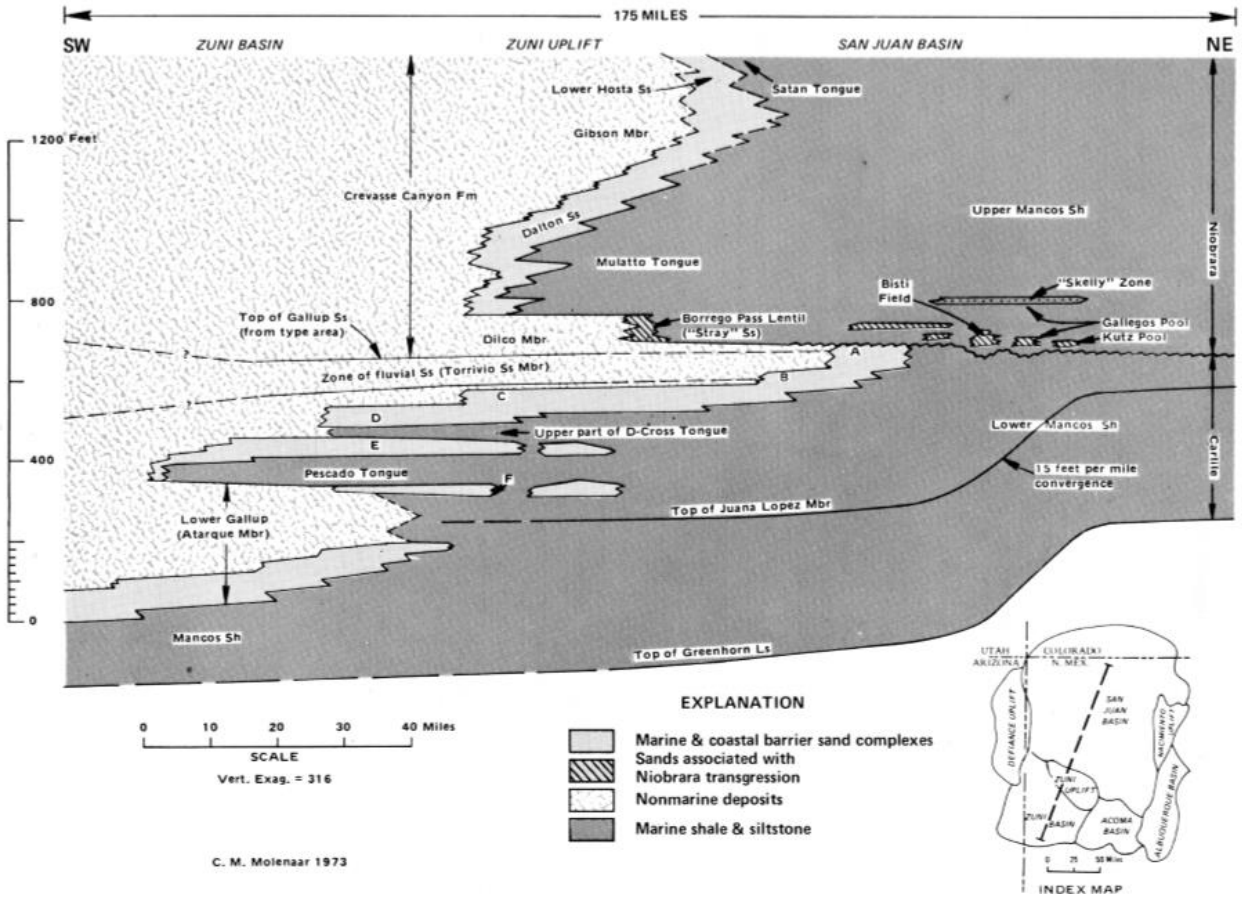

Figure 6. The first major accepted regional correlation of the Gallup sandstone as modified from Molenaar (1973). Note the six prograding sandstone tongues labelled A-F with F being the oldest. It is important to note the lack of important stratigraphic surfaces (i.e. sequence boundaries, systems tracts), and lack of any data detailing shoreline trajectory.

Recent work has utilized the approach of high-frequency sequence stratigraphy in order to reinterpret the Gallup Sandstone in terms of accommodation successions and shoreline trajectory (Figure 7). Two laterally extensive regional bentonite layers were used as reliable

datum's (Lin & Bhattacharya, 2017), splitting the unit into the 'Upper' and 'Lower' Gallup (Figure 7), in order to quantify the timescales of sea level fluctuation observed within the Gallup. In total, 5 sequences comprising 16 parasequence sets made up of 32 parasequences were identified within the Lower Gallup Sandstone and 6 sequences with 23 parasequence sets built out of 61 parasequences make up the Upper Gallup Sandstone (Lin & Bhattacharya, 2017).

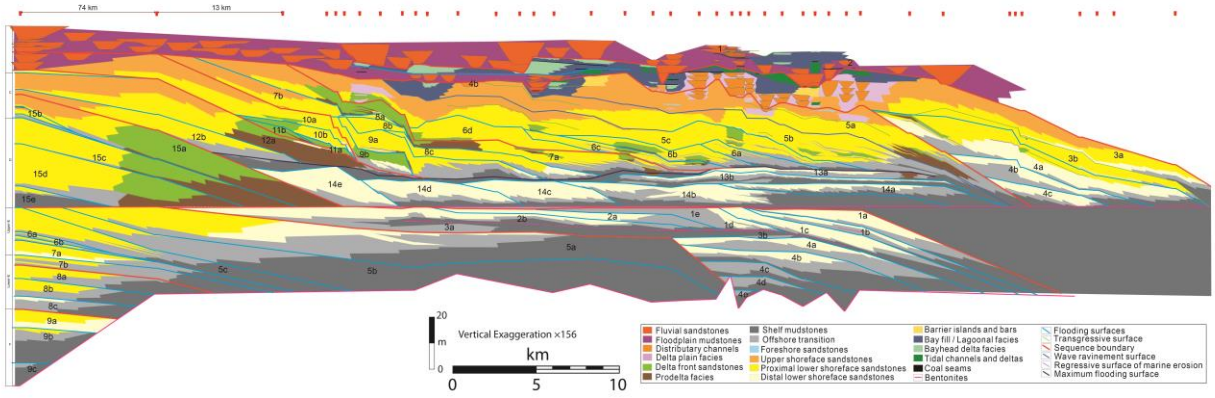

Figure 7. High-resolution sequence stratigraphy of the Gallup sandstone. Note the complexity and changing shoreline trajectory throughout the Gallup in comparison to Figure 5, (from Lin & Bhattacharya, 2017).

This work shows strong storm-influence in the deltaic deposits coupled with a degradational accommodation succession (Neal & Abreu, 2009) and presents evidence of forced regression resulting in a Falling Stage Systems Tract (FSST), which will be expanded on within this thesis (see Chapter 6). Along strike facies variations from deltaic facies into dune scale cross-bedded features interpreted as shoreface deposits (Lin & Bhattacharya, 2017), demonstrate that the Gallup exhibits some features consistent with the wave-influenced deltaic model (Dominguez, 1996; Bhattacharya & Giosan, 2003).

2.2 Field Site

The measured sections and bedding diagrams presented herein were collected in the northern part of the Gallup outcrop belt near the Shiprock area. Two sites were examined in detail: Rock Ridge, within Parasequence 5a, and Sanostee, within Parasequence 7a-6d (Figure 7; Lin & Bhattacharya, 2017).

A)

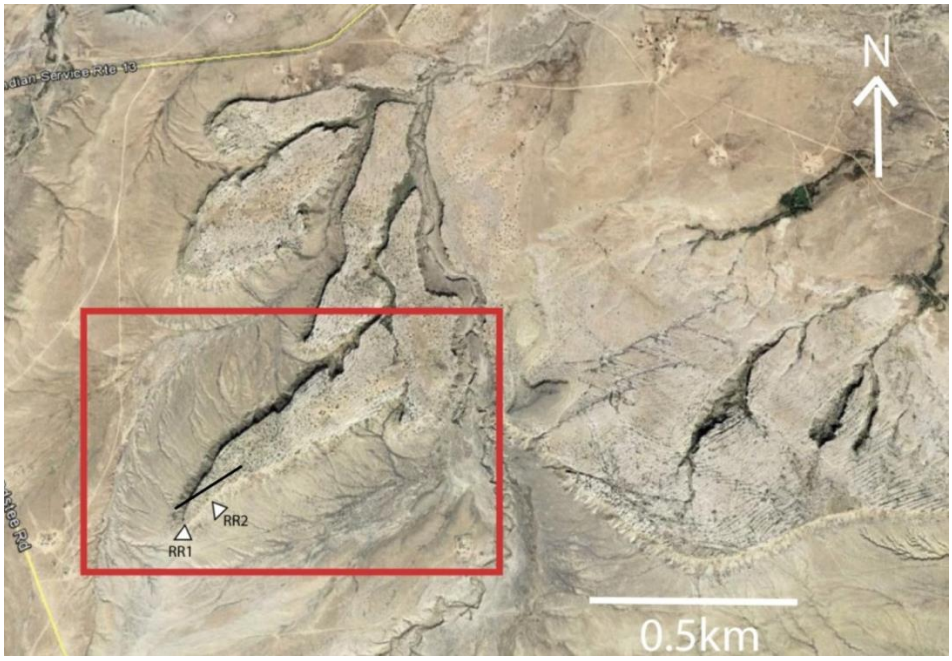

B)

Figure 8. Field map of locations presented in this thesis. A) Rock Ridge outcrop, and B) Sanostee outcrop. Black line indicates track of Gigapan images.

Chapter 3 – Methodology

Outcrop information collected included sedimentological and stratigraphic data from the outcrops, such as grain size, bedding thickness, bioturbation index, ichnofacies, and sedimentary structures. Three measured sections were taken at Sanostee and two at Rock Ridge. These sections (2.80m-7.12m) were measured at the centimeter scale in order to track high frequency facies changes. The measured sections were used to identify sandstones, which could then be correlated between sections.

High resolution gigapan photomosaics were collected in order to track the lateral variability of the sandstones within the heterolithic units. Measured sections were then placed on the photomosaics in order to identify the nature of key beds. The photomosaic is obtained by using a gigapan to take a series of images and then stitching them together to make a high resolution image in order to view all the thin beds within the heterolithic exposure. The image makes it possible to evaluate the degree of correlation of sandstones between sections.

Grain size measurements were taken using the Wentworth classification and a handheld grain size card. Silts and clays were differentiated by colour and texture and quantified within beds on a percentage scale. Field data was collected with a rock hammer, hand lens, camera for high quality photographs, and a Silva compass to collect paleocurrent data. A handheld GPS was used for navigation and to plot the location of measured sections in Google Earth. Measured sections were digitized in Adobe Illustrator. Grain size and facies characterizations were uploaded into Microsoft Excel for statistical analysis to determine the processes of deposition and the percentages of each facies association.

In order to perform this analysis, the sandstone dimensions were displayed on a scatterplot and the R^2 value computed. All sandstones, regardless of facies, were included as well as separate gutter plots for sandstones identified as gutter casts (presented in section 5.1.3).

Chapter 4 – Results: Facies

In the 5 measured sections taken, 12 facies were observed, which are presented below.

Facies 1: Structureless Mudstone

Structureless mudstone (Figure 9a and b) was observed in all sections and was characterized as 85-90% clay, with no silt or sand components. These muds were found in thin beds not exceeding 2 cm thick with sharp contacts. In some beds evidence of bioturbation was recorded and trace fossils observed were; *Chondrites, Planolites, Paloephycus, Asterosoma,* and *Zoophycos*. In beds where bioturbation was observed Bioturbation (BI) index ranges from 1-3, all other beds had BI values of 0. Abundant organic matter and fish scales were observed on bedding planes. Structureless mudstone beds were observed sharply overlying sandstone beds. Some beds exhibit normal grading into Facies 2 (F2) or Facies 3 (F3; refer to measured sections in Chapter 5), while others had sharp contacts.

Facies 1: Interpretation

Stuctureless mudstone can also be referred to as fluid mud (Dalrymple et al., 2012), defined as bottom-hugging subaqueous body of fine-grained sediment with a concentration of solids >10g/L (Kirby & Parker, 1983). These sediment-rich flows are formed when sediment is re-suspended during times of higher velocity flow and begins to deposit once the velocity slows (Ichaso & Dalrymple, 2009). Deposition occurs rapidly followed by dewatering and compaction. The speed of deposition does not allow colonization by biota during deposition but subsequent erosion could expose top layers of mud to top down colonization (Dalrymple et al., 2012). Lack of diversity within the ichnofauna coupled with a lack of wave-influenced structures and

stratigraphic proximity overlying sandstones indicates F1 to be deposited during waning flows with high sedimentation rates.

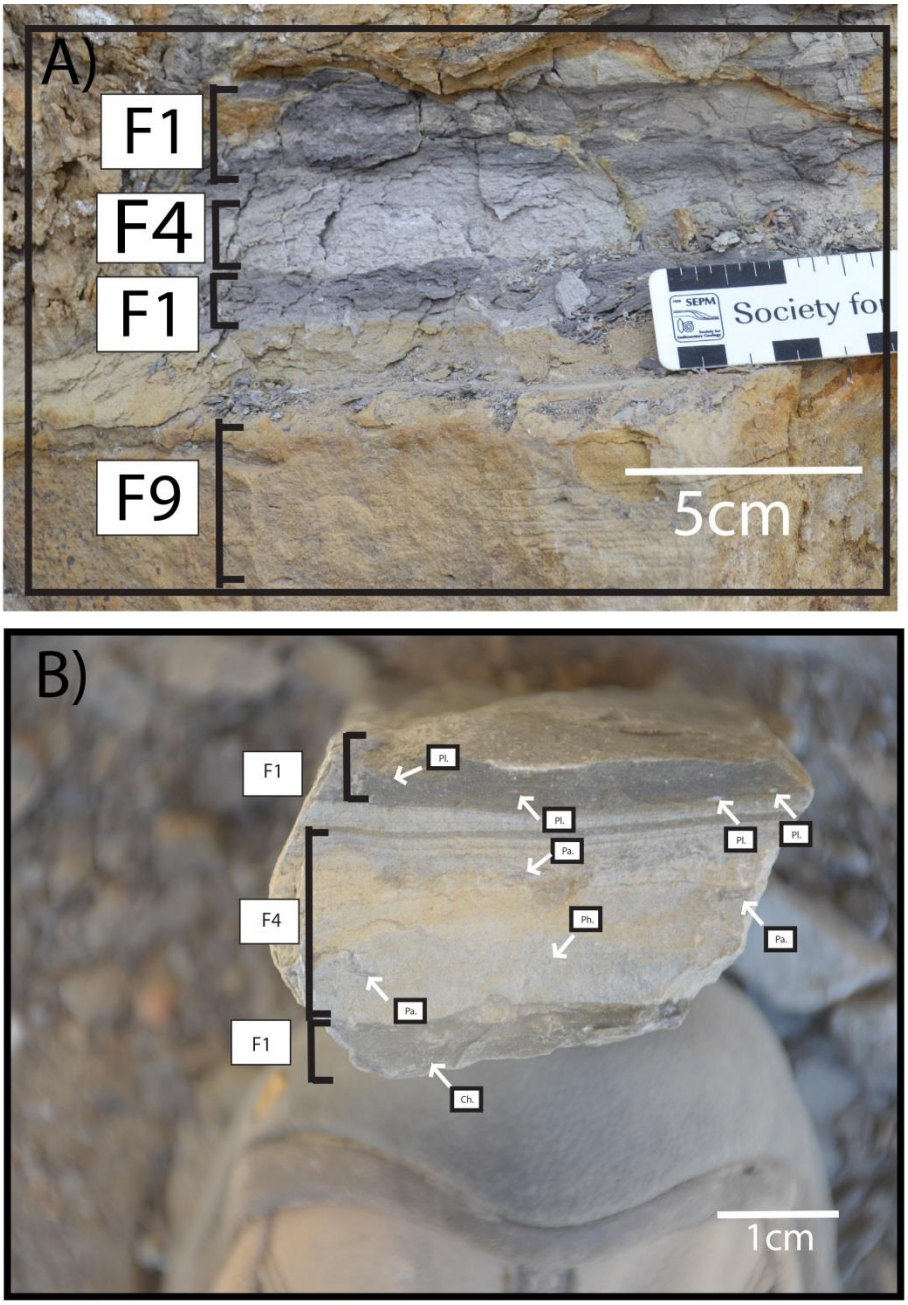

Figure 9. Multiple facies displayed. A) View of heterolithic bedding, F1 structureless mudstone, F4 muddy siltstone, and F9 HCS, B) Zoomed in view of F1 and F4. Evidence of trace fossils present within F1, in this case *Planolites* (Pl.) and *Chondrites* (Ch.); F4 contains *Paleophycus* (Pa.), and *Phycosiphon* (Ph.).

Facies 2: Laminated Mudstone

Laminated mudstone (Figure 10) is made up of 80% or greater clay sized particles with some minor silt lamina. Laminations are planar to wavy, with some evidence of starved ripples made of silt sized particles. BI ranges from 0-2, with a low diversity of ichnofauna, made up of *Phycosiphon*, *Planolites*, *Chondrites*, and *Zoophycos*, characteristic of the *Cruziana* ichnofacies. Laminated mudstone units vary in thickness from less than 1cm up to 10cm. Plant debris and other organic matter is common on bedding surfaces. Some beds exhibit normal grading into F3 or F4 and occasionally inverse grading into F1(refer to measured sections in Chapter 5), other beds have sharp contacts.

Facies 2: Interpretation

Laminated mudstone is indicative of multiple processes of deposition. The mud is interpreted to be the result of deposition from suspension out of low energy flows due to the presence of bioturbation, however, the coarser grained silty laminations are indicative of high energy flows in a distal location, possibly via sediment gravity flows (Collins et al., 2016). In some cases bioturbation occurs after deposition based on disturbance of laminations by burrowing.

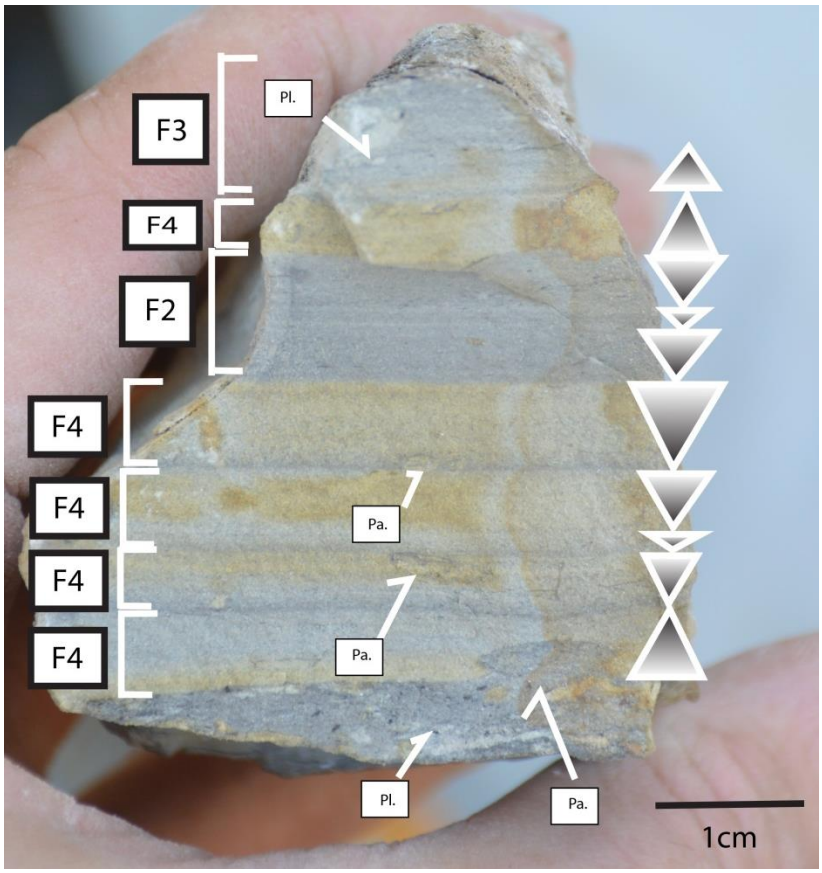

Figure 10. Laminated mudstone facies (F2), with F4 and F3. Trace fossils include *Paleophycus* (Pa.), and *Planolites* (Pl.). Beds show normally to inversely graded profiles.

Facies 3: Silty Mudstone

This facies (Figure 10) is characterized by the proportion of clay to silt, which was classified as 60%-40% based on field observations (refer to Chapter 3 for specific methods). The silty mudstone facies shows BI 0-2 for the majority of observations however there are some select intervals with a BI of 5. There is a low diversity of trace fossils including *Planolites*, *Phycosiphon*, and *Chondrites*, all of which are part of the *Cruziana* ichnofacies. The silt inclusions could be indicative of bioturbation or of higher energy environments than either F1 or

F2. Plant debris and other organic matter are commonly found on bedding surfaces. Some beds exhibit normal grading into F4 while others show inverse grading into F2 or F1.

Facies 3: Interpretation

F3 differs from F1 due to the clay-silt proportion, where F3 has on average 40% silt versus F1 which is 100% clay. The degree of bioturbation is indicative of lower sedimentation rates and lack of erosive currents allowing for a higher degree of colonization in comparison to F1. F3 is commonly associated with F2 and F4. Based on the variable bioturbation and the sorting, it is interpreted that the silty mudstone is deposited by suspension settling in low energy environments during waning flows with no evidence of wave influence.

Facies 4: Muddy Siltstone

This facies (Figures 9&10) is characterized by the clay to silt ratio, which was determined to be 40%-60% (refer to Chapter 3 for specific methods). Bed thickness varies from less than 1cm to 10cm, and is associated with F3. Some evidence of laminations are observed in some intervals of F4, laminations vary from planar to wavy. Some beds exhibit normal or reverse grading. BI varies from 0-2. Trace fossils observed are *Planolites*, *Chondrites*, and *Paleophycus* which are part of the *Cruziana* ichnofacies. In most cases F4 normally grades into mudstone, however in some instances it is sharply overlain by F1 or exhibits inverse grading (Figure 10). Most often bed contacts are not sharp based and gradationally overly F1, F2, or F3.

Facies 4: Interpretation

The presence of laminations, especially wavy laminations indicate that F4 was deposited in a moderate energy environment of oscillatory or combined-flow (Collins et al., 2016; Macquaker

et al., 2010). Wavy laminations are characterized as wave ripples. Inverse and normally graded beds, with a lack of a sharp base, are indicative of waxing and waning flow associated with hyperpycnal flows, likely to be a wave-enhanced sediment gravity flow in a storm-reworked prodelta (Plint, 2014; Bhattacharya & MacEachern, 2009; Mulder et al., 1995; Mulder et al., 2003). Lack of pervasive bioturbation throughout the facies, and apparent constraints upon the diversity of ichnofauna is indicative of a deltaic setting and sediment gravity flows or possibly fluid mud flow (MacEachern et al., 2005). In addition, the presence of plant debris and organic matter indicates proximity to a river mouth (Collins et al., 2016) leading to the interpretation of F4 being of deltaic origin.

Facies 5: Muddy Heterolithics

This facies (Figure 11) is mudstone dominated made up of clay to silt grains with up to 50% (very fine lower) vfl-vfu (very fine upper) sandstones. The sandstone laminations/thin beds vary from 0.2 cm – 2 cm in thickness. Internal structures are mostly asymmetrical cross lamination, and the majority of sand laminations/thin beds pinch out within 10 cm, indicating starved ripples. This facies has BI 0-1, and the only trace fossils observed are *Planolites* and *Chondrites*.

Facies 5: Interpretation

Due to the abundance of coarser grained sands this facies is considered more proximal than F1-F4. However, starved ripples are indicative that sand supply remained low. Asymmetric cross laminae are indicative of unidirectional current ripples (shown in Figure 13) resulting from an offshore directed current or oscillatory combined-flow (Collins et al., 2016). Lack of bioturbation could be indicative of a highly stressed environment frequently affected by offshore directed flows (Bhattacharya & Willis, 2001).

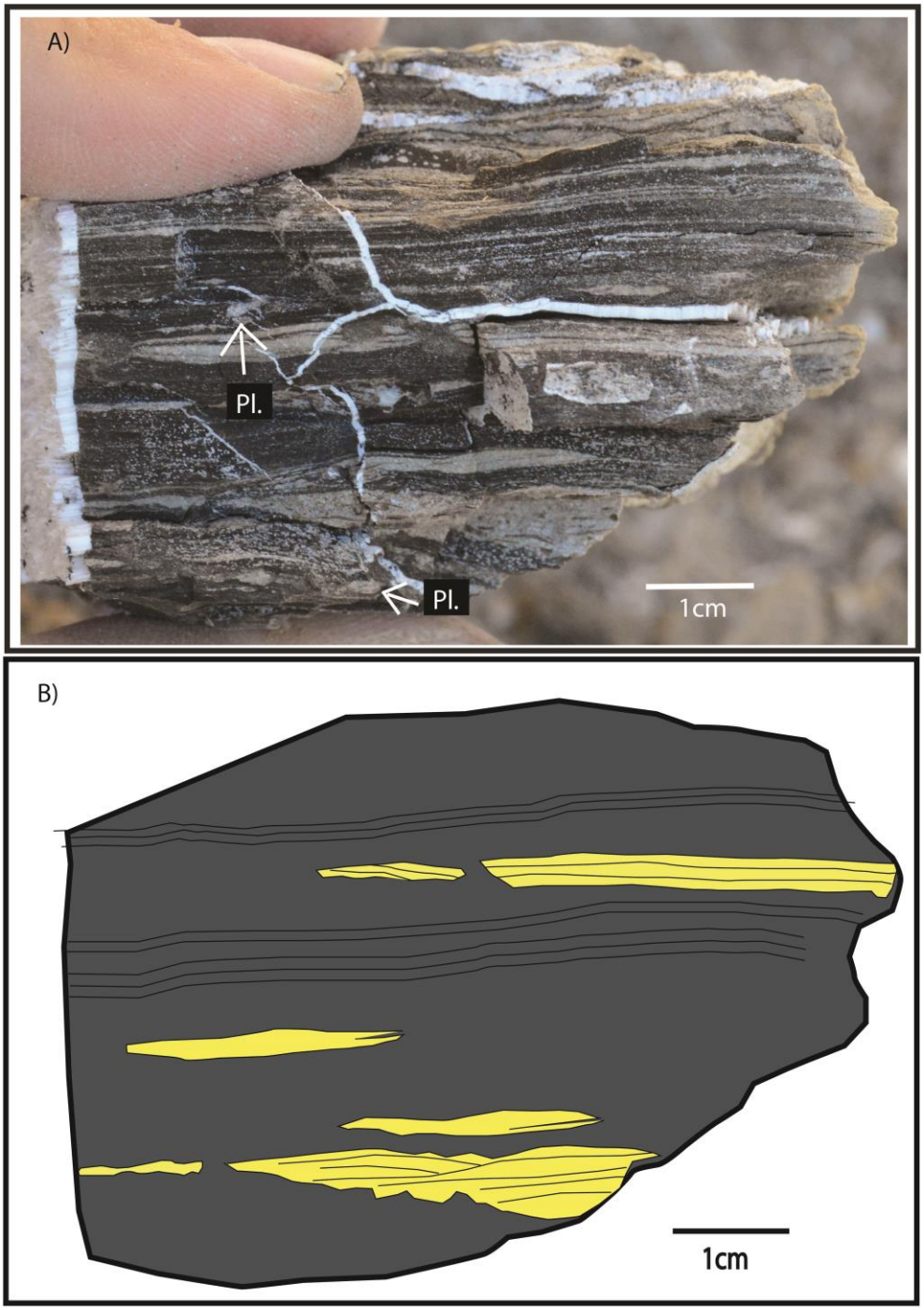

Figure 11. Muddy heterolithic facies (F5). A) showing silt-vfl sand starved ripples. Pl = *Planolites* trace fossil. B) Line drawing of sandstones. Note: micro-gutter at base.

Facies 6: Wave Rippled Sandstone

The first of three types of rippled sandstone (Figure 12) observed exhibit symmetrical cross-laminations. These units are classified as well sorted and made up of vfl-fL sand grains. Mud drapes were observed over some of the ripple crests. Bed thickness varies from 0.5 cm – 10 cm and have variable lateral extent from either 10 cm to 10 m. Bioturbation varies from 0-2 and few observable trace fossils include *Planolites, Chondrites, and Zoophycos* from the *Cruziana* ichnofacies.

Facies 6: Interpretation

Symmetrical cross-laminations are indicative of wave ripples produced by wave to possibly oscillatory combined flows and are common in wave-influenced delta fronts or distal shoreface (Bhattacharya, 2006; Plint, 2010). Lack of bioturbation and low diversity in ichnofauna could indicate deltaic influence. Wave ripple structures can also indicate some level of storm-influence.

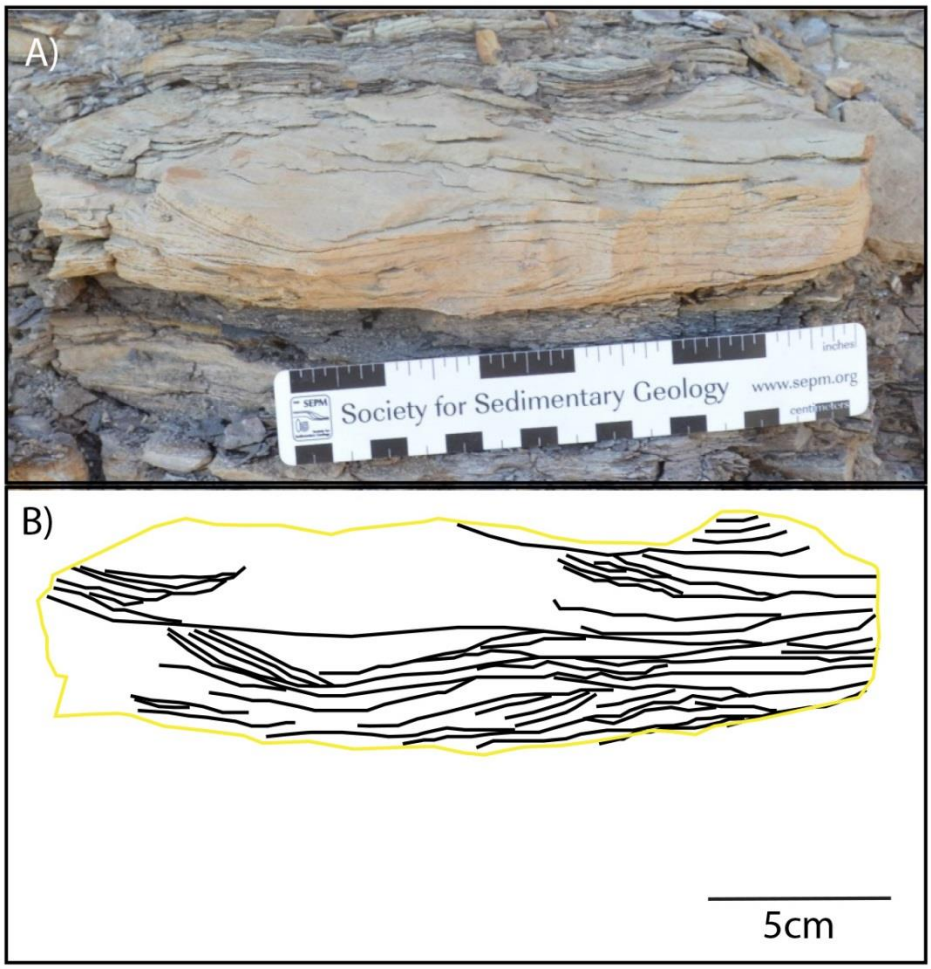

Figure 12. Wave rippled sandstone facies (F6). A) A typical observation of F6 in the Sanostee area, B) Line drawing exhibiting the lamination, note there is some evidence of combined flow. Due to storm influence there is no pure wave-rippled or current-rippled samples, all have some degree of combined flow.

Facies 7: Current Rippled Sandstone

Asymmetric cross-laminations makeup 5-10% of the structures recorded within all the measured sections; however they are important paleocurrent indicators. F7 (Figure 13) is characterized by vfl-fL sand grains with mud drapes observed over the ripple crests. The ripple foresets dip at the angle-of-repose. Bioturbation levels are low, similar to F6, with BI values of 0-1. Only

Planolites and *Chondrites* trace fossils were observed. Bed thickness varied from 2cm – 5cm and beds were had a variable lateral extent.

Facies 7: Interpretation

F7 is deposited by unidirectional currents in high energy environments causing the deposition of larger grains then previous facies, as well as higher sedimentation rates resulting in low levels of biologic activity. This indicates F7 was deposited in a more proximal, higher energy environment then F1-F5. Lack of bioturbation and diversity in ichnofauna suggests a stressed environment and rapid deposition. In these types of marine settings unidirectional current ripples have been associated with distinct event beds in turbidites caused by turbidity flows downslope or decelerating inertial flows (Mulder & Alexander, 2001; Lamb et al., 2008).

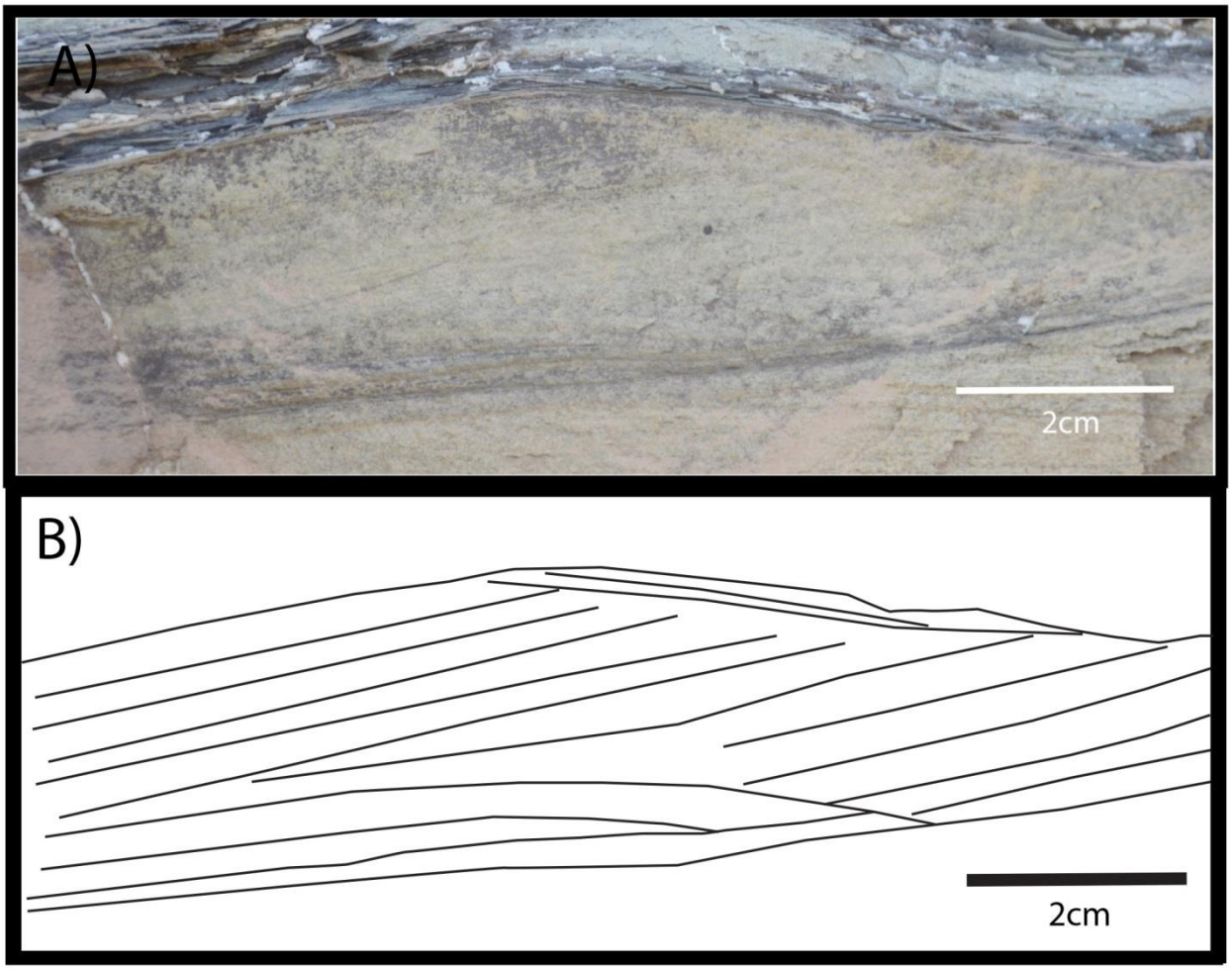

Figure 13. Example of asymmetric cross-laminations (F7) from Sanostee. A) Photo, B) Line drawing showing unidirectional current to the left of the page.

Facies 8: Combined Ripple Sandstone

This facies (Figure 14) is made up of vfl-fL sandstone with some mud drapes observable over ripple crests. Bed thickness varies from 2 cm-50 cm with a lateral extent that ranged from 1m-40 m. Combined flow ripples are characterized as ripple structures that have both a unidirectional and oscillatory component (Myrow & Southard, 1991). Bioturbation is generally low throughout F8 and BI ranges from 0-2. Observed trace fossils are *Planolites*, *Chondrites*, and *Paleophycus*.

Most instances of ripples observed in this study had some combined influence, however F8 is defined by those structures that exhibit equal parts unidirectional and oscillatory features.

Facies 8: Interpretation

Combined flow ripples form due to oscillatory currents, leading to the symmetrical laminations, with a distinct unidirectional current overprint. Such types of combined flows show both wave and current influence and are associated with storm-wave processes (Collins et al., 2016; Dumas & Arnott, 2006; Kerr & Eyles, 1991). Therefore combined flow ripples are associated with tempestite deposits and form as the storm flows wane (Dumas & Arnott, 2006). F8 is often found in association with HCS/SCS beds.

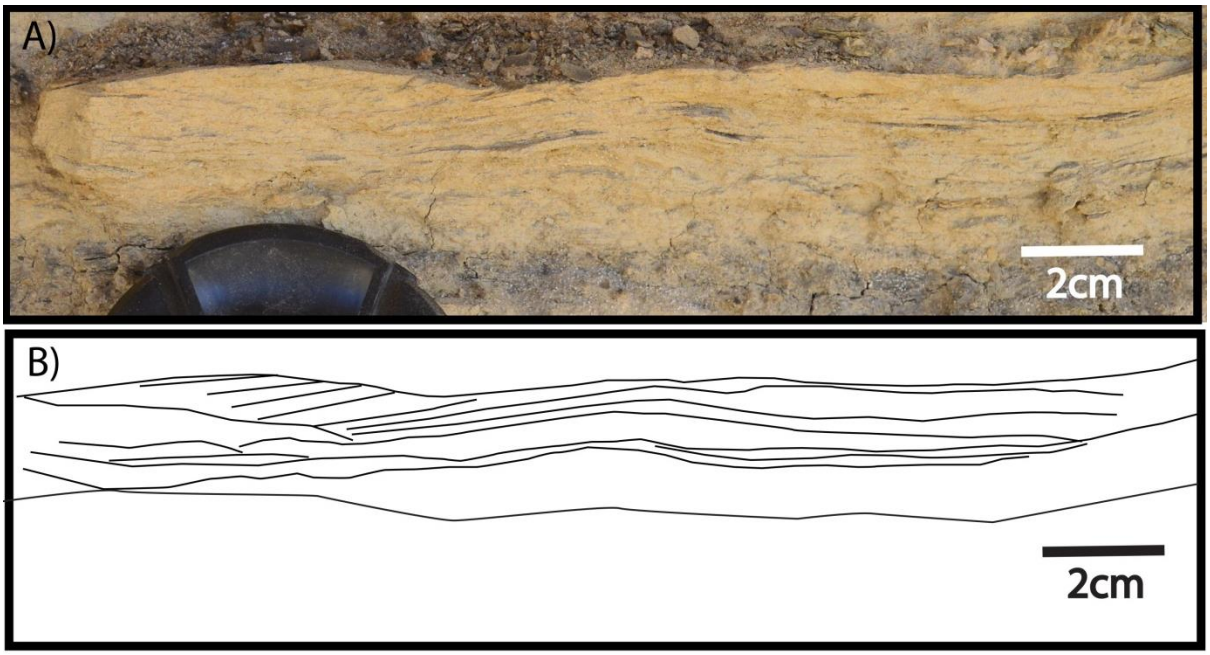

Figure 14. Combined flow rippled sandstone (F8). A) Photo, B) Bedding diagram. Note occurrence of both asymmetric cross-lamination with convex and concave up laminations indicative of combined flow. Note: outcrop oriented oblique to paleoshoreline.

Facies 9: Hummocky/Swaley Cross-Stratified Sandstone (HCS/SCS)

This facies (Figure 15) is made up of vfl-vfu sand grains with bed thickness varying from 5cm-15cm. No discernable trace fossils were observed. Some of the hummocky units are capped by a thin (1-2cm) layer of F6. Units are typically made up of both convex-up laminae (i.e. the hummock), and convex-down (i.e. the swale), which can either laterally terminate other or non-erosively end against each other (Duke, 1985). The SCS units are differentiated by common downlap and a lack of convex up laminae sets (Duke, 1985). Some units do show muddy laminations draping the sand laminations.

Facies 9: Interpretation

Hummocky and swaley cross-stratification has been interpreted to be caused by oscillatory dominated combined flows during storm events, with both erosion and subsequent deposition occurring (Duke, 1985; Dumas & Arnott, 2006). Mud laminations indicate instances of waning flow to allow mud to settle (Duke, 1985). Subsequent deposition of sands could be due to multiple storm flows within relatively short periods of time. F9 has been interpreted to be indicative of tempestite deposits (Collins et al., 2016; Kerr & Eyles, 1991).

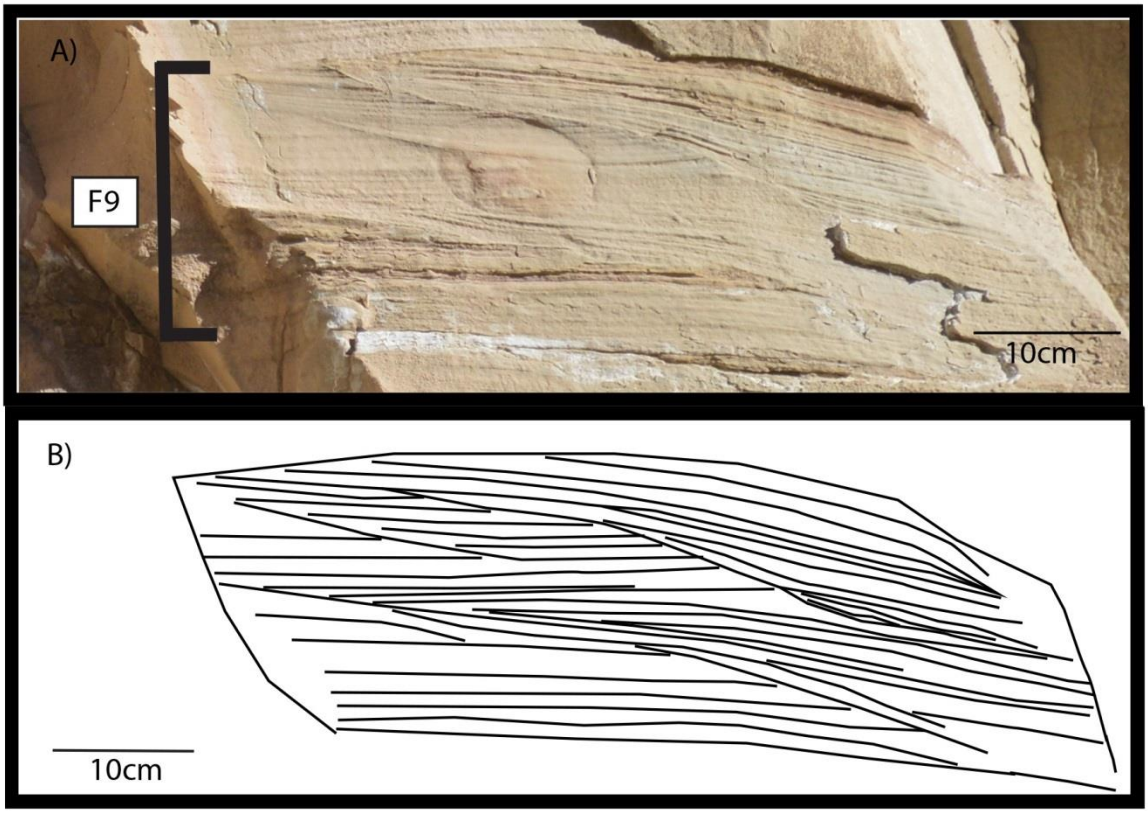

Figure 15. HCS sandstone facies (F9). A) Photo, B) Bedding diagram of internal HCS structure.

Facies 10: Laminated Sandstone

The fifth type of sandstone facies is laminated sandstone which has both low angle (1^{o}-5^{o}) lamination and horizontal planar lamination (Figure 16). Mud drapes are observed within some beds and some internal discontinuity or erosional surfaces are present, especially within the low angle laminated intervals. Laminated sandstone units are made up of vfl-vfu sand grains and are moderately sorted due to a small percentage (5%) of clay/silt content. Laminations are readily visible, indicating bioturbation is low with BI values ranging from 0-1. Observed trace fossils include *Planolites*, *Phycosiphon*, and *Zoophycos* all from the *Cruziana* ichnofacies (Seilacher, 1967; Gani et al., 2008).

Facies 10: Interpretation

Planar laminated sandstones have been found in various environments and therefore attributed to different processes, such as storm dominated shoreface (Bridge & Best, 1997), shallow marine tempestites (Kerr & Eyles, 1991), and wave-influenced turbidities (Lamb et al., 2008). Most examples of F10 in this study do not exhibit a high BI and therefore are interpreted to be deposited in higher energy environments susceptible to turbidity flow and storm activity, and the presence of low-angle laminations indicates some degree of wave influence.

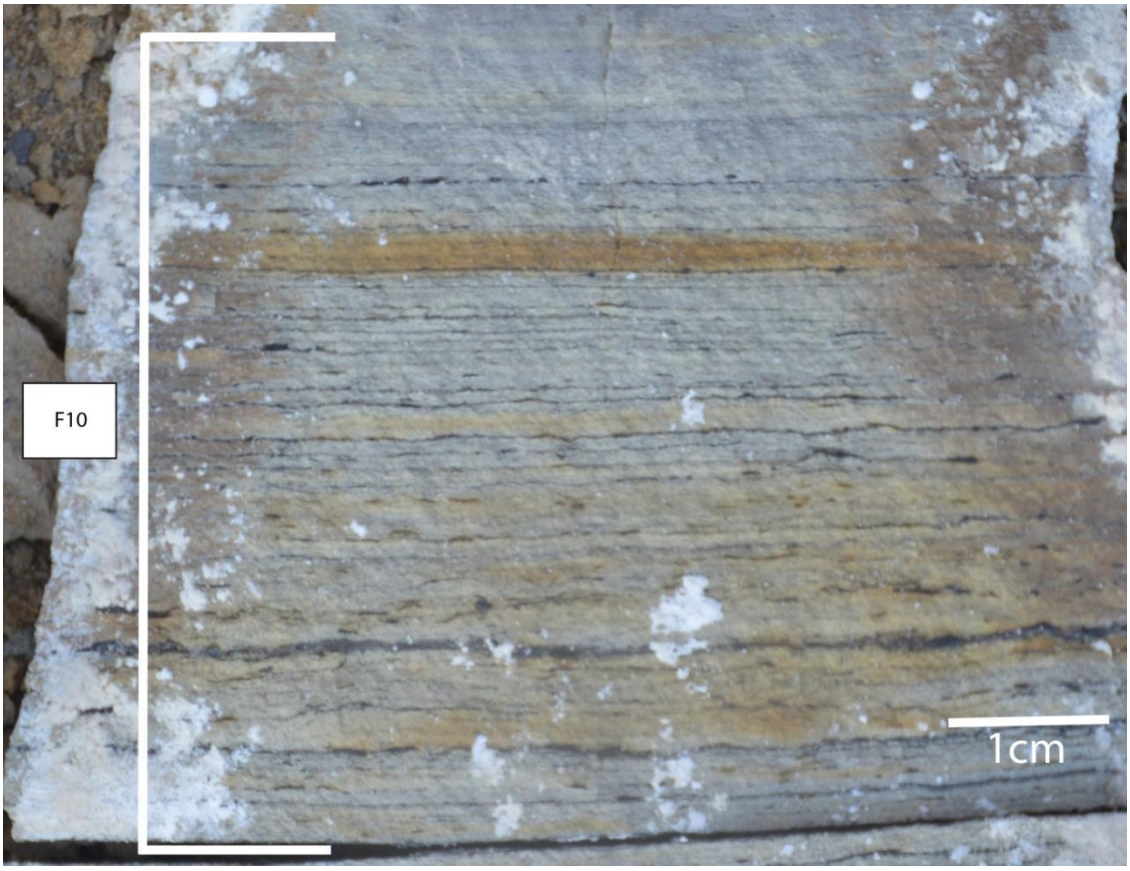

Figure 16. Planar Laminated sandstone facies (F10).

Facies 11: Massive Sandstone

The final sandstone facies (Figure 17) is massive with no evidence of any sedimentary structures. This facies is made up of sand grains ranging from vfl-fL, and is moderately sorted, as there is a

component (1-10%) of clay/silt size grains. Bioturbation is difficult to evaluate within F11 based on its massive nature could have a BI 0 or based on the inclusion of clays and silts could be BI 5. F11 exhibits BI 0. Beds in F11 have a thickness from 1-5cm and have a lateral extent from 0.5-10m.

Facies 11: Interpretation

Massive sandstone is made by rapid sedimentation rates where a turbulent flow moves downslope and rapidly slows to deposit the sediment without any observable sedimentary structures (Walker, 1978). The other possibility is that massive sands were originally deposited with primary sedimentary structures and subsequently bioturbated during times of low energy causing the obscuring of all structures and the mixing of various grain sizes within the unit. No direct evidence of bioturbation or other mixing was present, therefore, F11 is interpreted to be associated with turbidity flows based on the interpreted process of deposition and its occasional association with F10 within the measured sections.

Figure 17. Massive/bioturbated Sandstone facies (F11) overlain by F10. *Ophiomorpha* burrow in top left corner of image. Soft sediment deformation such as ball and pillow structures visible at bottom of the bed.

Facies 12: Guttered Sandstones

This facies (Figure 18) is characterized by a basal erosional scour that gives the base of the sandstone a channelized morphology. The scour surfaces observed within the Sanostee sections have a lateral extent of 1-2m. Gutters in the Rock Ridge section are much smaller, with an extent of 1-5 cm. Gutters are infilled with vf sand and several types of sedimentary structures are observed, most commonly HCS (F9), low angle lamination (F10) as well as occasional combined ripples (F8). The rationale behind separating F12 from F8, F9, and F10 is that every instance of F12 includes one or more other facies however the other facies are found in tabular beds in addition to gutter- fills. The presence of gutters leads to a different interpretation than if the bed

was tabular necessitating separation into a unique facies category. Gutters are filled with multiple stacked event beds separated by erosional surfaces. Bioturbation is low within the guttered facies with BI ranging from 0-1 and *Paleophycus* being the only trace fossil observed. Thickness of the guttered beds varies from 0.7-2m.

Facies 12: Interpretation

The gutter scour is interpreted as being formed by an oscillatory combined flow wave, which erodes previously deposited sediments and creates an elongate scour (Whitaker, 1973; Myrow, 1992). The infilling sand is deposited by subsequent storm waves, usually characterized by waning flow (Whitaker, 1973). Observed HCS distinguishes storm influence, and the lack of bioturbation, both during and post deposition indicates that the environment was never quiescent enough to allow for colonization. The erosive characteristics of gutter 'scour' (Whitaker, 1973) and subsequent fill are associated with storm-deposited tempestites.

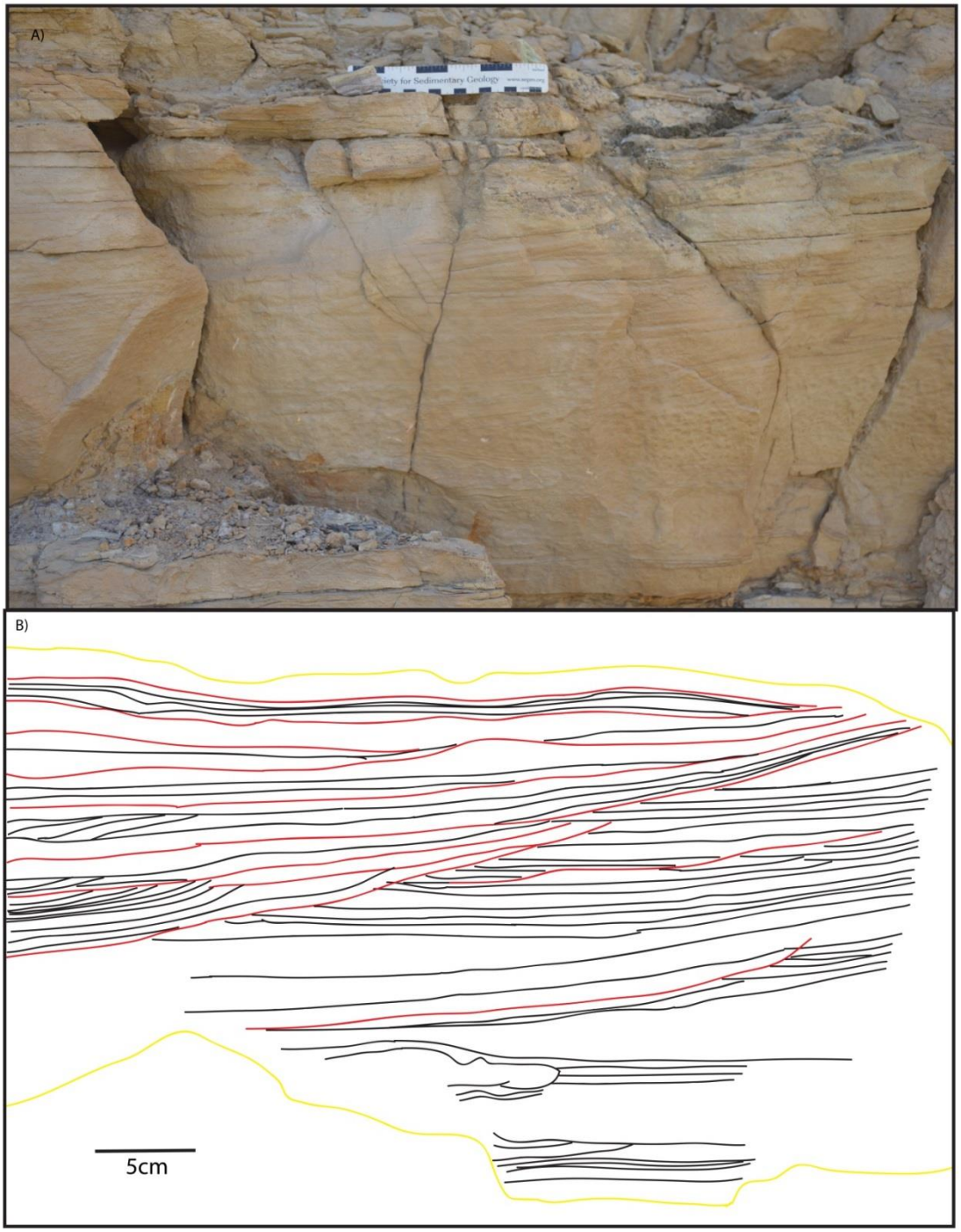

Figure 18. Guttered Sandstone facies (F12). A) One of the largest gutter casts found at Sanostee, analyzed in more detail in Chapter 5, scale ruler is 10 cm; B) Internal bedding structure of gutter. Note yellow surfaces mark sandstone boundary and gutter surface (Basal), red lines indicate erosional surfaces, and black lines indicate bedding surfaces which are truncated by erosional surfaces.

4.1 – Results: Facies Associations

The second part of facies analysis focuses on the stacking or vertical progression of facies in the sections. This is important to determine the dominant processes affecting deposition of sediment within the delta i.e. wave, fluvial, or tidal processes (Ainsworth et al., 2011; Bhattacharya, 2006). In similar studies, various methods have been used to determine facies associations. Collins et al. (2016), in their analysis of the heterolithics of the Baram Delta province, use a three-part classification system, splitting the facies patterns into mudstone dominated, heterolithic dominated, and sandstone dominated. This system specifically refers to the proportion of sand-to-shale within the facies.

Seepersad (2012) opted to identify associations based on the process of deposition in the heterolithics of the Ferron sandstone facies. Associations were classified into ignitive turbidites, hyperpycnites, tempestites, and sustained hyperpycnites/turbidites. Both methods have their uses with the Collins et al. (2016) method related to determining net-to-gross, important for reservoir classification, while process of deposition are key for determining the processes affecting the delta. Therefore, in this study, the process of deposition was determined for common associations, which included: ignitive turbidites, hyperpycnites, and tempestites. Facies associations were also classified based on the sand-to-shale ratio with the facies being broken down into; sandstones, mudstones, or heterolithics based on the percentage of sand present.

In this study, facies commonly associated with tempestites were F2, F6, F8, F9, F10, and F12. Tempestites followed a general progression from one of F12/ F10/F9 into F8, F6, F5 and some

would terminate in F2 before an increase in grain size would be observed indicating the following association. A typical progression is shown in Figure 19.

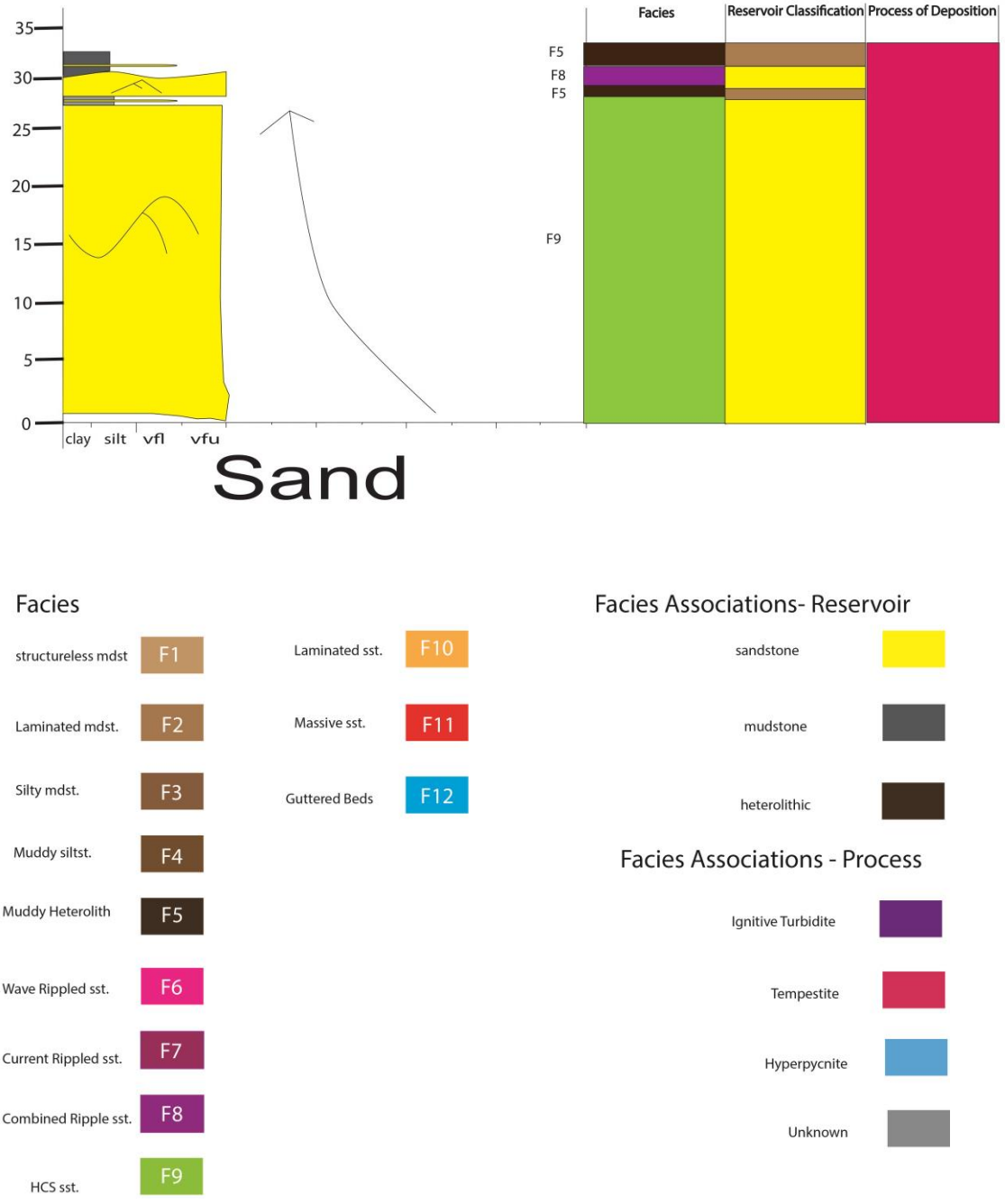

Figure 19. Tempestite facies association. Vertical scale is in centimeters. Legend with facies and association descriptions. For symbols see legend in Figure 22.

Several different types of turbidites have been described: ignitive and non-ignitive. Ignitive turbidites refer to those caused by a sudden input of force resulting in sediment failure such as an earthquake (Mulder & Syvitski, 1995; Mulder & Alexander, 2001; Mulder et al., 2003). Non-ignitive can refer to processes that are not sudden and more sustaining, meaning that non-ignitive turbidity flows can last longer e.g. hyperpycnal plumes, sometimes up to weeks; while ignitive turbidity flows only last up to a few hours (Mulder et al., 2003).

In this study the facies progression associated with ignitive turbidites are F11 intoF10, F6/F7/F8 and then grades into F2, F1 (see Figure 20) following a model similar to a traditional Bouma sequence showing normal grading due to waning flow (Bouma, 1962; Lowe, 2012; Stacey & Bowen, 1990).

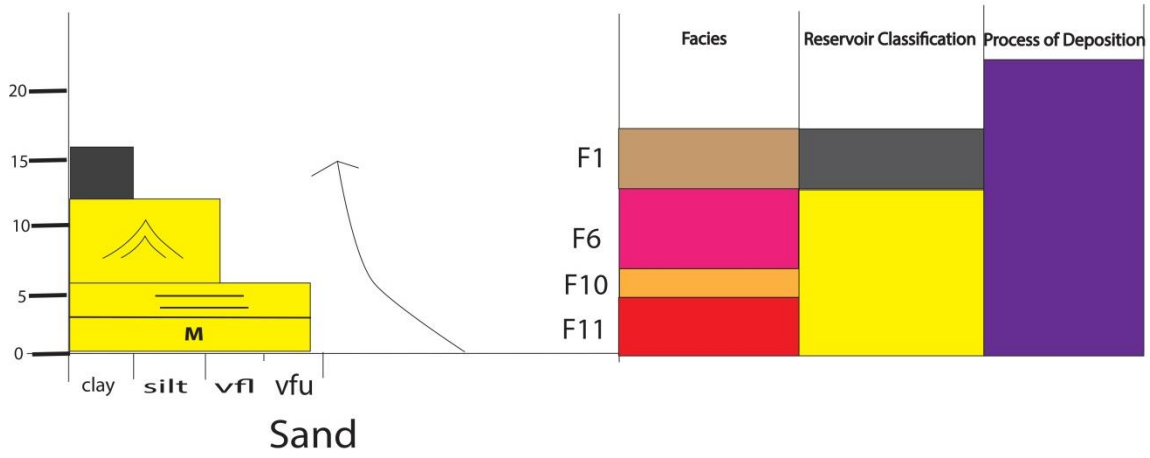

Figure 20. Facies Association of a typical turbidite deposit observed at Sanostee and Rock Ridge. Vertical scale is in centimeters.

In this study, hyperpycnites are identified by the presence of inverse grading (Bhattacharya & MacEachern, 2009; Mulder et al., 2003). Other facies found within this association were F1, F2, F3, F4, and F5 where contacts between the mud-dominated and sand-dominated beds were

graded instead of sharp, indicative of a hyperpycnal flow rather than an ignitive turbidity current. An example of a typical hyperpycnal facies progression observed in this study is shown in Figure 21.

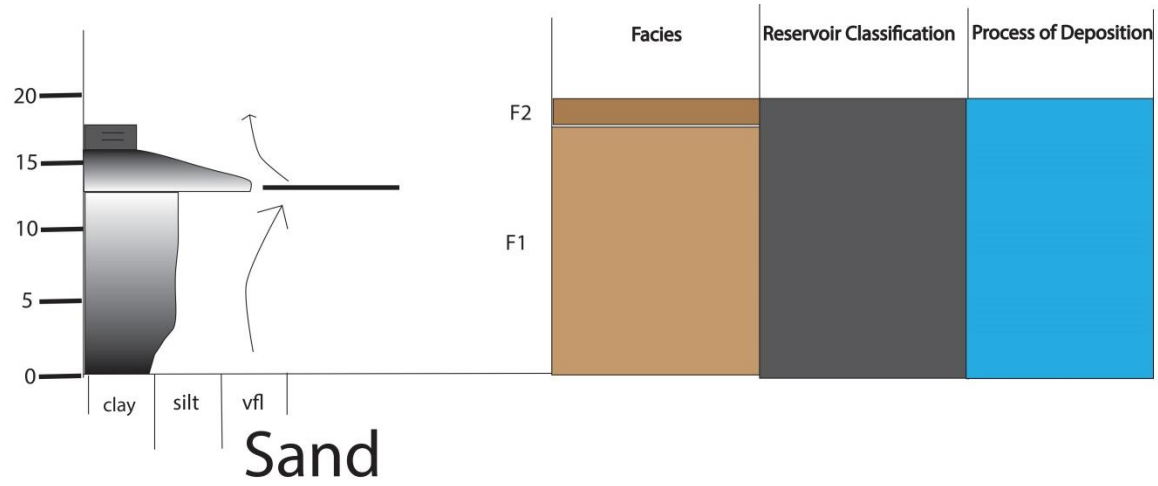

Figure 21. Hyperpycnite Facies Association. Vertical scale is in centimeters.

The second facies associations detailing lithology in terms of the sand-to-shale ratio (Collins et al., 2016) divides each interval into mudstone, heterolithics and sandstone. This classification quantifies net-to-gross within each measured section. Heterolithics are differentiated from sandstones based on the thickness and abundance within the interval. Laterally continuous sandstones, with a thickness of 5cm or less, are not classified as the sandstone facies association. These units are found in between mudstone facies therefore these intervals are considered to be part of the heterolithic facies association. Mudstone dominant units with starved ripples or sandy laminae (>2cm) were included in the heterolithic association, based on their sand content. Intervals classified in the mudstone facies association have no sand content and are made up exclusively of F1, F2, F3, and F4 (F2 only if laminations are silt grains). The sandstone facies

association is sandstone beds of 5cm or greater and often are made up of multiple stacked sandstones, mostly of facies F6, F7, F8, F9, F10, F11, and F12.

Chapter 5 – Results: Measured Sections, Net-to-Gross, Process of Deposition, and Correlations

The following sections display primary data collected, including measured sections and paleocurrents, as well as analysis and interpretations with facies associations and bedding diagrams.

5.1 - Sanostee

5.1.1 – Sections

In the measured sections two types of facies associations were distinguished based on: 1) the lithology of the association ; sandstone, mudstone, or heterolithic, and, 2) the process of deposition; turbidite, tempestite, hyperpycnite, or unknown (Li, et al., 2015; Snyder et al., 2016). This helps quantify the amount of influence each of the processes outlined in the coastal process classification plots model of Ainsworth et al. (2011) have within the Gallup delta.

Section 1 (S1) is 2.78m in length and is on the most southeasterly side of the exposure. The bioturbation index (Figure 22) in S1 varies from 0-3, though the majority of beds have a BI of 0-1. There are scattered intervals of BI 2, concentrated in mudstone beds (F1-F4, and F14-F15). Trace fossils observed in S1 include *Planolites, Phycosiphon, Chondrites,* and *Paleophycus,* which are included in the *Cruziana* ichnofacies (Pemberton et al., 1992).

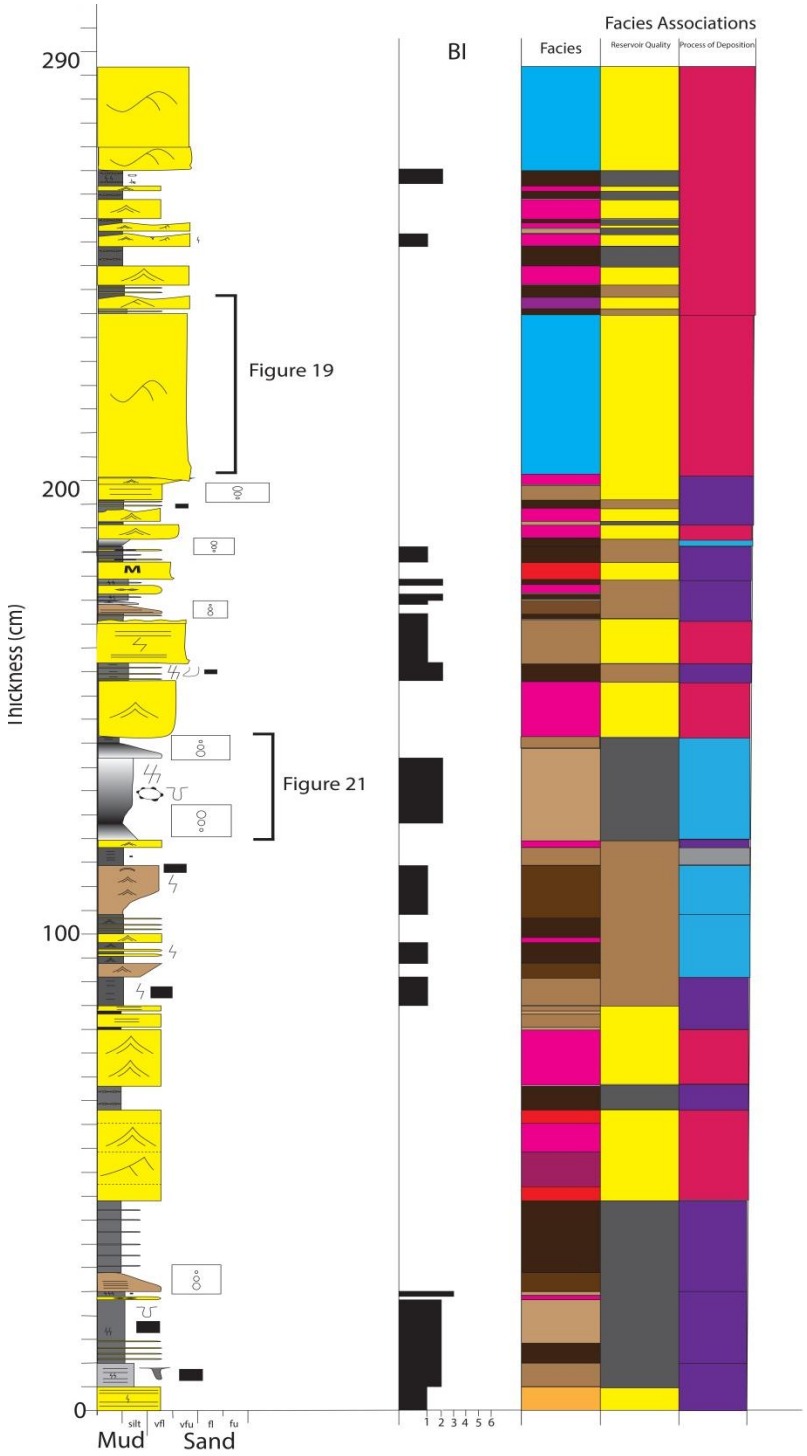
Facies Associations
BI
Facies
Reservoir Quality
Process of Deposition
290
200
100
0
Thickness (cm)
Figure 19
Figure 21
M
silt
vfl
vfu
fl
fu
Mud
Sand
1 2 3 4 5 6

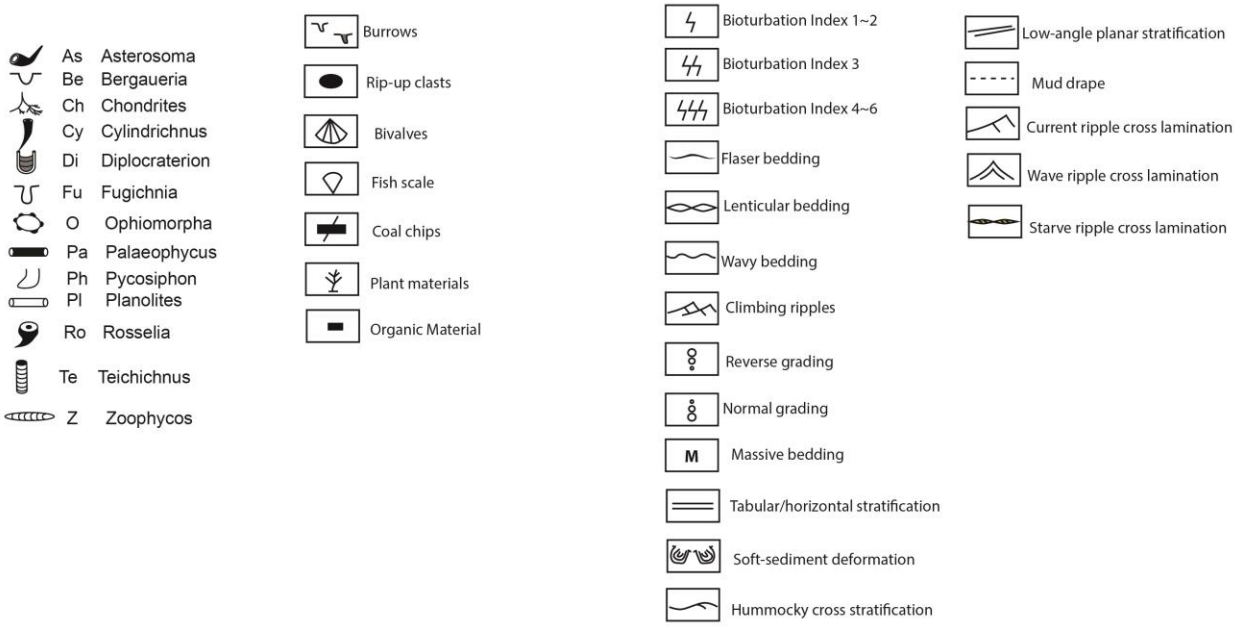

Figure 22. Sanostee Section 1 (S1) with symbols legend, for facies legend refer to Figure 19.

In S1, the facies breakdown shows that the most common facies within this section is F12, with 27% of the section being made up by this facies (Figure 23). Muddy heterolithics and wave-rippled sandstones make up a combined 42% of S1 (Figure 23).

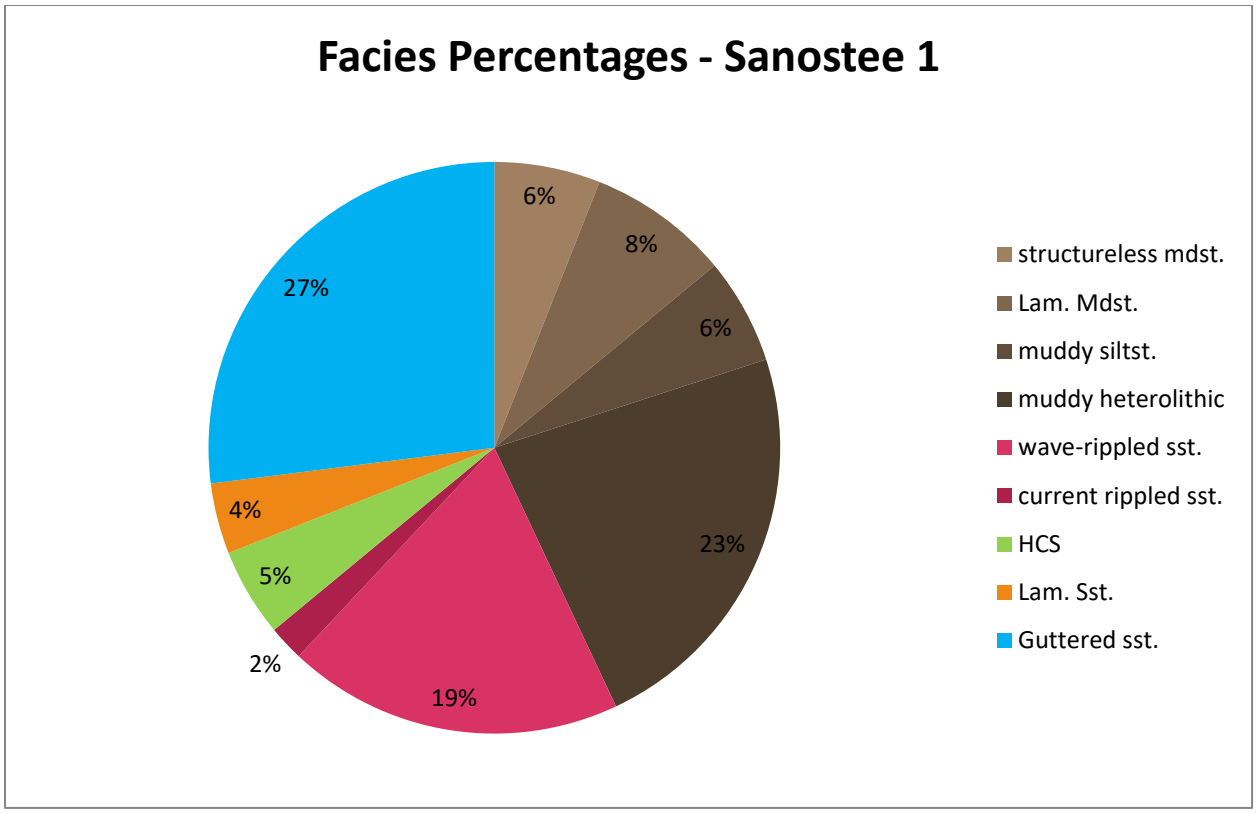

Figure 23. Facies percentages from section S1. Percentage reflects the total percent each facies accounts for the within the entire section.

Sand-to-shale analysis shows that S1 is made up of 50% sandstone, 26% mudstone and 24% heterolithics (Figure 24). Heterolithic intervals are defined by facies successions that are made up of F4, F3, F2, and F1 with minimal sandstone makeup, where sandstone beds do not exceed 2cm in thickness and are vertically discontinuous and separated by mud dominant intervals.

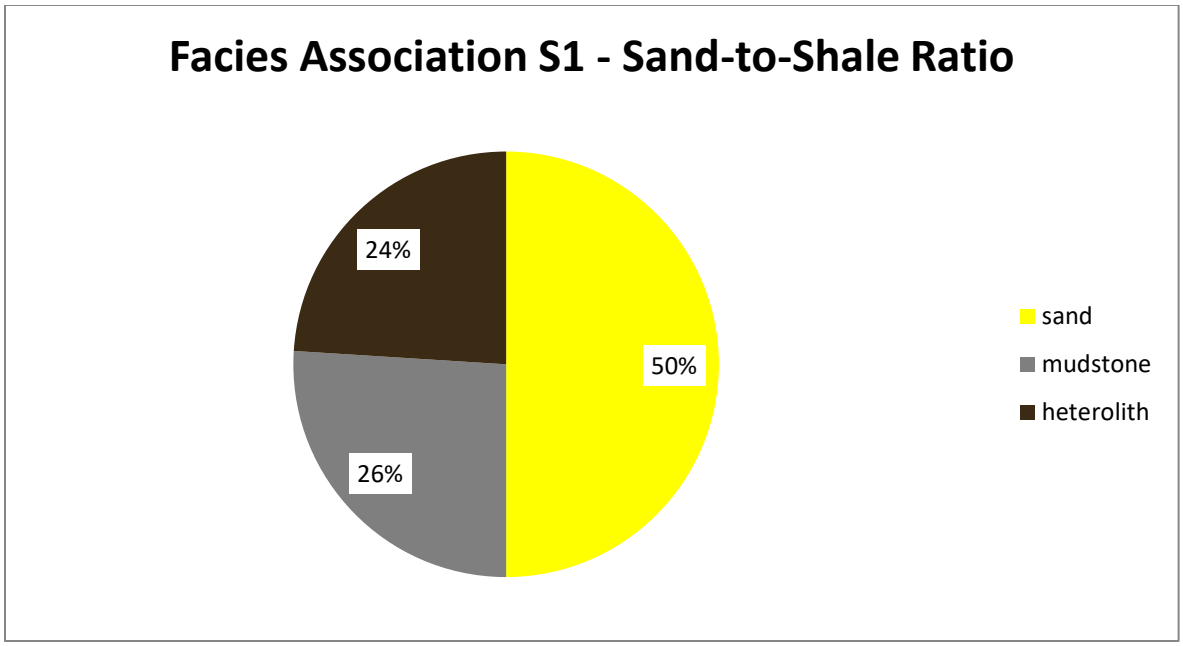

Figure 24. Facies associations based on sand-to-shale ratio from section S1.

In S1, the dominant process of deposition was found to be storm-deposited tempestites, making up 46% of deposits (see Chapter 4 for detailed description of the observed facies succession). Turbidites make up 35% of S1. The remaining 19% is made up of river induced hyperpycnal flows (18%) and 1% is of unknown origin. The unknown facies association is made up of mud dominated beds with variable levels of bioturbation that do not fit into the facies successions stratigraphically above or below the bed in question.

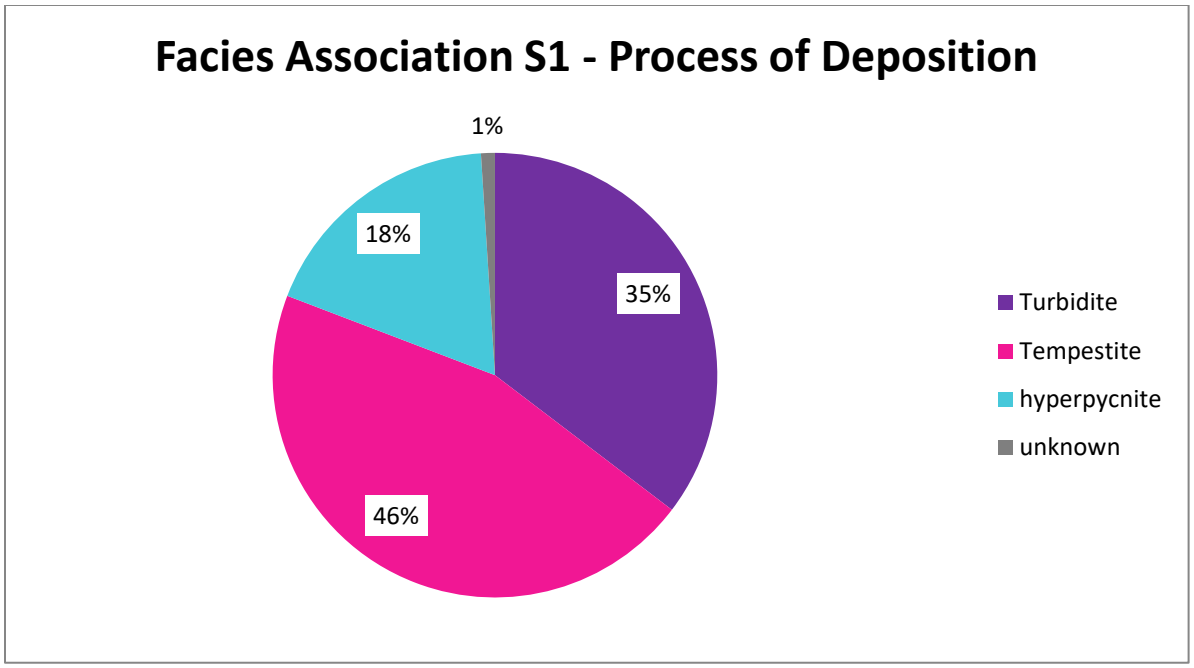

Figure 25. Facies associations for the entire section based on the process of deposition and influence; wave, fluvial, storm-wave.

Located in the middle of the exposure, S2 is similar in physical characteristics to S1 as it contains the guttered facies. Rare body fossils are observed within this section. Some of the mud-dominated units, F1 and F3, have abundant organic material present on bedding surfaces. Presence of mud drapes within some of the sandstones is recorded, and was not observed in S1 and found to be especially abundant within some of the guttered sandstone facies.

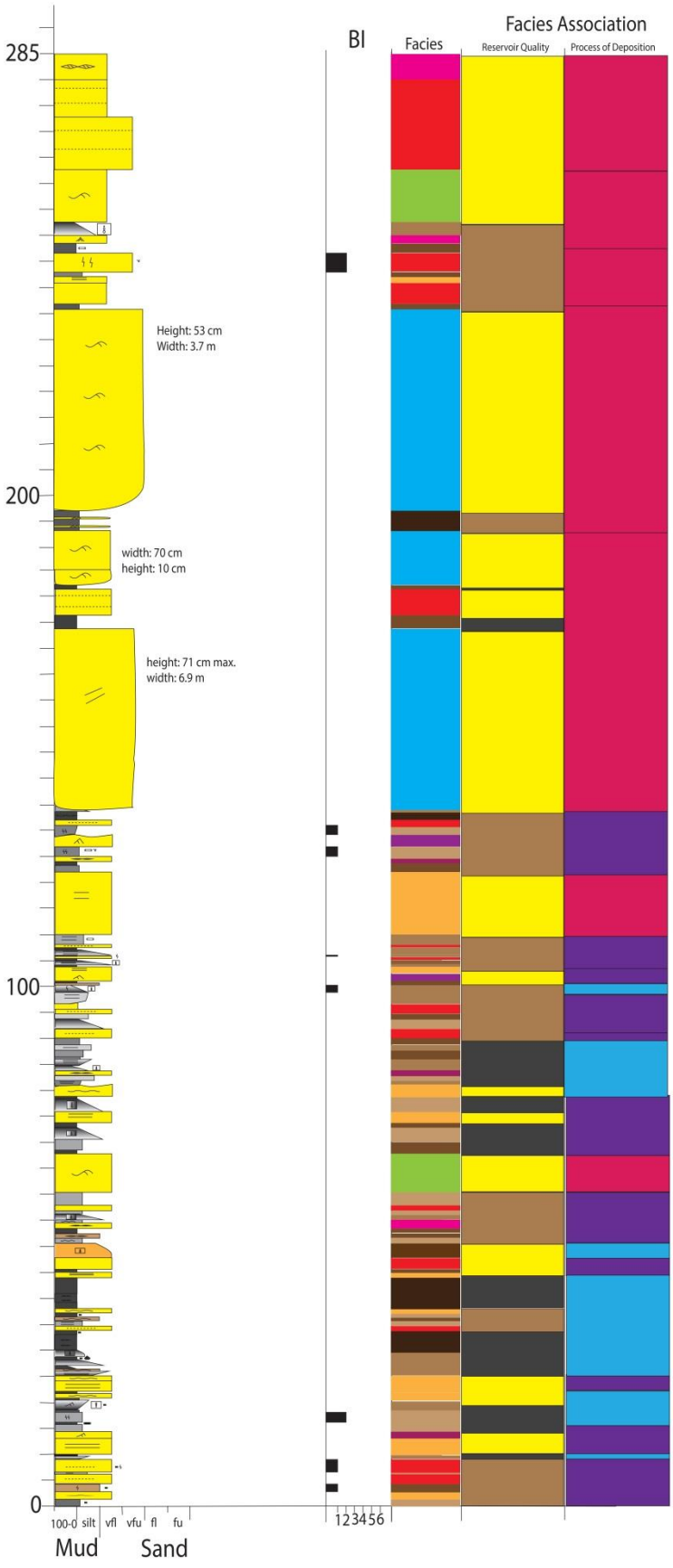
285
200
100
0
Height: 53 cm
Width: 3.7 m
width: 70 cm
height: 10 cm
height: 71 cm max.
width: 6.9 m
BI
Facies
Facies Association
Reservoir Quality
Process of Deposition
100-0
silt
vfl
vfu
fl
fu
1 2 3 4 5 6
Mud
Sand

Figure 26. Section S2 from Sanostee located 8.5m from S1 and 5m from S3.

Facies analysis demonstrates that the most common facies observed within S2 is F12 making up 29% of the section. Following F12 are F10 and F9, which make up 22% and 10% respectively. None of the other 10 facies observed within S2 exceed 10% (see Figure 27).

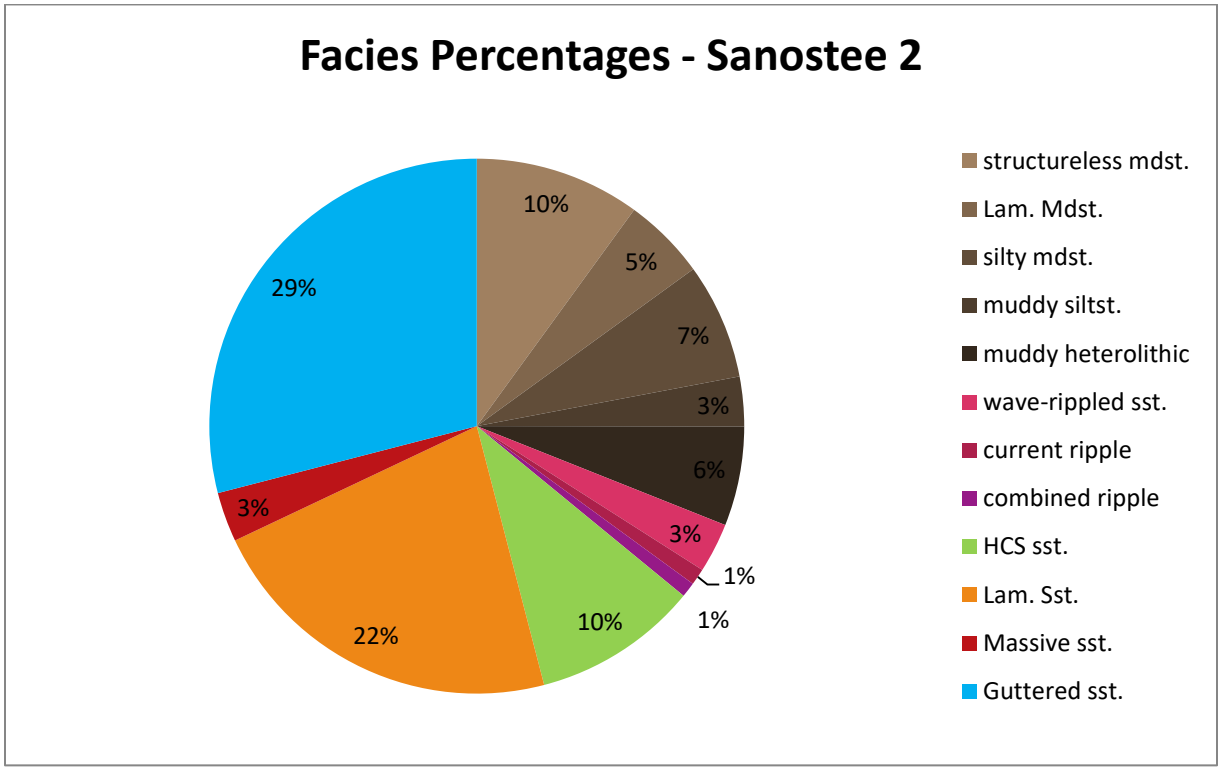

Figure 27. Facies percentage breakdown for section S2.

Sand content is slightly higher within S2 in comparison to S1, with 56% of the section being classified as sandstone (See Figure 28). Heterolithic reservoir units make up 29% of the section while the remaining 15% is mudstone.

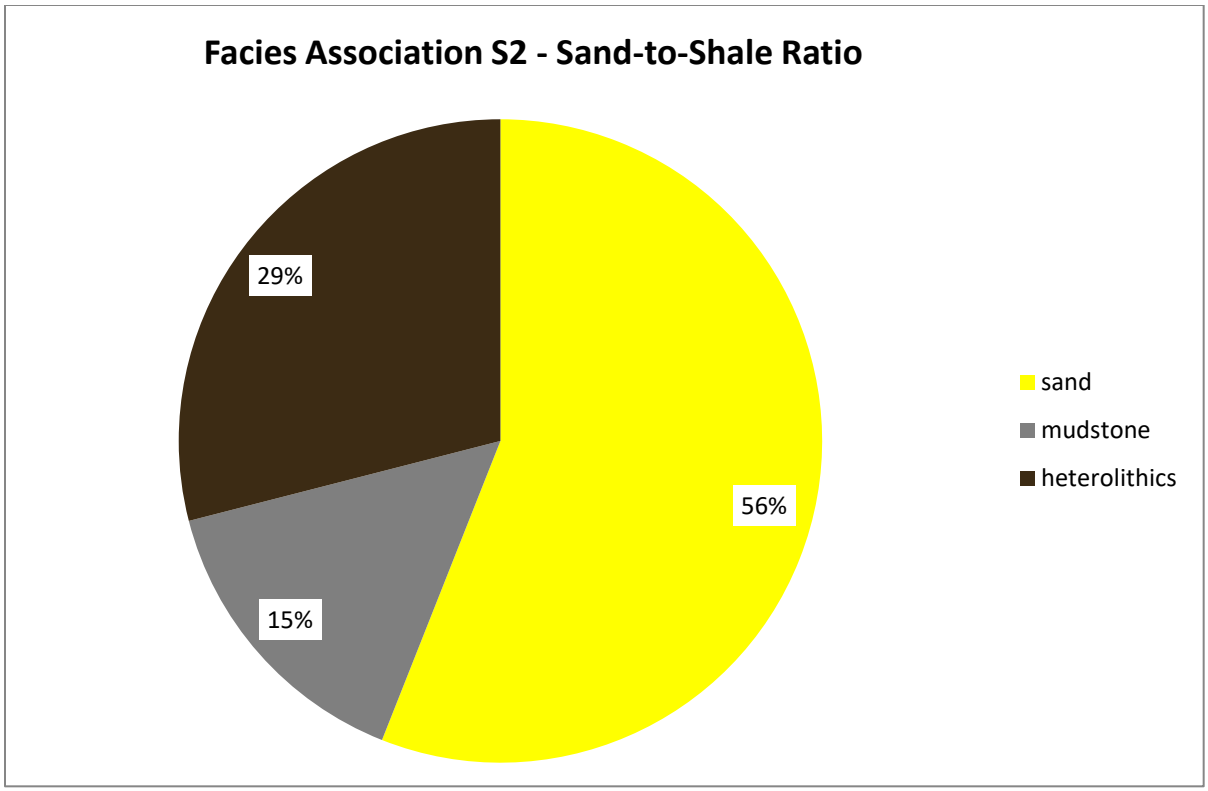

Figure 28. Facies association in terms of sand-to-shale ratio from S2.

The process of deposition has a similar breakdown to S1, where 53% of the section is interpreted to be deposited by tempestites. The second most prevalent process of deposition are turbidites accounting for 24% of the vertical section, with the remaining 22% being made up of hyperpycnites and 1% unknown origin possibly hypopycnal plumes.

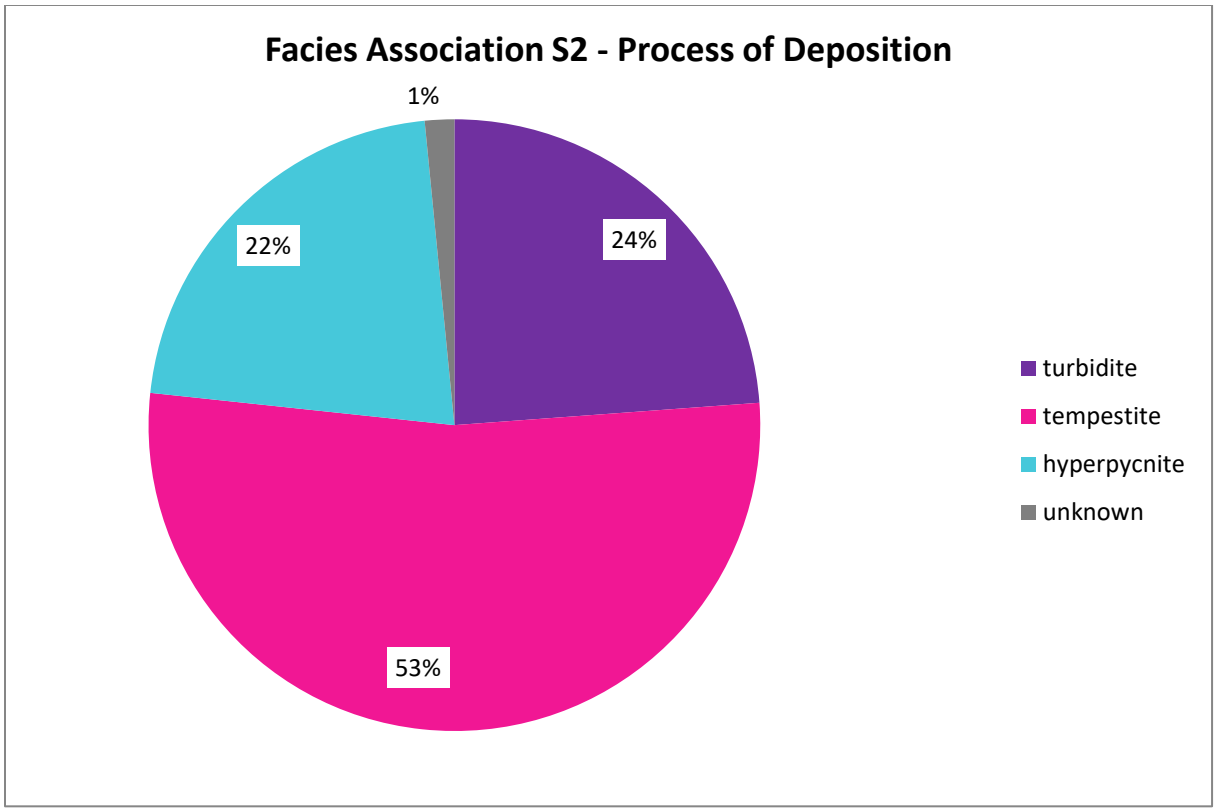

Figure 29. Facies associations based on process of deposition and relative influence of each process.

Total height of S3 is 2.8m (Figure 30). Bioturbation is much more prevalent throughout S3 in comparison to S2; however the range is the same as S1 and S2 varying from 0-3. Fish scales, organic matter, and shell fragments are observed on the bedding planes of some mud-dominated beds (F1 and F2).

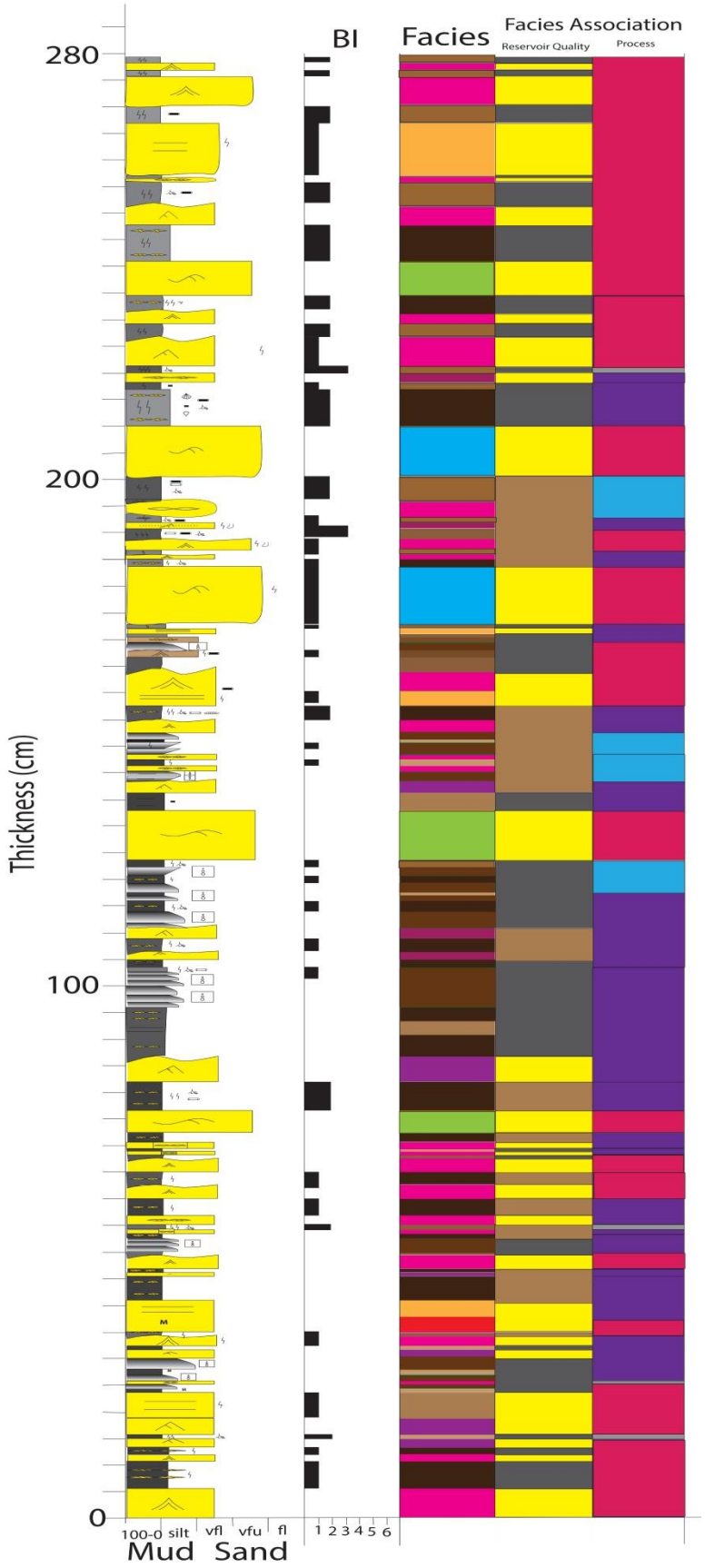
BI
Facies
Facies Association
Reservoir Quality
Process
280
200
100
0
Thickness (cm)
100-0 silt
vfl
vfu
fl
1 2 3 4 5 6
Mud
Sand

Figure 30. Section S3 from Sanostee, located 5m from S2. Legend in Figures 19 & 22.

Facies analysis shows a stark contrast from S2 and S1 with a much smaller proportion, 13%, of facies being attributed to F12 (see Figure 31). The two most prevalent facies are wave-rippled sandstone, 19%, and muddy heterolithic, 19%. No one other 9 facies observed exceed more than 8% of the total section.

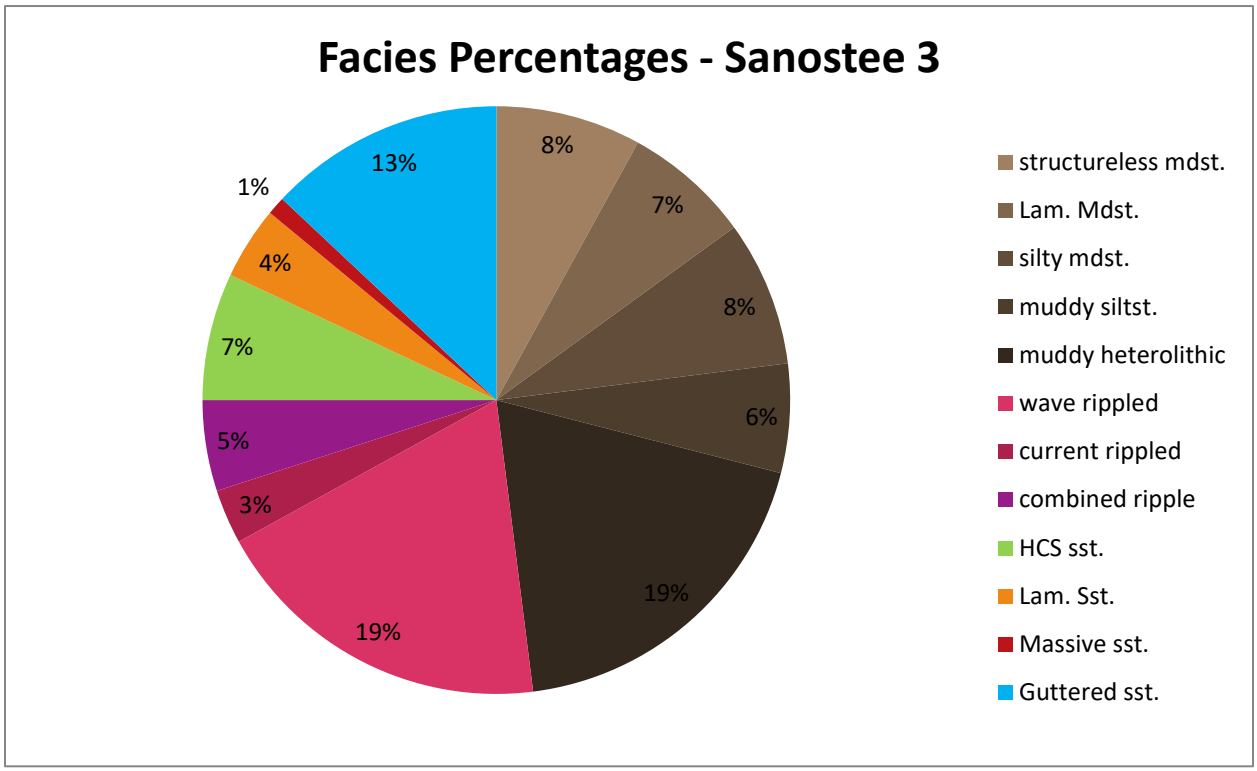

Figure 31. Facies percentages from S3.

The breakdown of the sand-to-shale ratio for S3 also differs from S1 and S2 with only 41% of the section being characterized as sandstone, with 39% shale, and 20% heterolithics.

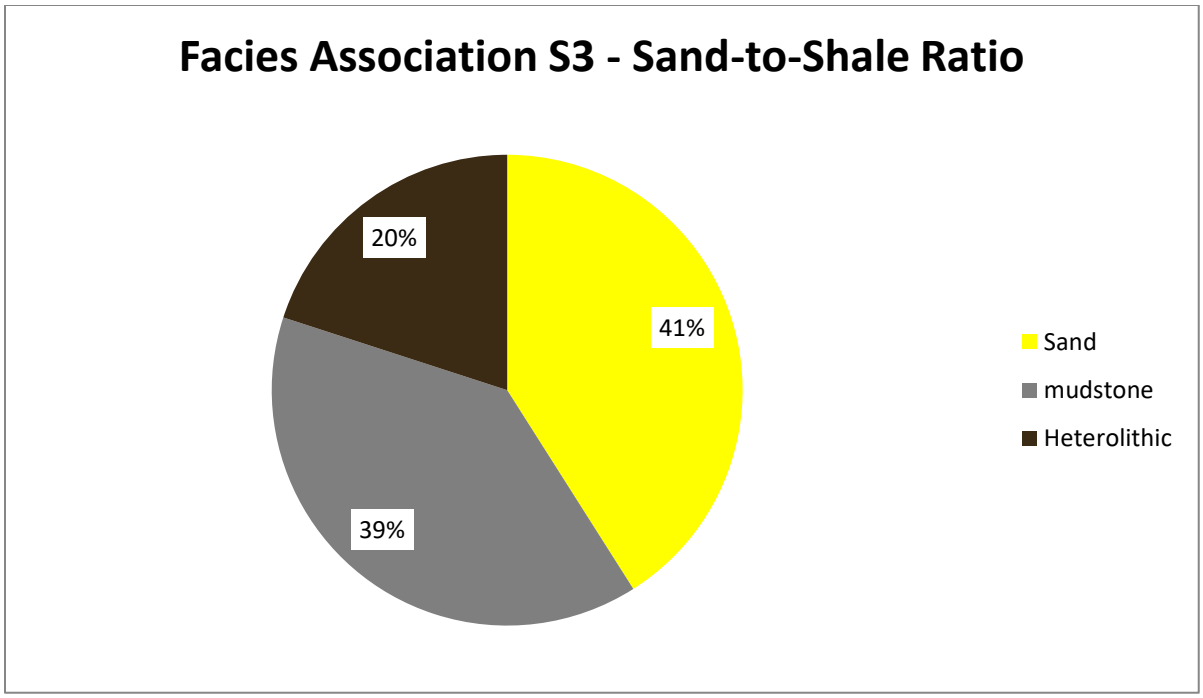

Figure 32. Facies association of the sand-to-shale ratio for S3.

In S3, similar to the other sections, tempestites make up the greatest percentage with 48%. Turbidites make up 40%, and hyperpycnites 8%.

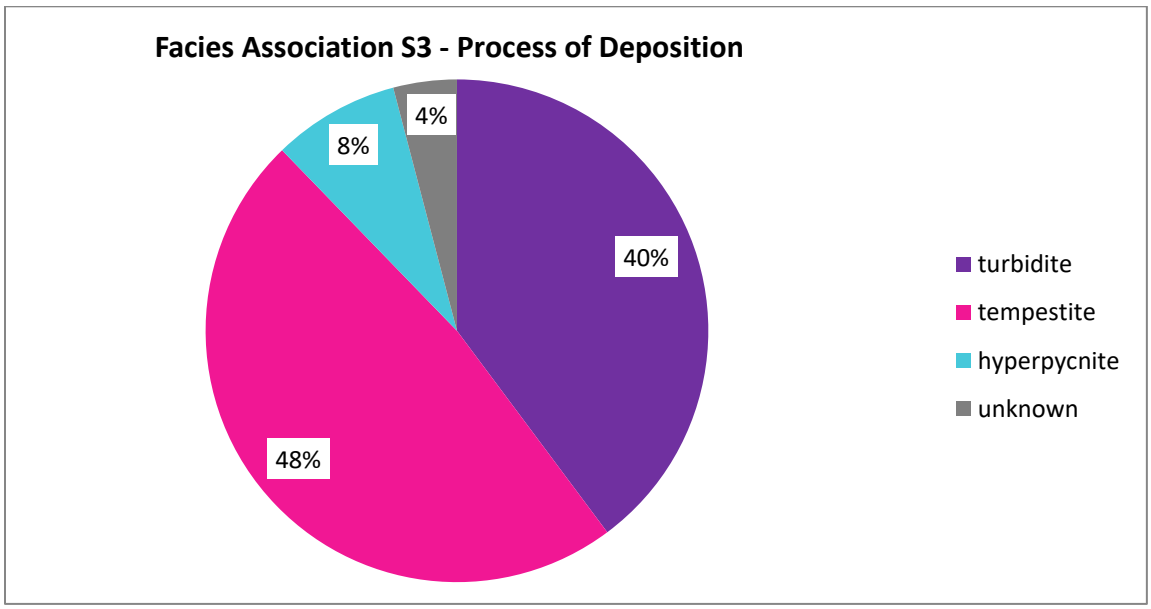

Figure 33. Facies associations based on process of deposition for S3.

5.1.2 – Sandstone Dimensions

Analysis of sandstone dimensions is done by comparing the thickness to width (i.e. lateral extent), in order to determine if there is a correlation between the two parameters, which is important to determine reservoir quality. The type of analysis presented here amplifies the importance of outcrop studies of such heterolithic intervals, as the average thickness of sandstones in the Sanostee exposure is 0.078m, which is below the resolution of typical logging tools (Passey, 2006a).

Figure 34 depicts the relationship between width and thickness of the sandstones measured at Sanostee. Three distinct clusters are observable, the first being located in the lower left corner of the graph depicting thin sandstones with a low lateral extent; the second in the lower right corner being made up of sands with a small thickness but a high lateral extent. The third cluster is made of sandstones with a high thickness and high lateral extent. The variation between the three clusters leads to a low R^2 value of 0.17.

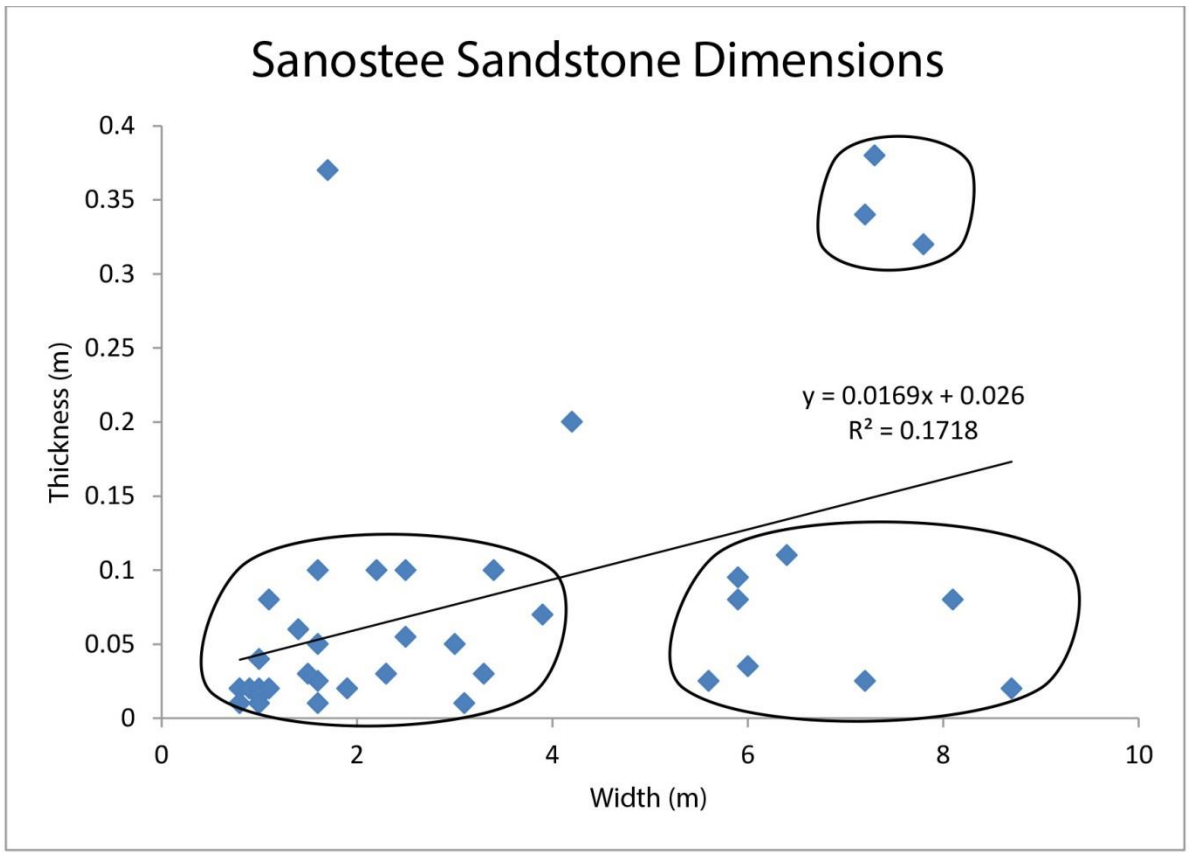

Figure 34. Scatterplot of width versus thickness of the sandstones at Sanostee. The R^2 value is 0.17, showing low correlation between thickness and width.

5.1.3 – Gutter Cast Analysis

Analysis of the gutter casts, found at Sanostee, includes a bedding diagram delineating the surfaces within and a plot of the dimensions. From Figure 18a, the internal structure is clear and undisturbed by bioturbation, which is common for the gutters observed. From the bedding diagram it is clear that there are numerous surfaces within the gutter. Multiple erosional surfaces which crosscut lower order depositional surfaces are visible, such as off lap surfaces towards the outer edges of the gutter, as well as top truncation and onlap surfaces on the right-hand side.

The plot of gutter cast dimensions (Figure 35) describes the relationship between the vertical thickness and lateral extent of these sandstones. Gutter size varies by an order of magnitude, with the smallest observed gutter being 2.5cm x 18cm, and the largest 71 cm x 690cm. Despite this large variation, the R^2 value of the plot is 0.71 indicating a strong correlation between the thickness and lateral extent of gutter casts.

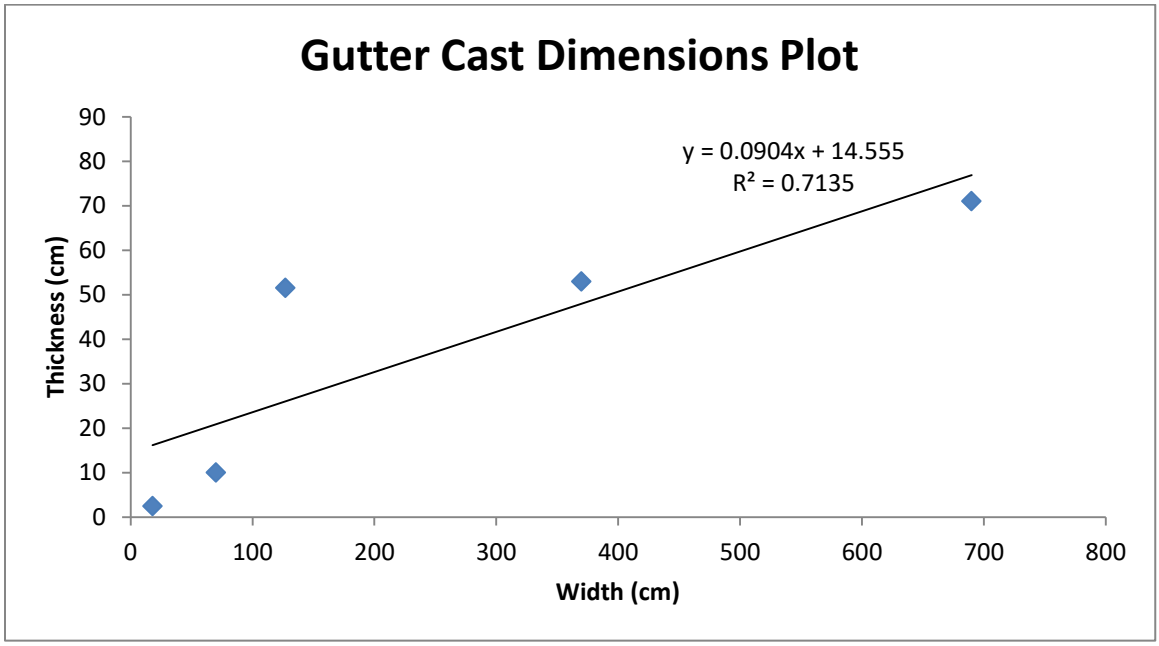

Figure 35. Scatterplot of gutter cast dimensions at Sanostee, width versus thickness, measured in centimeters. The R^2 value is 0.71.

The long axis of each gutter with an exposed basal surface was measured to determine the orientation of the cutting flow. Figure 36 shows a rose diagram with 7 measured orientations. The trend is in a northeasterly direction, with values ranging between 22^0NE – 96^0 SE.

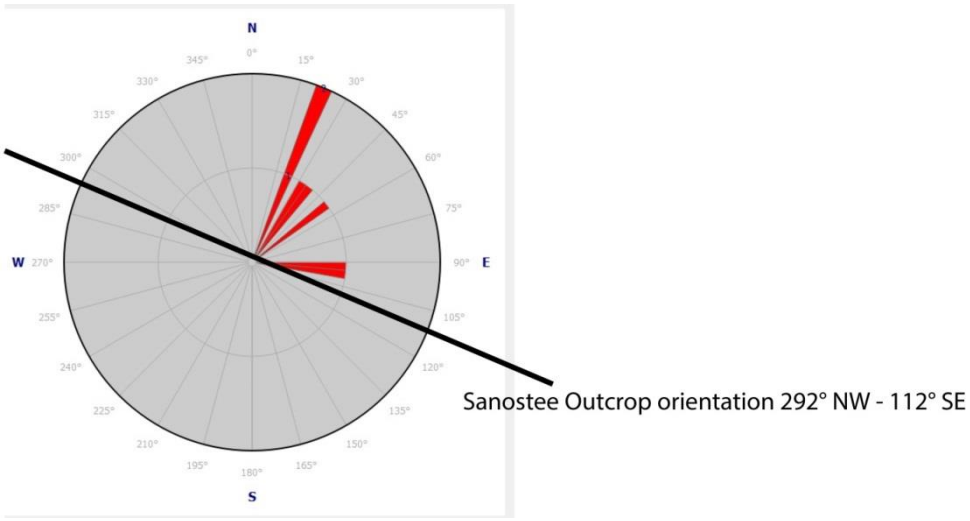

Figure 36. Gutter cast orientation based on scour surface measurements. N=7.

5.1.4 - Paleocurrent Analysis

Twenty paleocurrent measurements were taken at Sanostee, within sandstone beds with wave-ripple or current ripple laminations large enough to obtain an accurate compass reading. The overall trend observed is the dominant current trending 272^0 SW for current ripples (see Figure 37a) and in a northwest southeast direction for wave ripples (see Figure 37b). The outcrop shown in Figure 36, 37a, and b is oriented in the along-strike direction and matches regional paleoshoreline orientation (Molenaar, 1973, 1974, 1983). A northwest-southeast paleoshoreline is supported by the gutter cast orientations (Figure 36) with long-axes oriented perpendicular to the shore. Current ripple foresets and wave-ripple crests are oriented at slightly more oblique angles to the paleoshoreline indicating potential oblique wave approach, consistent with the asymmetric delta model.

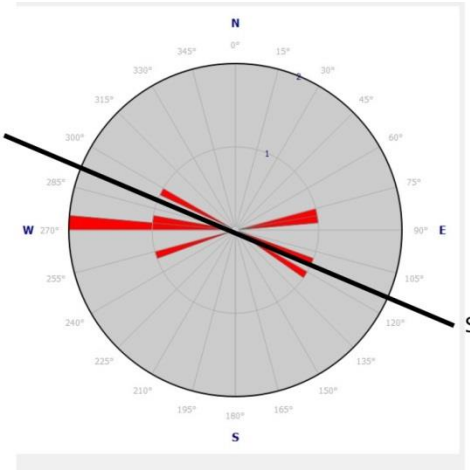

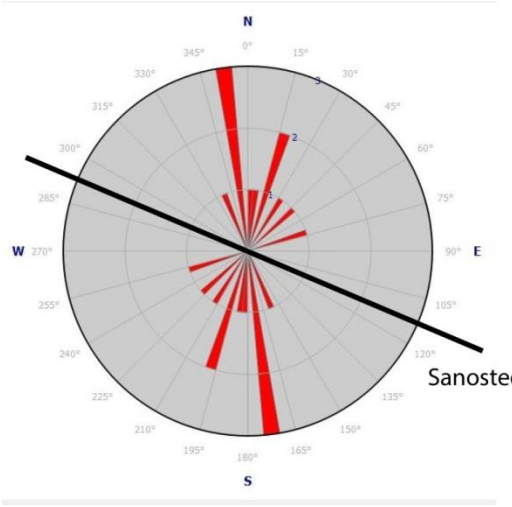

Figure 37. Paleocurrent analysis at Sanostee. A) Current ripple foresets, N=9, B) wave-ripple crests, N=10. Outcrop is oriented northwest-southeast.

5.1.5 – Correlation Panel

In Figure 38 the lateral continuity of the sandstones is documented. The facies transition from guttered sandstones, on the southeastern side of the panel, transitions to more tabular beds on the northwestern side. Thicker sandstones are found within the guttered facies, as shown in Figure 18 as well. The thinner sandstones on the northwestern side of the panel have a lower lateral extent (see Figure 38 b and c) than the guttered facies to the southeast. These thinner sands do not correlate much beyond 5m, whereas sandstones within the guttered facies can be correlated between multiple sections, S1 and S2, which are 8.5m apart. Two types of sandstone contacts are drawn in the correlation panel: red and black. These represent different types of surfaces within the interval. Black lines represent each separate sand bed, defined as an individual time of deposition corresponding to the scale of the measured section. Red lines indicate scour surfaces that were subsequently infilled by sand and mud units. These erosive surfaces crosscut depositional surfaces and are, in some cases laterally extensive between S1 and S2. The major erosive surface within S1 terminates (i.e. is crosscut) by the erosive surface within S2, indicating the cut in S2 and therefore subsequent fill is younger than S1.


NW
SE
5m

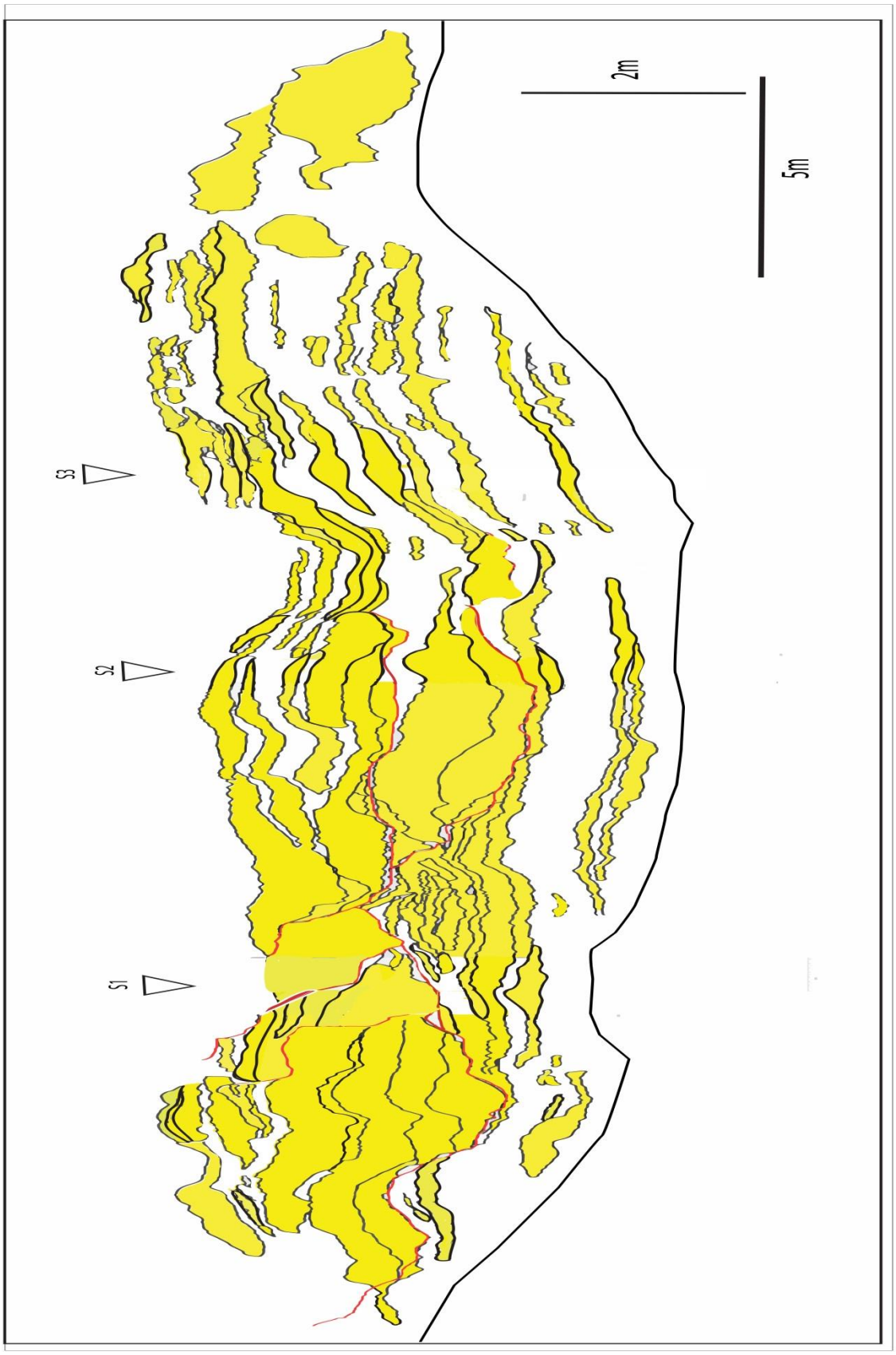
2m
5m
S3
S2
S1

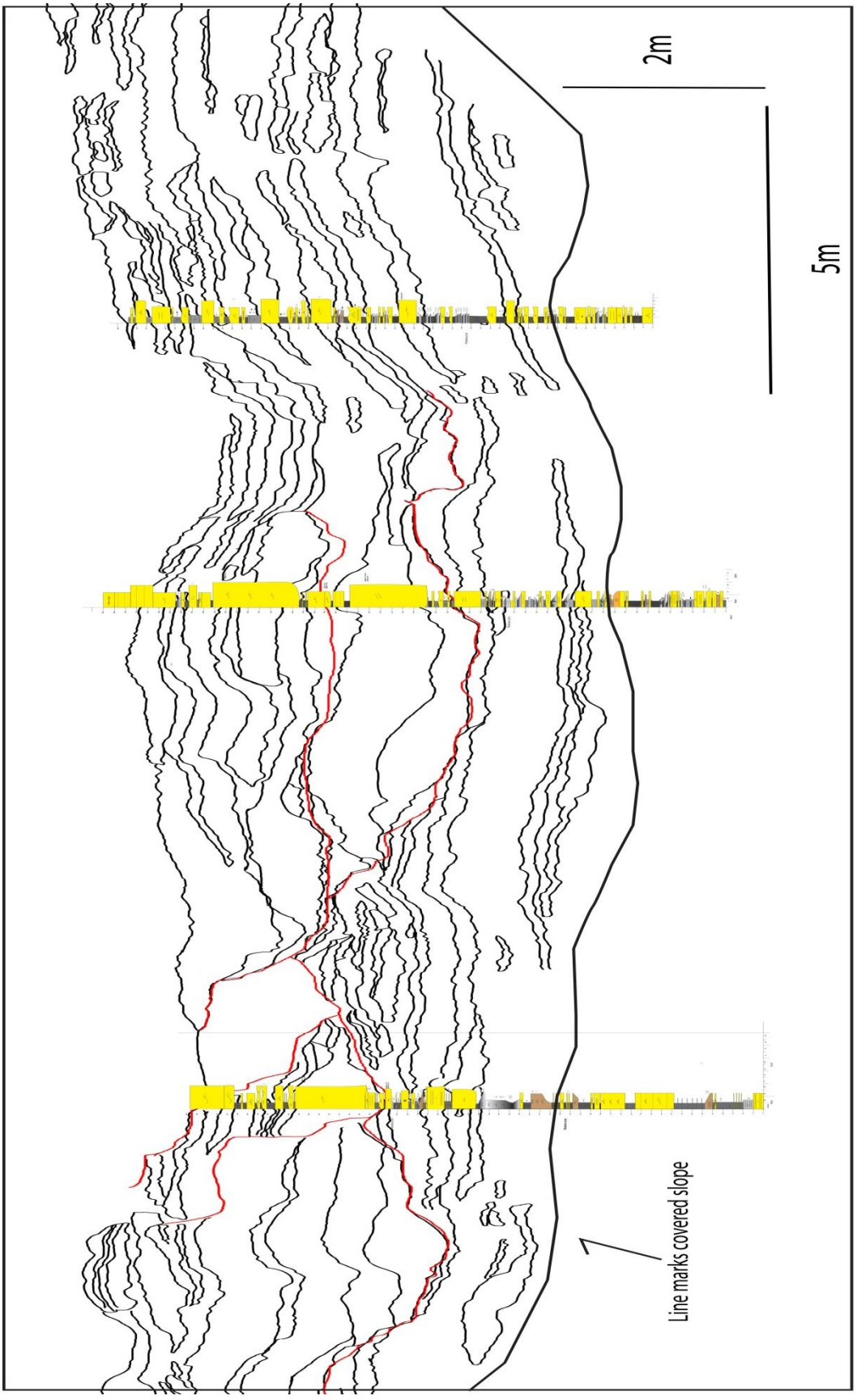
2m
5m
Line marks covered slope

Figure 38. Correlation panel of Sanostee. A) GigaPan photomosaic of Sanostee heterolithic exposure. Red box outlines the area that is analyzed in B, B) Sandstone diagram and correlation with measured sections (left to right) S1, S2, S3 labelled and associated sandstone contacts, C) Correlation diagram between sections S1, S2, S3. Red lines indicate scour surfaces formed by cutting erosive currents. Black lines indicate depositional surfaces which can be sandstone-shale or sandstone-sandstone contacts. Continuous line at base of correlations indicates the covered slope.

5.2 – Rock Ridge

5.2.1 – Sections

Two sections were taken at Rock Ridge (RR1 and RR2) separated by a distance of 10m. The outcrop at Rock Ridge is oriented slightly northeast-to-southwest with the exposure being at an oblique angle to the interpreted regional paleoshoreline (Campbell, 1979). Section RR1 was taken at the southwestern tip of the outcrop and RR2 10m to the northeast. The outcrop is made up of parasequences 3 and 4 (see Figure 7; Lin and Bhattacharya, 2017) and is the thickest package of exposed heterolithics observed with RR1 being 7.1m and RR2 6.8m. Both RR1 and RR2 exhibit coarsening upwards trends with increasing sand content towards the top of each respective section. Sandstone beds have both flat and guttered bases. Bioturbation is low, with BI ranging from 0-3, however most beds within RR1 do exhibit some degree of ichnological activity. Common trace fossils observed include: *Planolites*, *Chondrites, Zoophycos, Paleophycus, Ophiomorpha, Fugichnia*, and *Phycosiphon*. Bioturbation is more consistent throughout the entirety of RR1, while RR2 has a distinct increase in bioturbation following HCS sandstone 2.4m up the section. Both sections have a distinct HCS sandstone bed halfway up that corresponds to an overall increase in grain size compared to lower down in each (see Figures 39/40). Above this bed, sandstones jump from vfl-vfu to vfu-fu and increase in overall thickness.

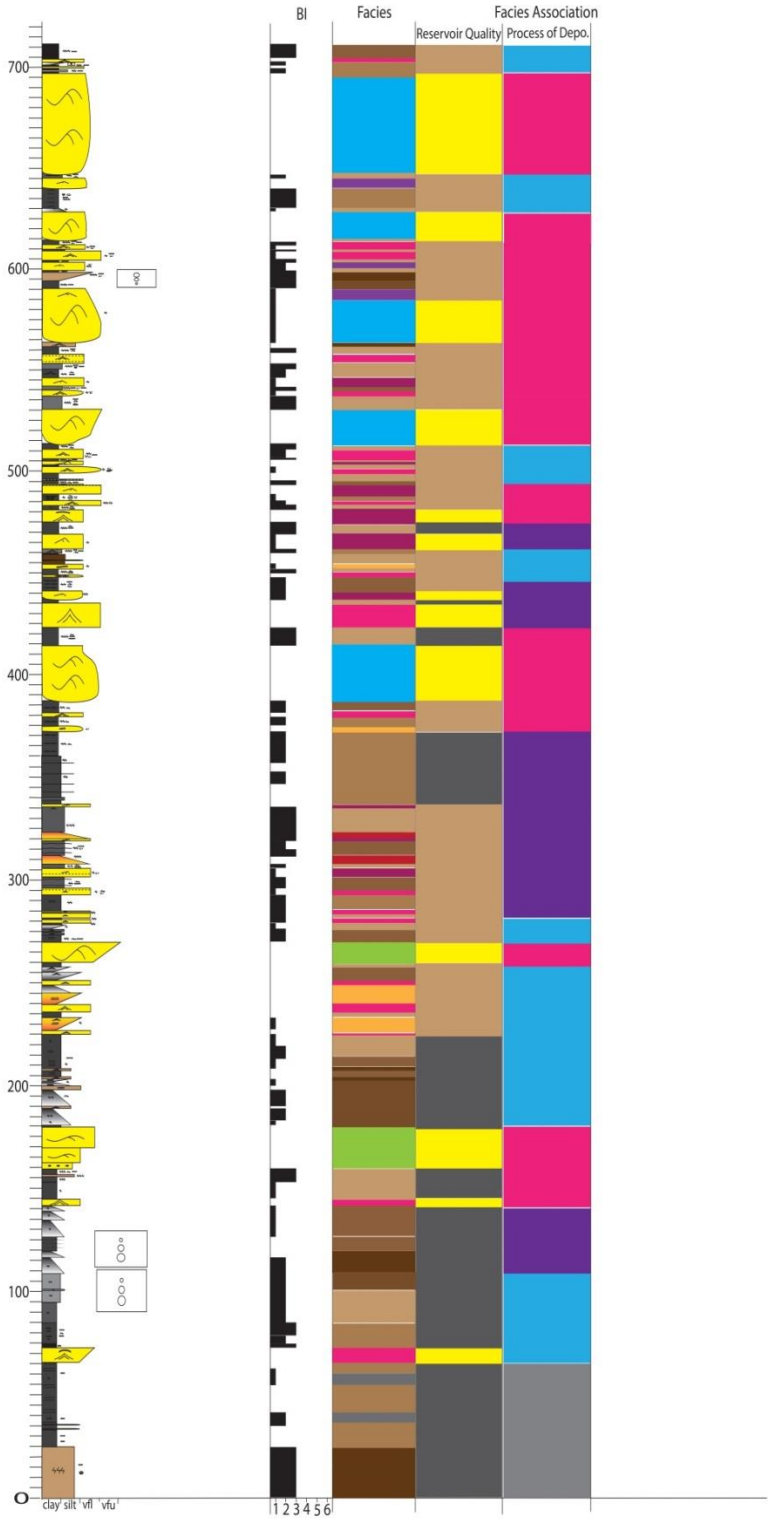

Figure 39. Section RR1. Columns from left-to-right are: lithology including thickness and structures, BI, Facies, and FA – Reservoir, FA – Process of Deposition. Legend is in Figure 19 & 22.

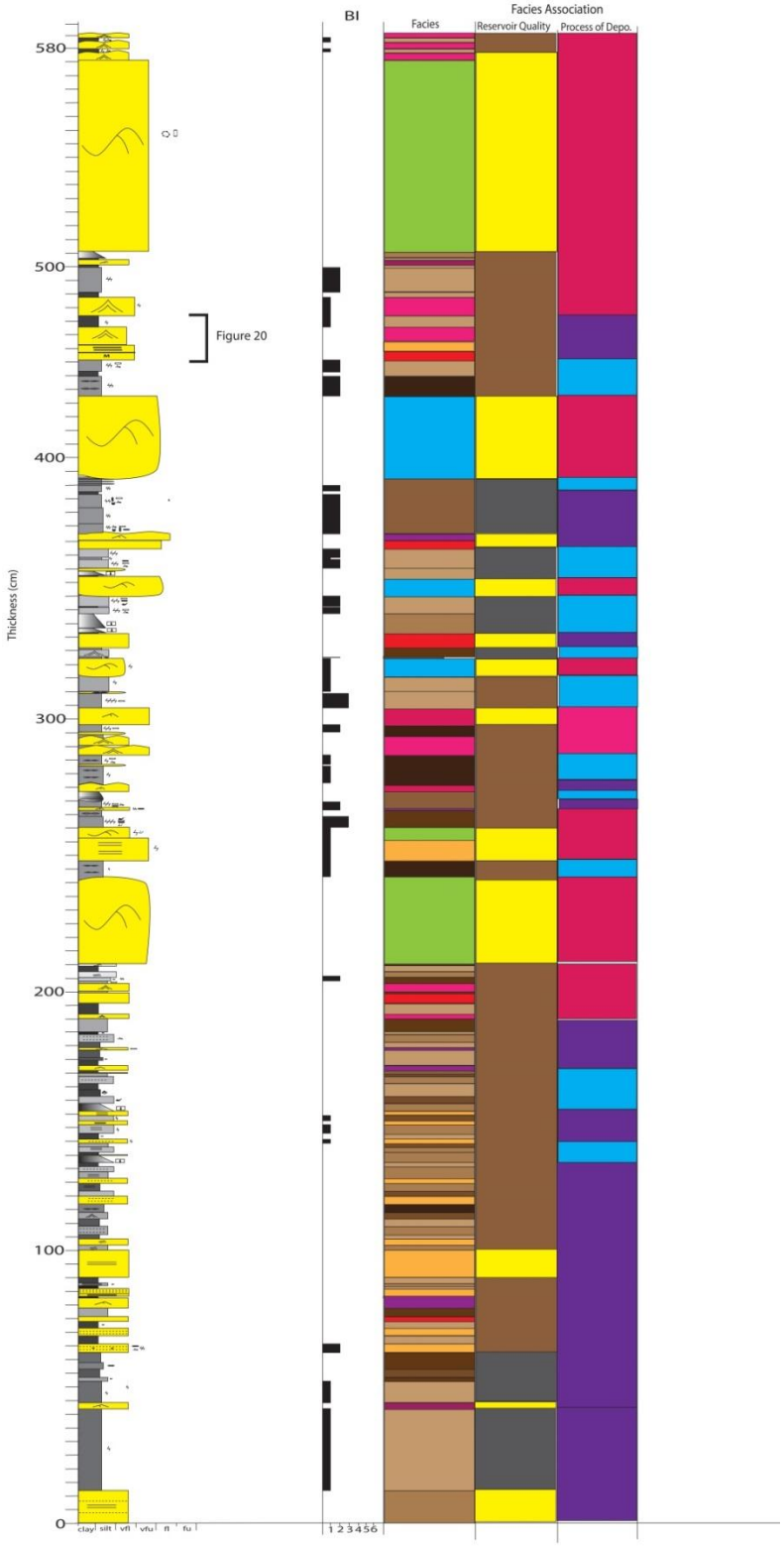

Figure 40. Section RR2. Columns from left-to-right are: lithology including thickness and structures, BI, Facies, and FA – Reservoir, FA – Process of Deposition. Legend is in Figure 19 & 22.

In RR1 the most common facies (Figure 41) is F12 , making up 20% of the entire section. The second most common facies are mudstones (F1-F2) which make up 18% and 16%, respectively. RR2 is made up of 21% F9 (Figure 42). F1 and F2 make up 28%, F2 being the second most abundant facies within RR2. Following F1 and F2 are F10 and F12, each making up 9% of the section. No other facies makes up more than 8% of the entire section.

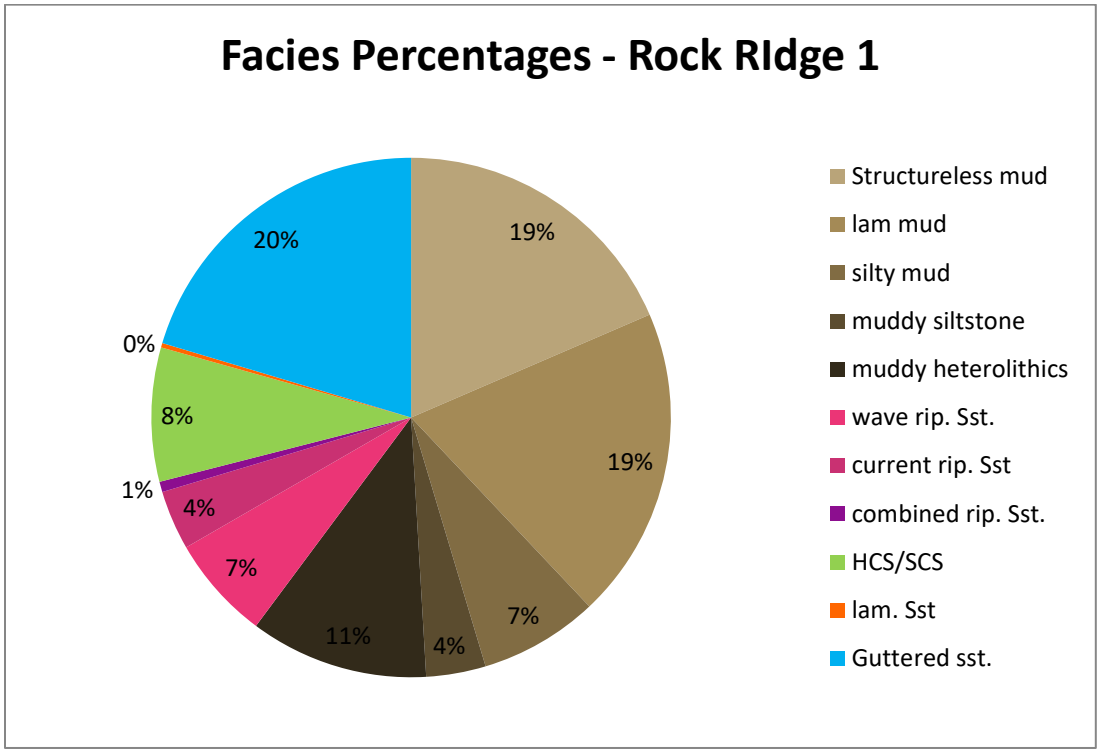

27

Figure 41. Facies percentages of section RR1.

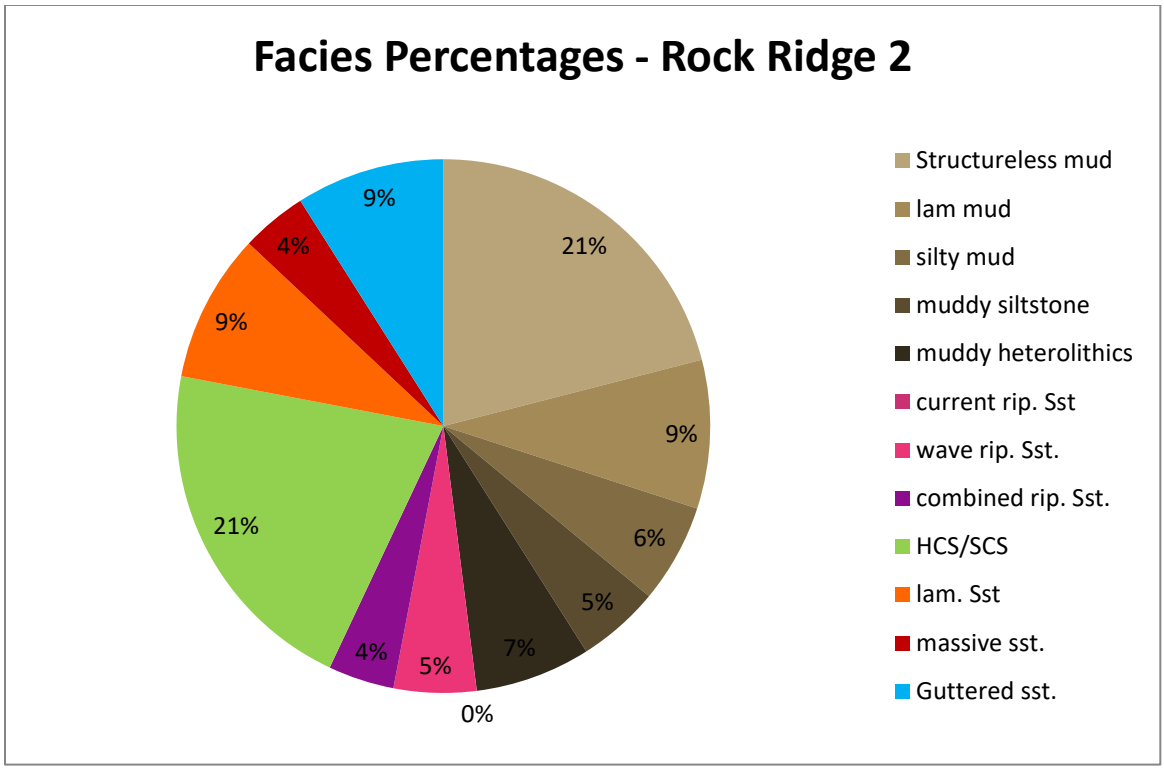

Figure 42. Facies percentages of section RR2.

Sand-to-shale analysis (Figure 43) presents differing results from Sanostee. Heterolithics make up the majority, 39%, of RR1 with mudstone following at 34%. Sand only makes up 27% of the total section with the majority of beds occupying the upper third of the section. The second section, RR2, is made up of 44% heterolithics, but differs from RR1 as it is made up of 38% sand and only 18% mudstone (Figure 44).

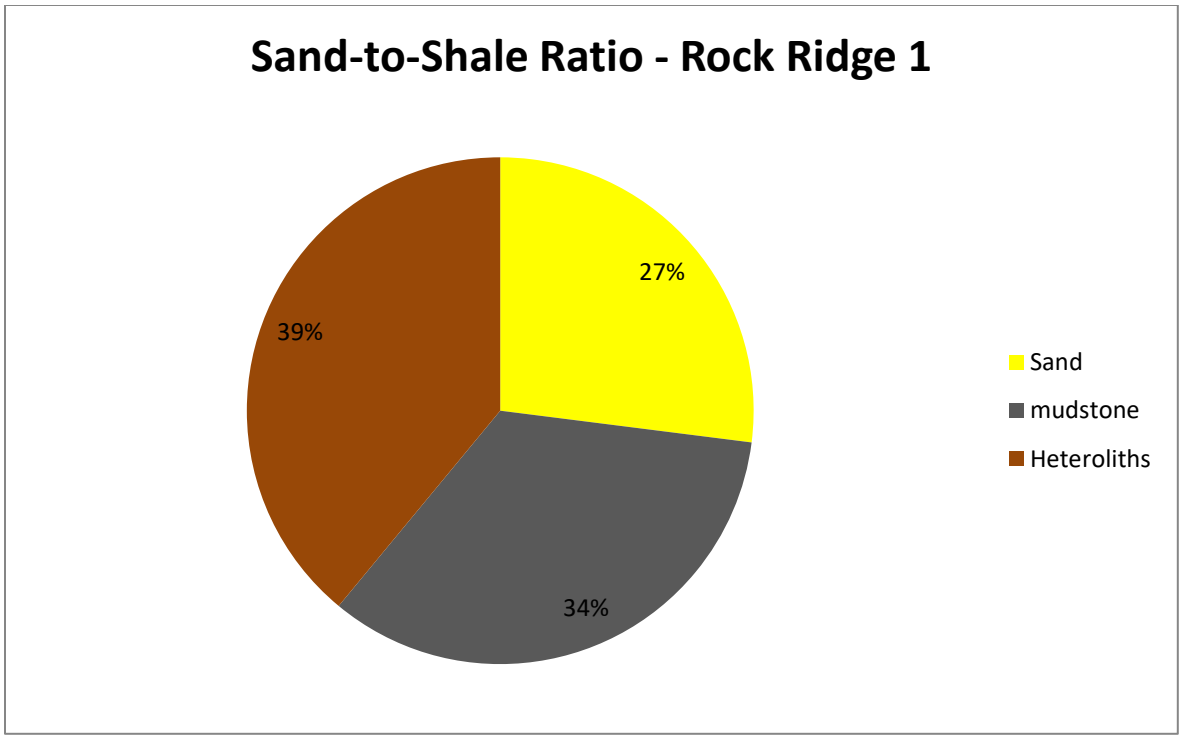

Figure 43. Facies association – sand-to-shale ratio for Section RR1.

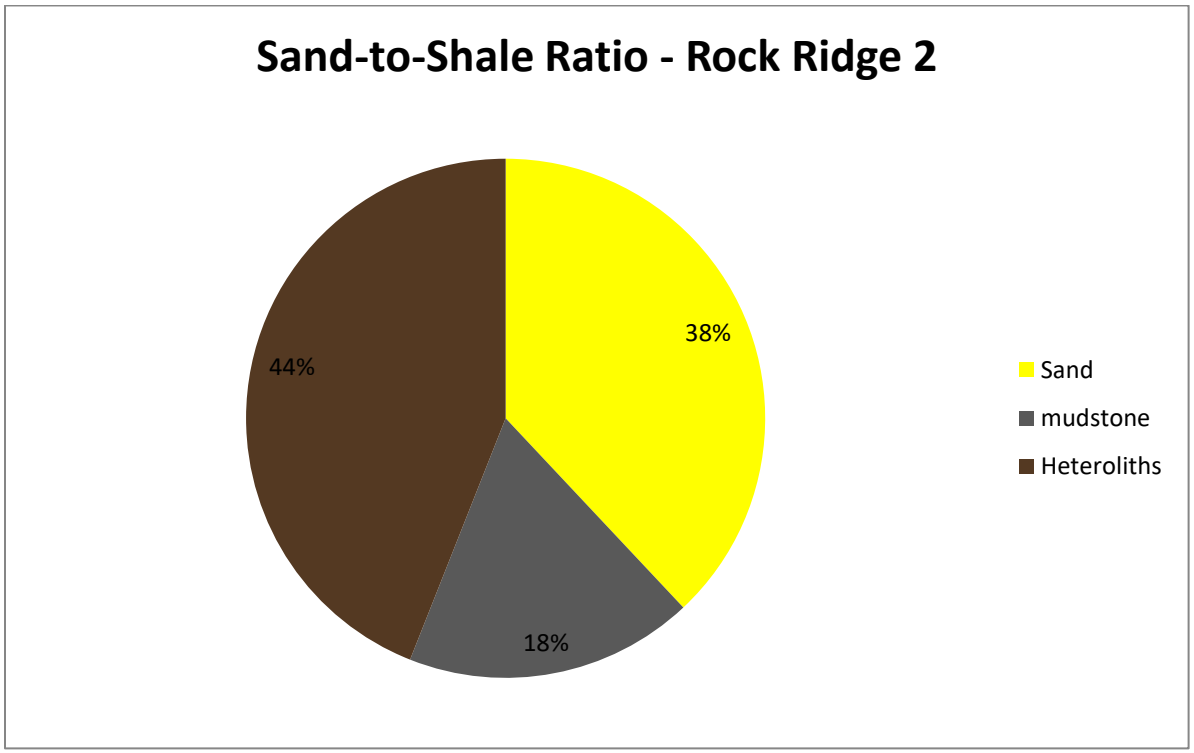

Figure 44. Facies association – sand-to-shale ratio for Section RR2.

The process of deposition for RR1 is broken down by turbidite, hyperpycnite, and tempestites (Figure 45). Turbidites make up 25% of RR1, while tempestites make up 40% and hyperpycnites 26%. In RR2 turbidities make up 39% of the section, while tempestites make up 43% and hyperpycnites make up only 18% (Figure 46).

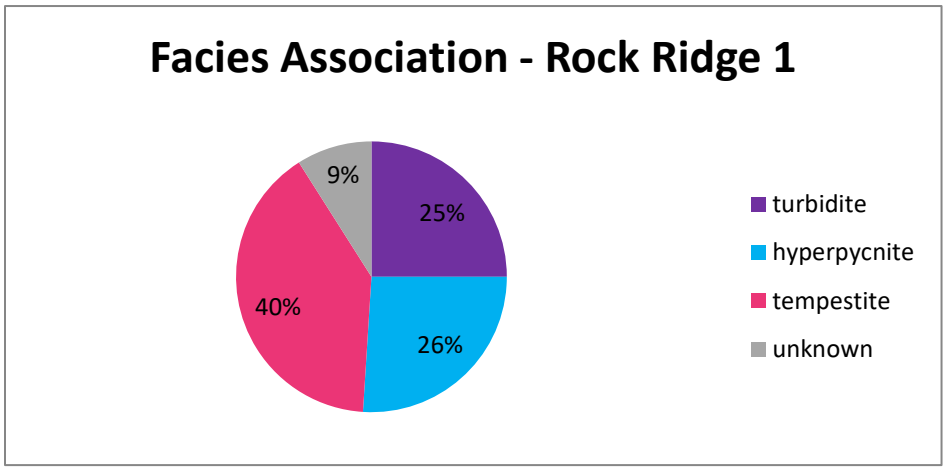

Figure 45. Facies association, process of deposition section RR1**.**

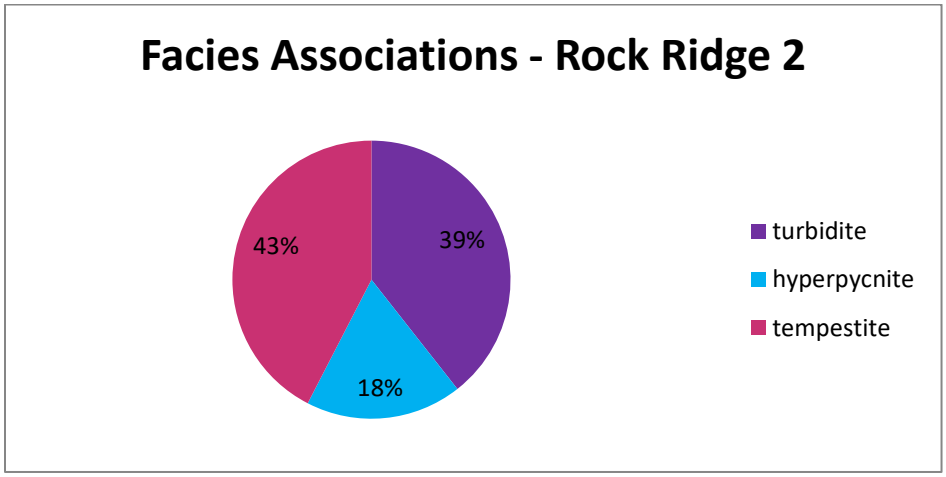

Figure 46. Facies association, process of deposition section RR2.

5.2.2 – Sandstone Ratios

Dimensional analysis (Figure 47) was performed on all sandstones observed within the sections at Rock Ridge. The thickest sandstone measured was 0.65m with the thinnest being 0.015m. Lateral extent varied over two orders of magnitude, with the least extensive sandstone measured to 0.65m and the longest 25.5m. Sandstones that were partly covered by slope were measured according to their inferred extent in Figure 50. The resulting scatter plot yielded an R^2 value of 0.73 indicating that there is a good correlation between sandstone thickness and lateral extent at Rock Ridge to be discussed at length in Chapter 6.

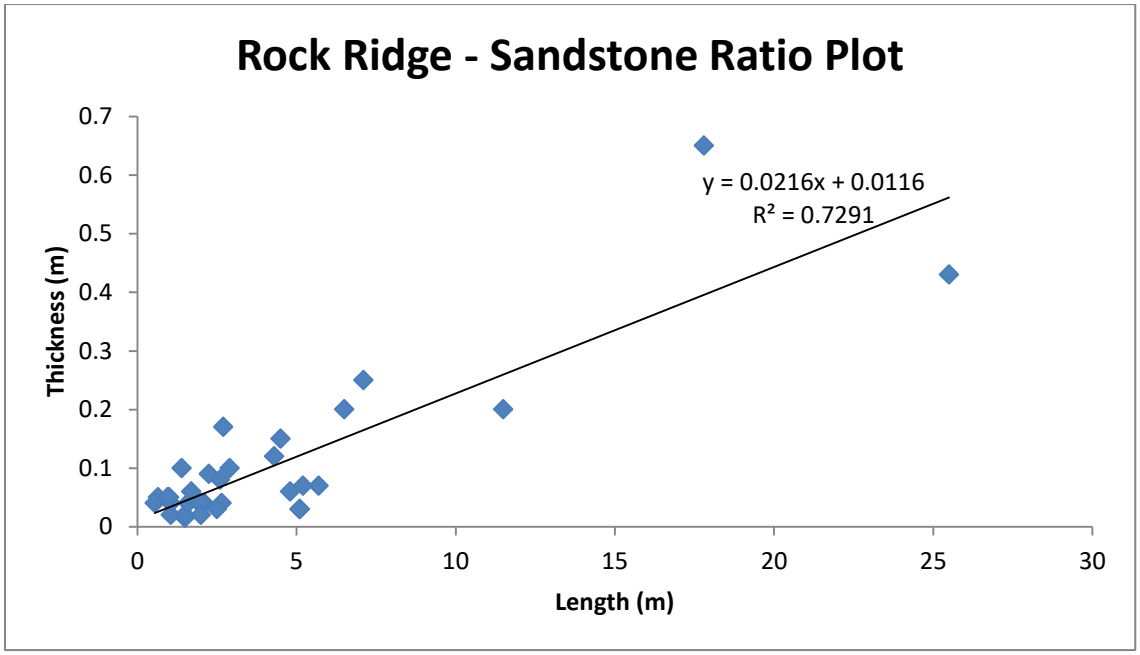

Figure 47. Plot of sandstone thickness versus length, measured in meters.

5.2.3 – Paleocurrents

Twenty-three paleocurrent measurements were taken at Rock Ridge, measuring wave ripple crests and current ripple foresets, as well as trough cross-bedding when it occurred. Paleoflow observations break down into three major directions. The main direction shown in Figure 48a is

SE-NW with a secondary component trending NE-SW. Direction of wave-ripple crests appears to be perpendicular to orientation of outcrop. In Figure 48b current ripple foresets trend 170° SE.

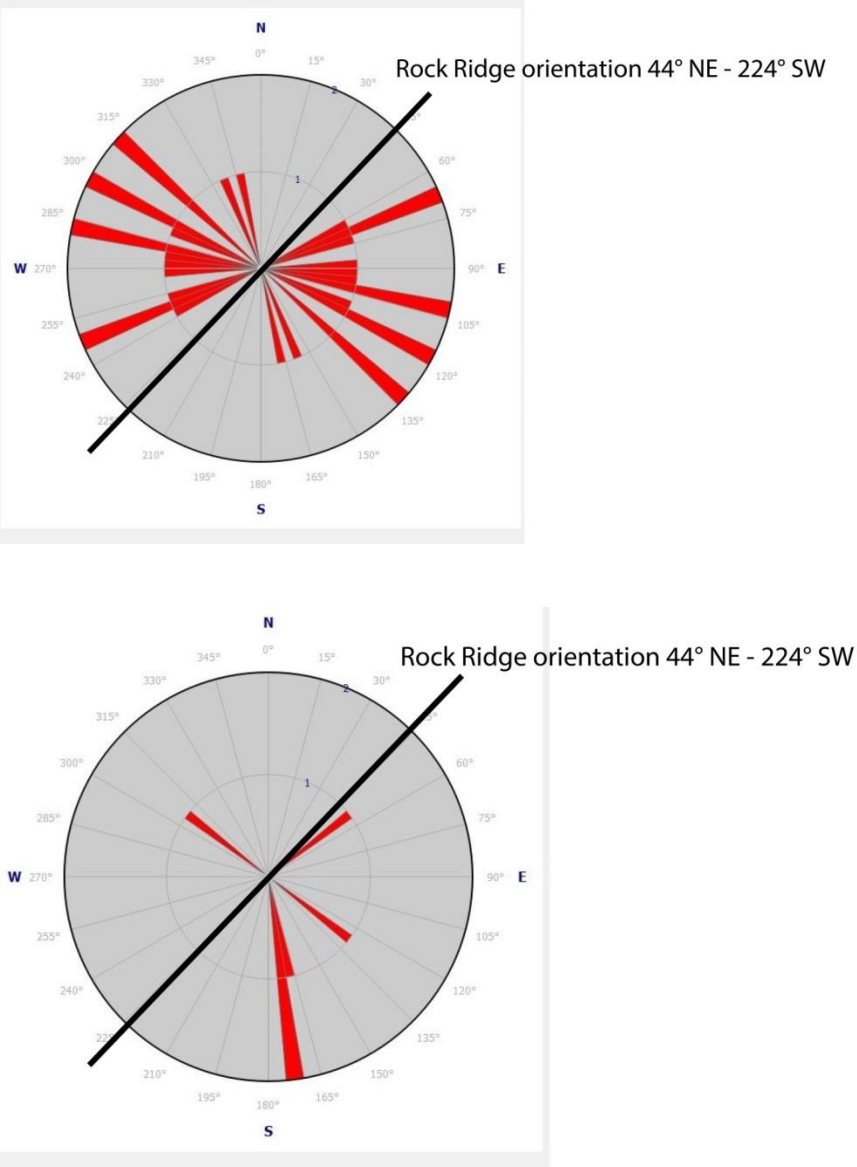

Figure 48. Measured paleocurrents of: A) wave, N=17 and B) current ripples, N=6 at Rock Ridge.

Due to the low number of measurements obtained past work was examined to augment the results presented here. Krueger (2011) took over 2000 paleocurrent measurements around Rock Ridge. Delta-front trough cross-bedding, upper shoreface trough cross-bedding, and wave-ripple crests were all documented. Kruger's results are presented in Figure 49.

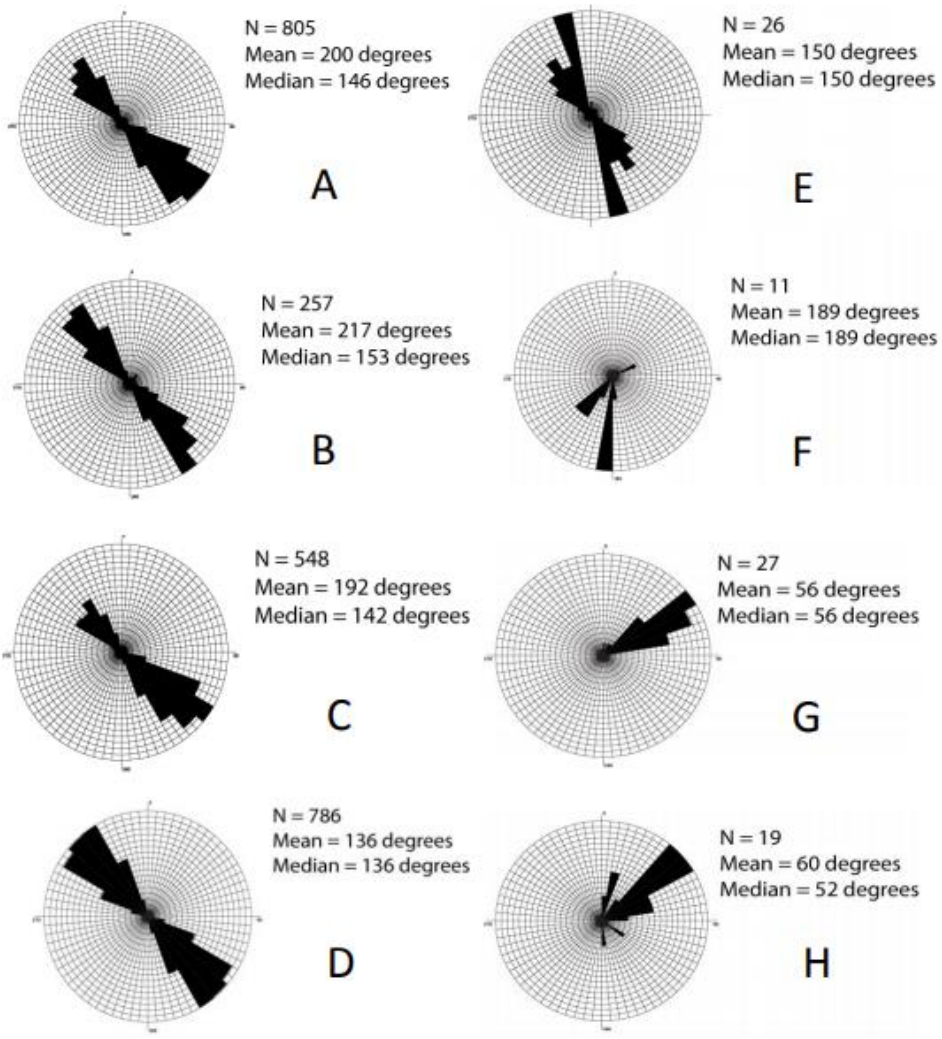

Figure 49. Rose diagrams of A) proximal delta-front trough cross-bedding, B) west side of Rock Ridge study are delta-front trough cross-bedding, C) east side upper shoreface trough cross-bedding, D) normalized upper shoreface/proximal delta-front trough cross-bedding, E) wave-ripple crest orientation, F) tidal channel cross-bedding, G) Torrivio fluvial trough cross-bedding, H) Torrivio fluvial lateral accretion bar strike section from

Krueger (2011). Note F-G are disregarded in terms of the data presented within this study as these refer to the Torrivio sandstone unit which overlays the Gallup.

From Figure 49E and Figure 48 it is clear that the orientation of wave-ripple crests, NW-SE, is consistent. Trough cross-bedding (A-D) matches the SE trend displayed in Figure 49. Unidirectional paleocurrent indicators trend in the SE direction, and wave paleocurrent indicators trend NW-SE and correlate with paleocurrent measurements presented within this study.

5.2.4 – Correlation

Figure 50. Correlation panel of the sandstones at Rock Ridge. A total of 10m separate sections RR1 and RR2.

From the two measured sections taken at Rock Ridge a correlation, similar to the one done at Sanostee, was performed using a high resolution gigapan photomosaic. Sandstones were able to be outlined and matched with those delineated in the sections and traced throughout the image to track lateral extent. Dashed lines on the correlation panel indicate areas where scree covered the outcrop and therefore no direct measurement of the rock could be taken. Correlation in these areas was performed using understanding of the area and the relationship between width and thickness (Figure 50) to estimate termination points of those covered sandstones.

Chapter 6 – Discussion

Results from this thesis document the heterolithic units of two separate parasequences within the Gallup sandstone and thus provide a case study to investigate the depositional mechanisms delivering sediment to the delta. The sharp contrast in the form of sandstones at either location provides insight into along strike variability within deltaic deposits and how mechanisms of sediment delivery can change spatially.

At Sanostee, towards the southeastern side of the exposure, sandstones are thicker with erosional bases and filled with HCS/SCS vfl-vfu sand grains (refer to Figure 18), with abundant gutter casts found on this side of the exposure (see Figures 18 and 38). On the northwestern side of the exposure, sands are much thinner (Figure 38) and have a lesser lateral extent. The transition from thick guttered to thin sandstones occurs within the range of measured sections (Figure 38) which spans 13.5m, meaning there is a process that has a higher degree of influence over the guttered facies and is mitigated 13.5m towards the northwest, along strike.

Gutter casts, present at Sanostee, are sharp-based and erosional with no evidence of soft-sediment deformation or dewatering structures, indicating that flows were entirely erosional (Collins et al., 2016). Gutters have U-shaped bases and are asymmetrical, (Figures 19 and 38) with sharp walls and no evidence of deformation or ‘caving-in’ within the gutter. Figure 18, depicts the internal structure of the gutter casts, demonstrating the degree of erosion and truncation within the fill. These erosional surfaces could result from one episode of cutting or could be a composite surface resultant from multiple storm events. The relief on the red surfaces reaches 2m in depth, making this a very large scour compared to other gutters observed (Collins et al., 2016). Therefore, these surfaces are interpreted as composite resulting from cutting during

multiple storm flows. Lack of a mud lag at the base of gutters indicates that the initial flow cut down into underlying mudstone units, leaving a scour. As the flow waned the fill was deposited, similar to gutters observed in the Miocene to modern Baram Delta Province by Collins et al. (2016). One difference with the Sanostee gutters is the presence of erosional surfaces within the fill, indicating that the original flow which cut the base did not fill the entire scour before another erosive flow came through and cut some of the previously deposited sand. This is indicative of multiple episodes of 'guttering-and-fill' (Goldring & Aigner, 1982) making the gutter casts observed at Sanostee amalgamated units, which are generally interconnected to sandstone beds (Figure 38). Gutters have been hypothesized to be cut by offshore directed unidirectional flows causing erosion (Whitaker, 1973; Myrow, 1992). Symmetrical 'pot casts' are cut by vortices at the base of the unidirectional flow caused by turbulence due to interaction with seafloor topography (Myrow, 1992). However, the gutters at Sanostee are filled with structures formed by oscillatory-dominated combined flow (Myrow, 1992; Collins et al., 2016). Due to the presence of multiple erosive surfaces within the fill coupled with gutter fill of HCS/SCS to combined flow ripples, the gutters at Sanostee were likely cut by a combined flow current that varied from unidirectional- dominant to oscillatory-dominant during waning. This is similar to the 'storm-flood' coupling phenomena or 'oceanic-flood' (Wheatcroft, 2000).

Dimensional analysis of the gutters determines that they range in thickness from 0.025m-0.71m and width 0.18m-6.9m. Average dimensions of a gutter cast at Sanostee are 0.37m thick by 2.55m wide. Figure 51b shows a plot of gutter dimensions with a line of best fit and an R^2 value 0.71, indicative of a moderate correlation between thickness and width relating to the size and strength of the erosive current (Collins et al., 2016; Myrow, 1992; Myrow & Southard, 1996). In comparison to other gutter dimensions published it is possible to compare those at Sanostee in

order to determine examples that may be useable analogues in order to analyze process of deposition and lateral continuity of sandstones. Figure 51 uses a plot from Collins et al. (2016) comparing dimensions of gutters from: the Belait Formation in Brunei (pink; Collins et al., 2016), the Lambir and Miri Formations (black; Collins et al., 2016), the Blackhawk Formation at Tusher Canyon within the Book Cliffs in Utah, USA (green), and published data (from Collins et al., 2016).

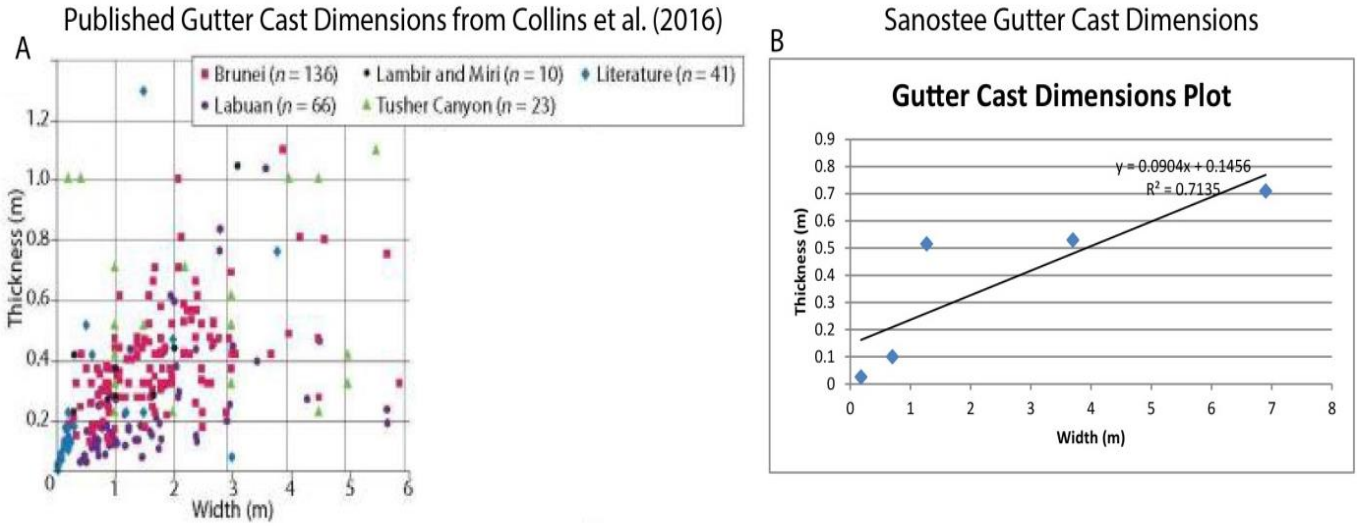

Figure 51. Gutter cast size plots. A) Modified from Collins et al. (2016) this plot summarizes the dimensions of previously published examples of gutter casts found in similar systems and environments to those measured in this study, B) the gutter cast dimension plot of those found at Sanostee.

Comparison of the two plots (Figure 51) shows that the gutters present at Sanostee are comparable in size to other gutters that have been published, specifically those of the Labuan and Brunei Formations. The largest gutter measured at Sanostee, with a thickness of 0.71m and width 6.9m, is wider across then any of the published gutters shown in A of Figure 51. This indicates that the strength of the flows affecting the Gallup shoreline were quite large and capable of causing offshore directed currents capable of eroding meters wide scours. This data also implies

that the gutters of the BDP presented in Collins et al. (2016) may be a good analogue for those at Sanostee.

Size and scale of the guttered facies is of interest due to its implications for reservoir dynamics. From the correlation presented in Figure 38 it is abundantly clear that the sandstone intervals are much thicker to the southeastern side of the panel i.e. within the guttered facies. As demonstrated by the internal bedding of the gutters (Figure 18) gutter casts tend to be amalgamated with overlying storm beds creating an abundance of sand-on-sand contacts due to the erosive nature of this prodelta transition zone to a more offshore environment caused by abundant storm-wave influence. Factors contributing to an erosive zone include: 1) Thin parasequence package due to progradation into shallow water; 2) wave-dominated delta with either distributary or fluvial channels nearby; 3) A sharp-based shoreface caused by rapid sea-level fall; 4) Parasequence thickness increases abruptly seaward due to pinchout of underlying shoreface sandstone (Eide et al., 2015) based on work done in the Cretaceous Blackhawk Formation. Looking at Parasequence 7a (Sanostee, Figure 7) it is clear that this package is prograding and thinning seaward. Data presented in the measured sections and facies analysis from Sanostee demonstrates an abundance of storm-wave features, such as tempestites, HCS/SCS bedding, low BI, and gutter casts, indicating storm-flood events. These factors support the observation of an erosive transition zone prodelta environment of the Gallup sandstone.

The abrupt lateral transition from guttered facies to a thinner, less extensive facies is important as an indicator of influence and transition of facies along-strike. Sand content is much higher within the guttered facies, which implies direct sediment input at this location. During storms, rivers flood and excess sediment is delivered to the shoreline (Bhattacharya & Giosan, 2003; Bhattacharya & MacEachern, 2009; Collins et al., 2016). Basins with a small distance (i.e.

<1000km), from source-to-sink, can be affected by a single storm from hinterland to basin (Romans et al., 2015) meaning that one storm could result in a corresponding offshore flow and input of sediment to the system. Based on the factors described by Eide et al. (2015) it is probable that the cause of the lateral facies shift observed at Sanostee is due to the presence of a fluvial, or more likely, a distributary channel in proximity to the guttered facies. Based on the distal nature of heterolithic deposits and grain size of sand being significantly smaller than the medium grained material found within the thick, overlying shoreface, it is likely that a distributary channel was feeding the sediment to this location. Within the thinner facies, the sand ratio decreases significantly (see Figures 34 and 38) indicating the input of sediment at this point had fallen as the distance from the channel mouth increased. This observation also indicates that these offshore directed oscillatory storm flows responsible for the formation of gutter casts are narrow (Myrow, 1992), in this case less than 10m wide.

Gutter casts are common features in many storm deposited sandstones (Collins et al., 2016; Krueger et al., 2010; Myrow, 1992; Plint, 2000; Plint, 2014) and those at Sanostee are not abnormally large in comparison to others that have been published (see Figure 51; Collins et al., 2016). However, those at Sanostee have a significant stratigraphic importance in the correlation of the Gallup sandstone (Lin & Bhattacharya, 2017). Sections taken at Sanostee (Lin & Bhattacharya, 2017) indicate an overlying sharp-based shoreface. A sharp-based shoreface is deposited due to erosion of offshore muds as fair-weather wave base descends into the shelf muds, this surface is termed a Regressive Surface of Marine Erosion (RSME), due to an abrupt fall in sea-level with no change in sediment input (Plint & Nummedal, 2000; Plint, 1996; Eide et al., 2015). Sharp-based shoreface deposits are indicative of a ‘Forced Regression’ where sea-level abruptly drops with no corresponding increase in sediment input (Plint & Nummedal,

2000). The position of the sequence boundary is the object of much debate with some arguing that it belongs on top of the shoreface (Plint, 1996) while others argue the RSME is the sequence boundary because this surface indicates the first drop of base-level (Posamentier & Morris, 2000).

The significance of the gutters present at Sanostee is that in all the sections taken within the study area, no other gutters of this size and scale were observed. Due to this fact the sequence boundary was placed on the continuous surface separating tabular heterolithic sandstones and the guttered facies (i.e. a RSME by Lin & Bhattacharya, 2017). From Figure 7, parasequence 7a is the start of a FSST leading into lowstand.

Observations presented in this study differ from previous work on the same stratigraphic intervals (Waller, 2016). Firstly, this study focuses on taking multiple measured sections across an exposure in order to perform lateral continuity correlations and some of these sections, particularly at Sanostee are taken at slightly different locations to those in Waller (2016). However, significant differences emerge in facies analysis which leads to changes in corresponding associations and process interpretation. Waller (2016) finds the most dominant facies to be bioturbated mudstone (low, moderate, and high) which make up a total of 38.25% of the total section. While this study presents the most predominant facies to be guttered and wave-rippled sandstones with very low levels of bioturbation throughout all three sections. Another major difference is determining the dominant processes. Waller (2016) attributes this location to be fluvial dominated with wave influence (Ainsworth et al., 2011). However, as noted above this study observes dominant tempestites; therefore, it is likely that the data collected in Waller (2016) was taken either up or down strike and therefore missed the guttered facies. Such a

difference between two studies demonstrates the complexity of these heterolithics and why extensive outcrop work is vital to analyze such intervals.

The deposits measured at Rock Ridge contrast with those at Sanostee in multiple ways. Rock Ridge falls within Parasequence set 5 and the deposits measured here are part of Parasequence 5a, located in a Highstand Systems Tract (HST; see Figure 7). Orientation of the outcrop is slightly north-northeast to south-southeast making it oblique to regional strike and more down-dip from the paleoshoreline. Firstly, 60% of RR1 and 48% of RR2 are made of mud-dominated facies (F1-FF5 and F12; See Figures 43-44), results which agree with those of Waller (2016) who found 50.7% of those sections to be mudstone-dominated. Presence of F12 is indicative that storm-influence is a major factor in deposition of these thin-beds (see Figure 42-43). In total, tempestites make up 40% and 43% of RR1 and RR2, respectively. Waller (2016) argues that Rock Ridge exhibits fluvial to mixed dominance, which does align with the findings of this study. Hyperpycnites, make up 26% and 18% of sections RR1 and RR2, respectively indicating fluvial influence. The abundance of mud could be indicative of river-fed turbidites, coupled with increasing levels of bioturbation up section would be consistent with fluvial influence. However, the abundance of F12 and F9 make it difficult to classify Rock Ridge as river dominated. Observed gutters are evidence of oscillatory offshore directed combined flows complicating the interpretation of Rock Ridge. Due to the gutter casts it can be stated that storm-floods influence the deposition of sandstones at Rock Ridge in a significant manner.

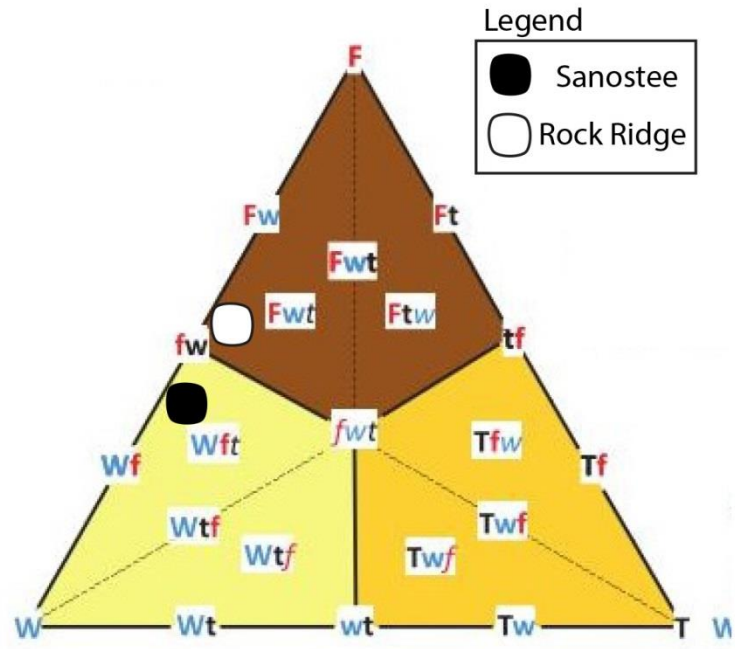

Figure 52. Plotting the Gallup deltas examined within this study based on the classification method of Ainsworth et al. (2011) and extensive facies analysis presented in Chapters 4 and 5. The sections observed at Sanostee are indicative of wave-dominance and fluvial influence, while Rock Ridge is classified as wave-dominated and fluvial-influenced as well.

Based on the facies observations made within this study (Figures 22,27,31,42,43, and 44) the Gallup deltas can be classified using the method devised by Ainsworth et al. (2011), mentioned in Chapter 1, to determine degree of influence. From Figure 52, Sanostee is classified as wave-dominated and fluvially-influenced due to the abundance of oscillatory combined-flow structures found within S1-S3. Rock Ridge is also wave-dominated and fluvially-influenced, but in this case the fluvial portion plays a larger role based on the lack of large gutter casts and a greater presence of grading and a larger proportion of hyperpycnites in comparison to Sanostee.

Clearly sandstones correlate over a larger distance than those at Sanostee. Dimensional analysis of the sandstones at Rock Ridge shows a moderate correlation between thickness and lateral extent, in addition to the thicker sandstones correlating between both sections and continuing over the entire exposure. Three sandstones correlate between RR1 and RR2, a distance of 10m, exceeding the lateral extent of any sandstone at Sanostee. Sandstones correlate in a horizontal manner and pinch-out to the north, at an oblique angle to the paleoshoreline. Correlation shows that no individual sand cross-cuts another, unlike at Sanostee where higher order erosional surfaces cross-cut lower order surfaces. Guttering is more common and net-to-gross rises further up section, above the second correlatable bed (Figure 50), most likely indicating proximity to the shoreline. However, despite the presence of F12, degree of amalgamation between guttered sandstones is minimal, unlike Sanostee, which makes the majority of sandstone units vertically isolated from each other.

Clearly, Rock Ridge exhibits significant differences in the type and form of heterolithic sandstone deposits in comparison to Sanostee; which can be explained by examining the stratigraphic context within which the sands are deposited. The location of Parasequence 7a, discussed earlier within this section, is within a FSST caused by forced regression. While Parasequence 5a is higher up stratigraphically (Figure 7) and also lies in a seaward direction indicating it is younger than 7a. In terms of accommodation successions and shoreline trajectory, Parasequence 5a lies within a progradational-aggradational system above a Transgressive Systems Tract (TST) making it part of an HST. This HST follows the previous sequence capped by the sequence boundary at the RSME found at Sanostee. High sediment input, coupled with steady sea-level, lends itself to being conducive of sediment gravity flows creating more elongate, flat-based sandstones (Bhattacharya, 2006). Furthermore, the difference in F12

between the two locations indicates that the size, scale, and placement of those gutters observed at Sanostee are stratigraphically significant.

Correlation of these thin-to-medium bedded sandstones over their entire exposure, 35m (Sanostee) and 44m (Rock Ridge) displays the complex bedding of heterolithic deposits. Vertical conductivity is affected by the difference between the guttered and tabular sandstone facies as is the net-to-gross ratio. Within the guttered sections, a number of amalgamated sandstone beds with abundant sand-on-sand contacts are evident making for a higher degree of connectivity and therefore a higher vertical conductivity within the heterolithics. In stark contrast to the tabular facies, where the majority of sandstone beds are isolated from the others by intervening mudstone layers, effectively acting as baffles to vertical flow. Eide et al. (2015) have done some large scale modelling of the permeability differences in such reservoirs based on sandstone facies. Comparing between guttered and tabular facies it is clear that permeability is higher in reservoirs that have a higher percentage of guttered facies (Eide et al., 2015).

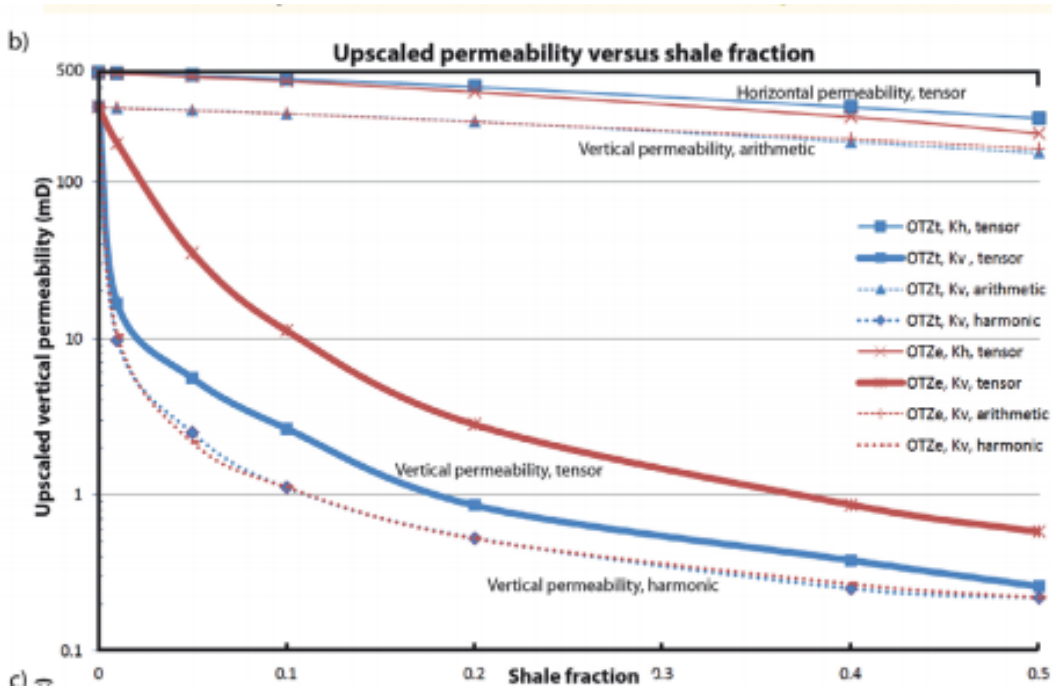

Figure 53. Graph modified from Eide et al. (2015) depicting their modelling of vertical permeability through heterolithic reservoirs. Bold red line represents heterolithic sandstones defined by guttered facies, whereas blue represents more tabular sandstones.

Results such as these can be applied to the correlation performed in this study to better analyze heterolithic reservoirs. Though vertical conductivity is better within the guttered facies, strike continuity is not. Based on the findings presented in Chapter 5, the section with the highest sand net-to-gross percentage were S1 and S2 (within the guttered facies) with percentages of sandstone units making up 50% and 56% respectively. These intervals do not include the sand content within the heterolithic facies association. No other section has greater than 41% sand and RR1 and RR2 only have 27% and 38%. These results would indicate that within the intervals investigated as part of this study, the guttered facies at Sanostee has the highest degree of vertical conductivity and the highest sand content. Though the tabular deposits of Rock Ridge have a greater lateral continuity, it must be noted/considered that the orientation of the deposits (strike vs. oblique/dip-direction) may play a role in affecting the lateral continuity.

Chapter 7 – Conclusion

The central questions addressed in this thesis are: 1) What is the process of deposition that is dominant within the prodelta heterolithics of the Gallup sandstone; and 2) How do these sands correlate with distance? With the goal of the study being to provide an analysis of these sandstones to better understand their form and stratigraphic significance.

From this study one can conclude that:

1. Processes of sediment delivery can be observed and quantified by performing high-resolution (i.e. centimeter scale) facies analysis of prodelta heterolithics within the Gallup Sandstone of northwestern New Mexico.
2. Sandstone facies interpreted as storm-deposited tempestites are the dominant facies association responsible for sandstone deposition within the heterolithic intervals at Sanostee, in contrast to previous work done on these units i.e. Waller (2016).
3. Sanostee sections (S1 and S2) dominated by tempestites have a greater sandstone percentage then sections dominated by turbidites or hyperpycnites (S3, RR1, RR2).
4. Large scale scours found at Sanostee represent composite surfaces of many oscillatory combined storm flows responsible for numerous episodes of cut and erosion. Subsequent fill of scours is made up of many erosive surfaces indicating the process to ‘cut-and-fill’ these gutters happened over multiple storm events.
5. Transition from guttered to tabular sandstone facies within a horizontal distance of 10m is indicative of the presence of a distributary channel feeding the sediment into the gutter fill and demonstrates the abrupt along-strike transition of facies in thin-bedded reservoirs.

6. Sandstones within the guttered facies correlate over smaller horizontal distances (8.5m) in comparison to more tabular sandstones which can correlate over distances >10m.
7. Sandstones in the guttered facies have a higher degree of amalgamation than those in the tabular facies making thicker sand packages. While tabular sandstones found at Rock Ridge have a greater degree of lateral continuity.
8. Guttered facies have a higher degree of sand-on-sand contacts, while tabular sandstones are isolated giving guttered reservoirs a higher degree of vertical conductivity.
9. The unique presence of gutters of such scale at Sanostee is indicative of an RSME caused by rapid sea-level fall which is clear evidence to identify a FSST due to a forced regression.

References

Ainsworth, R. B., Vakarelov, B. K., & Nanson, R. A. (2011). Dynamic spatial and temporal prediction of changes in depositional processes on clastic shorelines : Toward improved subsurface uncertainty reduction and management. *AAPG Bulletin*, *95*(2), 267–297.

Barrell, J. (1912). Criteria for the recognition of ancient delta deposits. *Geological Society of America Bulletin*, *23*(1), 377-446.

Bhattacharya, J. P. (2006). Deltas In R. G. Posamentier, H.W. and Walker (Ed.), *Facies Models Revisited*, 237–292. SEPM (Society for Sedimentary Geologists).

Bhattacharya, J. P., & Willis, B. J. (2001). Lowstand deltas in the Frontier Formation, Powder River Basin, Wyoming: implications for sequence stratigraphic models. *AAPG Bulletin*, *85*(2), 261-294.

Bhattacharya, J. P., & Giosan, L. (2003). Wave-influenced deltas: geomorphological implications for facies reconstruction. *Sedimentology*, *50*(1), 187–210.

Bhattacharya, J. P., & MacEachern, J. A. (2009). Hyperpycnal rivers and prodeltaic shelves in the Cretaceous Seaway of North America. *Journal of Sedimentary Research*, *79*, 184–209.

Blakey, R. C. (2014). Paleogeography and Paleotectonics of the Western Interior Seaway , Jurassic-Cretaceous of North America In *Search and Discovery Article*, *30392*. AAPG.

Bouma, A. H. (1962). Sedimentology of some flysch deposits: a graphic approach to facies interpretation. Elsevier Pub. Co..

Bridge, J. & Best, J. (1997). Preservation of planar laminae due to migration of low-relief bed

waves over aggrading upper-stage plane beds : comparison of experimental data with theory. *Sedimentology*, *44*, 253–262.

Campbell, C. V. (1971). Depositional Model - Upper Cretaceous Gallup Beach Shoreline, Shiprock Area, Northwestern New Mexico. *Journal of Sedimentary Petrology*, *41*(2), 395–409.

Campbell, C. V. (1973). Offshore Equivalents of Upper Cretaceous Gallup Beach Sandstones, Northwestern New Mexico In *Four Corners Geological Society Memoir Book*, 78–84.

Campbell C.V. (1979). Model for beach shoreline in Gallup Sandstone (Upper Cretaceous) of northwestern New Mexico. New Mexico Bureau of Mines & Mineral Resources.

Collins, D. S., Johnson, H. D., Allison, P. A., & Guilpain, P. (2016). Coupled " storm-flood " depositional model : Application to the Miocene – Modern Baram Delta Province , north-west Borneo. *Sedimentology*, *64*(5), 1203-1235.

Dalrymple, R. W., Baker, E. K., Harris, P. T., & Hughes, M. G. (2012). Sedimentology and Stratigraphy of a Tide-Dominated , Foreland-Basin Delta (Fly River , Papua New Guinea) In *Tropical Deltas of Southeast Asia- Sedimentology, Stratigraphy, and Petroleum Geology*, *SEPM Special Publication*, (76), 147–173.

Dane, C.H., G.O. Bachman, & Reeside, Jr., J.B. (1957). The Gallup Sandstone, its age and stratigraphic relationships south and east of the type locality, In C.J. Little and J.J. Gill, (Eds.), *Geology of Southwestern San Juan basin: Four Corners Geological Society Guidebook, 2nd Field Conference*, 114–120.

Dominguez, J. M. L. (1996). The São Francisco strandplain: A paradigm for wave-dominated

deltas In de Batist, M., and Jacobs, P. (Eds.), *Geology of Siliciclastic Shelf Seas: Geological Society of London, Special Publications*, *117*(1), 217-231.

Duke, W. L. (1985). Hummocky cross-stratification , tropical hurricanes , and intense winter storms. *Sedimentology*, *32*, 167–194.

Dumas, S.,& Arnott, R. W. C. (2006). Origin of hummocky and swaley cross-stratification — The controlling influence of unidirectional current strength and aggradation rate. *Geology*, (12), 1073–1076.

Eide, C. H., Howell, J. A., & Buckley, S. J. (2015). Sedimentology and reservoir properties of tabular and erosive offshore transition deposits in wave-dominated , shallow-marine strata : Book Cliffs , USA. *Petroleum Geoscience*, *21*, 55–73.

Galloway, W. E. (1975). Process Framework for Describing the Morphologic and Stratigraphic Evolution of Deltaic Depositional Systems. In *Deltas: Models for Exploration*, 87–98. Houston Geological Society.

Gani, R. M., Bhattacharya, J. P., & MacEachern, J. A. (2008). Using Ichnology to determine relative influence of waves, storms, tides, and rivers in deltaic deposits: examples from Cretaceous western interior seaway, U.S.A. *Applied Ichnology*, 209–225.

Goldring, R., & Aigner, T. (1982). Scour and fill: the significance of event separation, In *Cyclic and Event Stratification*, 354-362. Springer, Berlin, Heidelberg.

Ichaso, A. A., & Dalrymple, R. W. (2009). Tide- and wave-generated fluid mud deposits in the Tilje Formation (Jurassic), Offshore Norway Processes and Deposit Characteristics. *Geology*, *37*(6), 539-542.

Kerr, M. and Eyles, N. (1991). Storm-deposited sandstones (tempestites) and related ichnofossils of the Late Ordovician. *Canadian Journal of Earth Sciences*, *28*, 266–282.

Kirby, R. and Parker, W. R. (1983). Distribution and Behavior of Fine Sediment in the Severn Estuary and Inner Bristol Channel, U. K. *Canadian Journal of Fisheries and Aquatic Sciences*, *40*.

Krueger, R. (2010). *S*trike Variability within a wave-influenced delta, the Gallup Sandstone, Shiprock, New Mexico. University of Houston.

Lamb, M. P., Myrow, P. M., Lukens, C., Houck, K., & Strauss, J. (2008). Deposits from Wave-Influenced Turbidity Currents : Pennsylvanian MIinturn Formation, Colorado, U.S.A. *Journal of Sedimentary Research*, *78*, 480–498.

Li, Z., Bhattacharya, J. P., & Schieber, J. (2015). Evaluating along-strike variation using thin-bedded facies analysis , Upper Cretaceous Ferron Notom Delta , Utah. *Sedimentology*, *62*, 2060–2089.

Lin, W., & Bhattacharya, J. P. (2017) High-Resolution Sequence Stratigraphy, Shoreline Trajectory, Accommodation Successions, and Facies Association in the Cretaceous Gallup System, Shiprock, New Mexico, USA In *AAPG Annual Convention and Exhibition*.

LoParco, M. (2011). Application of the Asymmetric Wave - Influenced Delta Model to the Cretaceous Gallup Sandstone in Shiprock, New Mexico. University of Houston.

Lowe, D. R. (1979). Sediment gravity flows: their classification and some problems of application to natural flows and deposits. *SEPM Special Publication*, *27*, 75-82.

MacEachern, J., Bann, K. L., Bhattacharya, J. P., & Howell, C. D. (2005). Ichnology of Deltas:

Organism Responses to the Dynamic Iinterplay of Rivers, Waves, Storms, and Tides. *SEPM Special Publication*, (83), 49–85.

Macquaker, J. H. S., Bentley, S. J., & Bohacs, K. M. (2010). Wave-enhanced sediment-gravity fl ows and mud dispersal across continental shelves: Reappraising sediment transport processes operating in ancient mudstone successions, *Geology*, (10), 947–950.

McCubbin, D. G. (1982). Barrier-island and strand-plain facies, In Scholle, P.A. & Spearing, (Eds.), Sandstone Depositional Environments, *AAPG Memoir, 31*, 247-280.

Milliman, J. D., & Syvitski, J. P. (1992). Geomorphic/tectonic control of sediment discharge to the ocean: the importance of small mountainous rivers. *The Journal of Geology*, *100*(5), 525-544.

Molenaar, C. M. (1973). Sedimentary Facies and Correlation of the Gallup Sandstone and Associated Formations, Northwestern New Mexico. *Cretaceous and Tertiary Rocks of the Southern Colorado Plateau - Memoir, 1973*.

Molenaar, C. M. (1974). New Mexico Geological Society Cretaceous , Eastern San Juan and Acoma Basins , New Mexico. In *Ghost Ranch*, 251–258.

Molenaar, C. M. (1983). Principal reference section and correlation of Gallup Sandstone, northwestern New Mexico, In Hook, S.C. (compiler), *Contributions to Mid-Cretraceous Paleontology and Stratigraphy of New Mexico: New Mexico Bureau of Mines and Mineral Resourcees, Circ. 185*, 29-40.

Mulder, T., & Syvitski, J. P. M. (1995). Turbidity Currents Generated at River Mouths during Exceptional Discharges to the World Oceans. *The Journal of Geology*, *103*(3), 285–299.

Mulder, T., & Alexander, J. A. N. (2001). The physical character of subaqueous sedimentary density flows and their deposits. *Sedimentology*, *48*.

Mulder, T., Syvitski, J. P. M., Migeon, S., Faugeres, J.-C., & Savoye, B. (2003). Marine hyperpycnal flows : initiation , behavior and related deposits. A review. *Marine and Petroleum Geology*, *20*, 861–882.

Myrow, P.M. and Southard, J. B. (1996). Tempestite Deposition. *Journal of Sedimentary Research*, *66*(5), 875–887.

Myrow, P. M. (1992). Pot and Gutter Casts From the Chapel Island Formation, Southeast Newfoundland. *Journal of Sedimentary Petrology*, *62*(6), 992–1007.

Neal, J., & Abreu, V. (2009). Sequence stratigraphy hierarchy and the accommodation succession method. *Geology*, *37*(9), 779–782.

Noad, J. (2015). When storms go bad : their impact on gutter cast distribution and dimensions , based on new data from the Miocene of eastern Borneo. In *GeoConvention 2015*,1–5. Geoscience New Horizons.

Nummedal, D., and Molenaar, C. M. (1995). Sequence Stratigraphy of Ramp-Setting Strand Plain Successions : The Gallup Sandstone , New Mexico. In van Wagoner, J.C. and Bertram G.T. (Eds.), *Sequence Stratigraphy of Foreland Basin Deposits, AAPG Memoir, 64*, 277–310.

Pemberton, S. G., Maceachern, J. A., & Ranger, M. J. (1992). Ichnology and Event Stratigraphy: The Use of Trace Fossils in Recognizing Tempestites. *Applications of Ichnology to Petroleum Exploration, a core workshop,* Core Workshop, 17 Edited by: Pemberton, S.g. 1-

32. Society of Economic Paleontologists and Mineralogists.

Plint, A(1996). Marine and nonmarine systems tracts in fourth-order sequences in the Early-Middle Cenomanian, Dunvegan Alloformation, northeastern British Columbia, Canada. In Howell, J.A. and Aitken, J.F. (Eds.), *High Resolution Sequence Stratigraphy: Innovations and Applications*, 159–191.

Plint, A. G. (2000). Sequence stratigraphy and paleogeography of a Cenomanian deltaic complex : the Dunvegan and lower Kaskapau formations in subsurface and outcrop , Alberta and British Columbia , Canada. *Bulletin of Canadian Petroleum Geology*, *48*(1), 43–79.

Plint, A.G. (2010). Wave and storm-dominated shoreline and shallow-marine systems. In *Facies Models 4*, 167-200.

Plint, A.G. (2014). Mud dispersal across a Cretaceous prodelta : Storm-generated , wave-enhanced sediment gravity flows inferred from mudstone microtexture and microfacies. *Sedimentology*, *61*, 609–647.

Plint, A., & Nummedal, D. (2000). The falling stage systems tract : recognition and importance in sequence stratigraphic analysis. In Hunt, D., Gawthorpe , R.L. (Eds.), *Sedimentary Responses to Forced Regressions*, 1–17. Geological Society, London.

Posamentier, H. W., & Morris, W. R. (2000). Aspects of the stratal architecture of forced regressive deposits. *Geological Society, London, Special Publications*, *172*(1), 19-46.

Romans, B. W., Castelltort, S., Covault, J. A., Fildani, A., & Walsh, J. P. (2015). Earth-Science Reviews: Environmental signal propagation in sedimentary systems across timescales.

Earth Science Reviews, *153*, 7-29.

Schieber, J., Southard, J., Thaisen, K., & Sorby, H. C. (2007). Accretion of Mudstone Beds from Migrating Floccule Ripples. *Science*, *318*, 1760–1763.

Seepersad, D. (2012). Thin-bedded Facies Analysis of a Ferron Storm-dominated Delta Front and Prodelta: Cretaceous Ferron Sandstone, Utah (Doctoral dissertation).

Snyder, C. J., Khan, S. D., Bhattacharya, J. P., Glennie, C., & Seepersad, D. (2016). Thin-bedded reservoir analogs in an ancient delta using terrestrial laser scanner and high-resolution ground-based hyperspectral cameras. *Sedimentary Geology*, *342*, 154–164.

Stacey, M. W., & Bowen, A. J. (1990). A comparison of an autosuspension criterion to field observations of five turbidity currents. *Sedimentology*, *37*(1), 1-5.

Tillman, R.W., & Merewether, E.A. (1994) Field guide for valley-fill, estuarine, and shelf ridge sandstones, mid-Cretaceous Frontier Formation, central Wyoming. *AAPG Annual Meeting Field Trip Guidebook*, pp. 90.

Walker, R. G. (1978). Deep-Water Sandstone Facies and Ancient Submarine Fans : Models for Exploration for Stratigraphic Traps ’. *AAPG Bulletin*, *62*(6), 932–966.

Waller, Z. (2016). Thin Bed Architecture of Cretaceous Gallup Prodelta Shales, New Mexico (Bachelor's Thesis). McMaster University.

Wheatcroft, R. A. (2000). Oceanic flood sedimentation: a new perspective. *Continental Shelf Research*, *20*(16), 2059-2066.

Whitaker, J. H. M. (1973). “Gutter Casts”, A new name For Scour-and-Fill Structures: With

Examples From The Llandoverian of Ringerike and Malmoya, Southern Norway. *Norsk Geologisk Tidsskrift*, *53*, 403–417.

Wilson, R. D., & Schieber, J. (2014). Muddy Prodeltaic Hyperpycnites in the Lower Genesee Group of Central New York , USA : Implications for mud Transport in Epicontinental Seas. *Journal of Sedimentary Research*, *84*, 866–874.